Investigations on Temporal and Spatial Variation of Slope-Scale SOC Erosion and Deposition

Inauguraldissertation
zur
Erlangung der Würde eines Doktors der Philosophie
vorgelegt der
Philosophisch-Naturwissenschaftlichen Fakultät
der Universität Basel
von

Yaxian Hu

China

Basel, 2014

Genehmigt von der Philosophisch-Naturwissenschaftlichen Fakultät
auf Antrag von

Prof. Dr. Nikolaus J. Kuhn
University of Basel
Faculty representative / dissertation supervisor

Dr. Goswin Johann Heckrath
Aarhus University
Co-examiner

Basel, June 24, 2014

_____

Prof. Dr. Jörg Schibler
The Dean of Faculty of Science

ABSTRACT

The net effect of soil erosion on global carbon cycling, especially as a source or sink for greenhouse gas emissions, has been the subject of intense debate. The controversy arises, to a large degree, from the inadequate understanding of the variation of soil organic carbon (SOC) in eroded sediment, and from the limited information on the fate of eroded SOC whilst in-transit from the site of erosion to the site of deposition. During a slope-scale erosion event, soil fractions and associated SOC will be transported away from eroding sites mainly by overland flow. If by interrill erosion, eroded sediment is often enriched in SOC. While the reported SOC enrichment ratios (ER_{SOC}) are mostly greater than unity, they vary widely. Conservation of mass dictates that the ER_{SOC} of sediment must be balanced over time by a decline of SOC in the source areas material. Although the effects of crust formation on SOC erosion have been discovered, a systematic study on crust formation over time and interrill SOC erosion has not been conducted so far. In addition, the inherent complexity of soil properties and SOC erosion process may inevitably introduce variations between replicates in SOC erosion data. Yet, the significance of such variation has not been systematically investigated.

Even after erosion, SOC distribution in eroded soil also can change during transport. Regardless of selective interrill erosion or non-selective rill erosion, eroded soil will be either gradually re-deposited along hillslopes or further transferred to river systems. Under given flow conditions, the site of SOC deposition depends on the transport distances of sediment particles where the SOC is stored. Very often, soil and SOC erosion risk is assessed by comparing the SOC stock on eroding and colluvial depositional sites, or by applying the mineral particle specific SOC distribution observed from either site to estimate the SOC stock of its counterpart. However, soil is not always eroded as dispersed mineral particles, but mostly in form of aggregates. Aggregates possibly have distinct settling velocity from individual mineral particles, which may considerably change the transport distance of the associated SOC. In addition, SOC concentration in different aggregates probably differs from soil average SOC concentration, which also complicates the spatial re-distribution of eroded SOC. Yet, little has been known about the potential effects of aggregation onto the movement and fate of eroded SOC. Mineralization during transport may add an extra risk to SOC loss. Some reports claimed that most of the SOC transfer occurs during large-scale erosion events, rapidly transporting eroded SOC into depositional sites. Mineralization of eroded SOC during such rapid transport, therefore, is of minor importance and thus can be ignored when calculating carbon balances between eroding and depositional sites. Meanwhile, some other reports argued that erosion and transport tend to break down aggregates, expose previously protected SOC to microbes and atmosphere, and hence accelerate mineralization of eroded SOC during transport. To solve this discrepancy, it is required to understand the susceptibility of eroded SOC to mineralization during transport, especially for erosion events that mobilize soil but do not necessarily move it far enough to reach permanent depositional sites.

The above-described debate on the fate of eroded SOC highlights four knowledge gaps: 1) how does SOC enrichment in eroded sediment vary with crust formation over rainfall time, and how the accordingly derived systematic variability affects soil and SOC erosion prediction; 2) how does the inherent complexity of interrill erosion processes affect the variability of SOC enrichment in eroded sediment; 3) how aggregation affects likely

transport distance of eroded SOC; 4) whether or not erosion and transport induce acceleration of eroded SOC mineralization. In this study, a series of experiments was conducted to address the above-identified knowledge gaps: *SOC-Variability* experiment, SOC-Settling velocity experiment (*SOC-Settling*), SOC-Aggregation effects experiment 1 (*SOC-Aggregation 1*) and SOC-Aggregation effects experiment 2 (*SOC-Aggregation 2*).

The *SOC-Variability* experiment was conducted to identify the temporal variation of SOC enrichment with crust formation during prolonged rainfall time, by applying a simulated rainfall to two silty loams placed in round flumes for 6 hours. A two-step erosion model was developed, based on the erosional response data obtained from six selected sub-events, to examine the systematic variability derived from crusting evolvement over rainfall time. In addition, the simulated erosion events were repeated ten times, enabling reliable statistical analysis for inter-replicate variability. Key results are: 1) the temporal variation of SOC enrichment ratio shows that ER_{SOC} of eroded sediment cannot be always greater than unity, but varies with rainfall time, in agreement with conservation of mass; 2) the gradually improved systematic variability of SOC erosion prediction over rainfall time shows that observations from short events cannot be directly extrapolated to predict soil and SOC loss over prolonged events and vice versa; 3) the significant inter-replicate variability at maximum runoff and soil erosion rates suggests that variability remains significant even under ideal laboratory conditions. A settling tube apparatus was built up in the *SOC-Settling* experiment to fractionated soil samples according to the potential transport distances of various fractions. To further examine the aggregation effects onto the likely transport distance of eroded SOC, this settling tube apparatus was then applied in the experiment *SOC-Aggregation 1*, to fractionate eroded sediment generated from a silty loam. Results show that aggregation of source soil considerably reduces the likely transport distance of eroded SOC, and potentially increases its likelihood to be re-deposited along hillslopes. Based on this observation on a single soil in the experiment *SOC-Aggregation 1*, *SOC-Aggregation 2* was then carried out with two types of soils, a silt loam and silt clay. Furthermore, the fractionated sediments were incubated for 50 days to assess their long-term mineralization potential. Key results from the experiment *SOC-Aggregation 1*, and *SOC-Aggregation 2* show that: 1) Aggregation of source soil and preferential deposition of SOC-rich coarse sediment fractions potentially skew the re-deposition of eroded SOC into the terrestrial system. 2) Erosion and transport tend to accelerate mineralization of eroded SOC, demonstrating their potential to contribute additional CO_2 to the atmosphere.

Overall, this study demonstrates that both the temporal variation of SOC erosion and the spatial variation of SOC deposition on hillslopes have to be considered when assessing the role of soil erosion on net CO_2 emissions. Applying "constant" SOC enrichment ratios in erosion models will lead to bias estimation of SOC loss. Aggregation effects of source soil considerably reduce the likely transport distance of eroded SOC, potentially skewing the re-deposition of SOC-rich coarse sediment fractions towards the terrestrial system. Erosion and transport processes tend to accelerate mineralization of eroded SOC, and hence potentially contribute additional CO_2 to the atmosphere. Such findings may profoundly alter our current accounting for erosion-induced lateral SOC transfer, further suggesting that current recognition on deep burial of SOC on long-term depositional sites and the accordingly derived CO_2 sink strength would be over-estimated. Significantly accelerated mineralization of eroded SOC during transport adds a further error into current carbon sink balances. Therefore, results from this study suggest that soil erosion is more likely to be a source of atmospheric CO_2.

ACKNOWLEDGEMENT

Thanks to numerous and invaluable supports, help and advices from many people, my study and life in the University of Basel pursuing a PhD degree are full of pleasant surprises, interesting experiences, and new knowledge of all kinds. First, I would like to give my sincere gratitude to Prof. Nikolaus J. Kuhn, for his kind encouragement at our first meet in China inspiring me to pursue advanced study abroad; for his help to fulfil this wish by giving me the opportunity two years later to start this PhD study in the University of Basel; and also for his patience, gradual guidance and profound knowledge that trained me to transform from an agricultural engineer to a geoscientist. I also would like to thank Dr. Wolfgang Fister, who has been always determined as well as attentive to show me the correct way to think, talk and work as a real geoscientist; and also who guided me through my first two years as a freshman in geoscience field with his incredible patience and considerate advices. I am especially grateful to China Scholarship Council for sponsoring my expenses abroad, which enabled me to commence the research in the University of Basel.

I also would like to give my thanks to other colleagues in research group of Physical Geography and Environmental Change: MScs. Ruth Strunk for her kindly teaching me and assisting all my laboratory measurements; our secretary Ms. Rosmarie Gisin for her kind help to find the apartment so that I could settle down upon arrival, and her helping hand on all kinds of issues during the past four years; our technician Mr. Hans-Rudolf Rüegg for his talents in building all the experiment instruments and gifted hands to solve all the technical problems during my experiments; Dr. Phil Greenwood for his generosity to correct my papers and improve my English language skills with his critical and always shrewd comments; MSc. Matthias Hunziker for his input to my first ever German article, his typical Swiss patience and kind heart, getting me to know local Swiss cultural with great joy.

I am also very grateful to other colleagues in our research group: Chatrina Caviezel, Judith Hinger, Kathrin Naegeli, Liangang Xiao, Mathias Würsch, Miriam Widmer, Ryan Studer, Samuel Kuonen, Simon Käch, Susann Tesch, and Wolfgang Schwanghart, who either assisted my work in the lab, or joyfully shared their daily time, experience or office with me. I particularly would like to thank Michelle Marbach, whose cheerful personality and considerate accompanying during my first few months in Basel helped me to get along with my new life in Basel with much more joys. Many thanks also go to all the other colleagues, who have always been ready to give comments and suggestions to improve my experiments, papers, presentations or posters.

I also would like to acknowledge the support of Dr. Franz Conen from Research Group Environmental Geosciences, Department of Environmental Sciences, for helping me to establish the

experimental rationale and generously lending me his Gas Chromatograph machine to investigate soil mineralization potentials. I would also like to thank Severin Kym from Bäumlihof and Edi Hilpert from Eulenhof, Möhlin, Switzerland, for allowing access to their fields and providing soil samples.

I particularly would like to remember Marianne Caroni, a member of the laboratory staffs, whose passing was much too premature and who is still sorely missed in the department. Her jolly characteristics in daily life, professional attitude at work and readiness to assist others will always be cherished in the rest of my life.

At last, I would like to thank my parents and my elder brother, without whose loving understanding and selfless supports I could have never accomplished this research.

TABLE OF CONTENTS

Chapter 1

Introduction

1.1. Soil erosion and global carbon cycling

1.1.1. Global carbon budget

The terrestrial carbon pool is the third largest carbon pool on the Earth. Within in the terrestrial carbon pool, dead organic matter in litter and soils contain about 1500 to 2400 petagram carbon (Pg C), three times as organic compounds in living biomass (450 to 650 Pg C) (IPCC, 2014). In addition, the soil carbon pool is actively interconnected with other carbon pools. For example, the cumulative net CO_2 emissions from land use changes between 1750 and 2011 are estimated at 180 ± 80 Pg C (IPCC, 2014). Accelerated soil erosion, as one of the most widespread forms of soil degradation in the terrestrial system, is potentially responsible for the net CO_2 emission of about 1 Gt $C \cdot yr^{-1}$(Lal et al., 2004). Quinton et al. (2010) estimated that globally about 0.08 Pg C is delivered to river systems every year by soil erosion. Van Oost et al. (2007) proposed that if 26% of the lost carbon is replaced on eroding sites through biomass incorporation, a global carbon sink of 0.12 Pg $C \cdot yr^{-1}$ could result from erosion in the world's agricultural landscapes. All these observations suggest that any changes in soil erosion processes, no matter being alleviated or accelerated, will have a significant impact onto global carbon cycling.

1.1.2. Soil erosion

There are four manners of soil erosion: mass wasting, water erosion, wind erosion and tillage erosion. In this study, we mainly investigate soil erosion by water. Within soil erosion by water, three types are generally recognized: interrill, rill and gully erosion. Linear erosion by concentrated flow on agricultural land is called rill erosion, while erosion by non-concentrated runoff, enhanced by the impact of raindrops, is referred to as interrill erosion (Kuhn et al., 2012). When the volume of runoff is further concentrated, the rushing water cuts deeper into the soil, deepening and coalescing the rills into larger channels termed gullies (Brady and Weil, 2002). Gully erosion is out of the scope of this study.

1.1.3. General impacts of soil erosion onto global carbon cycling

Substantial literature has discussed the impacts of soil erosion by water onto global carbon cycling (Pimentel et al., 1995; Stallard, 1998; Harden et al., 1999; Smith et al., 2001; Jacinthe and Lal, 2001; Jacinthe et al., 2001; Lal, 2003; Berhe et al., 2007; van Oost et al., 2007; Kuhn et al., 2009; Lal and Pimentel, 2008; Quinton et al., 2010; Berhe, 2011; Nadeu et al., 2012; Doetterl et al., 2012). The effects of soil erosion on soil organic carbon (SOC) dynamics can be summarized into seven processes (Figure 1-1): 1) slaking or disruption disintegrates macro-aggregates into smaller and easily transportable fractions by

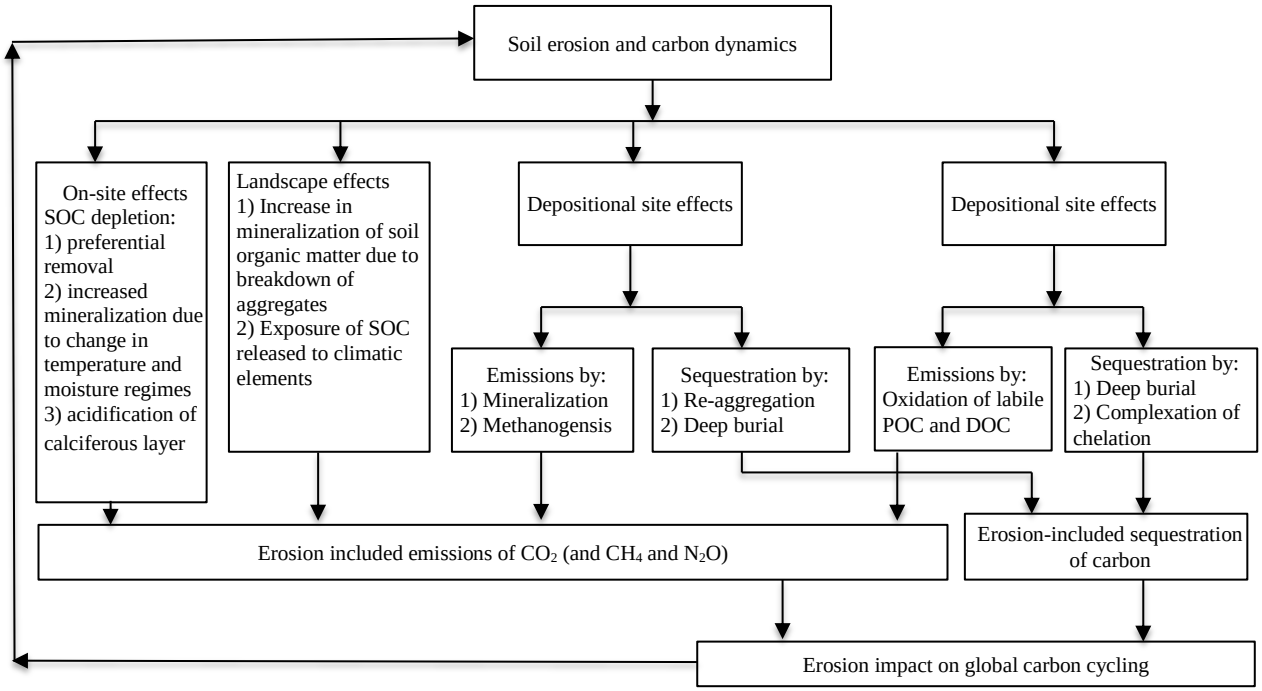

Figure 1-1 Processes affecting soil organic carbon (SOC) dynamics. Arrows pointed upward indicate emissions of CO_2 into the atmosphere. This figure is adopted from Lal et al. (2004).

runoff (Le Bissonnais et al., 1989; Le Bissonnais, 1990; Darboux and Le Bissonnais, 2007); in addition, slaking or disruption of aggregates exposes the previously protected SOC accessible to microbes and hence accelerating mineralization (Six et al., 2002; Lal and Pimentel, 2008; van Hemelryck et al., 2010); 2) preferential removal of carbon in runoff water or dust storms, facilitating soil carbon loss and significantly deteriorating soil quality (Sharpley, 1985; Moore and Singer, 1990b; Singer and Shainberg, 2004; Kuhn, 2007; Schiettecatte et al., 2008; Kuhn et al., 2009); 3) partial replacement of lost SOC by inputs of decomposing plants on the surface of eroding sites (Stallard, 1998; Harden et al., 1999; van Oost et al., 2007); 4) re-distribution of displaced SOC over the landscape and transported in rivers, resulting in a great scale of lateral transfers (Starr et al., 2000; Lal, 2003; Mora et al., 2007; Dlugoß et al., 2012); 5) mineralization of SOC on eroding sites, during transport and on depositional sites(Gregorich et al., 1998; van Hemelryck et al., 2010, 2011; Fiener et al., 2012); 6) re-aggregation of soil through formation of organo-mineral complexes at the depositional sites, protecting the freshly deposited SOC back into aggregates (Berhe et al., 2007; Berhe, 2011); 7) deep burial carbon-enriched sediments in depositional sites, flood plains and reservoirs and ocean floor (Stallard, 1998; van Oost et al., 2012; Hoffmann et al., 2013). Although a great amount of research has been devoted to study these processes, our knowledge on SOC dynamics is still very limited. A detailed discussion on the knowledge gaps in current studies of SOC erosion on hillslopes will follow in section 1.3. Out of the numerous unaddressed knowledge gaps, crust formation evolvement over time, the accordingly induced variations of SOC erosion, and the biogeochemical fate of displaced SOC during transport, will be the major issues addressed in this study.

1.2. Carbon dynamics in the terrestrial system

1.2.1. Carbon dynamics on eroding sites

A considerable amount of literature has reported that SOC erosion is dependent on numerous factors: 1) soil erodibility which is related to soil texture, aggregate stability, initial SOC content, and soil moisture (Tisdall and Oades, 1982; Le Bissonnais et al., 1995; Fitzjohn et al., 1998; Barthes and Roose, 2002; Darboux and Le Bissonnais, 2007; Zehe et al., 2010); 2) rainfall erosivity associated with intensity, kinetic energy, frequency, raindrop size and distribution (Beuselinck et al., 2000; Jacinthe et al., 2004; Kuhn and Bryan, 2004; Assouline and Ben-Hur, 2006; Jin et al., 2009; Berhe et al., 2012; Martínez-Mena et al., 2012; Iserloh et al., 2013); 3) soil surface conditions such as crust formation and surface roughness (Moore and Singer, 1990b; Le Bissonnais et al., 1998; Römkens et al., 2002; Kuhn and Bryan, 2004; Le Bissonnais et al., 2005; Anderson and Kuhn, 2008); 4) topography such as slope gradient, length and connectivity (Cerda and Garcia-Fayos, 1997; Fox et al., 1997; Fox and Bryan, 2000; Assouline and Ben-Hur, 2006; Olson, 2010; Armstrong et al., 2011); and 5) land use (Bradford and Huang, 1994; Govers et al., 1996; Jacinthe et al., 2002b; van Oost et al., 2005; Boix-Fayos et al., 2008; Wang et al., 2008; Olson, 2010). By integrating these factors in one way or another, different approaches have been developed to predict SOC erosion. For instance, SOC loss can be log-linearly related to soil loss, or simply obtained by multiplying soil loss with the percent of SOC in the near-surface soil and a SOC enrichment ratio (Sharpley, 1985; Schiettecatte et al., 2008), or estimated by extrapolating particle size specific SOC distribution in a runoff plot scale to that in river watershed scales (Massey and Jackson, 1952; Starr et al., 2000). Parameters in these approaches are often based on average values obtained over a certain monitoring setting. But both soil loss and the percent of SOC in near-surface soil may change with time (Vanmaercke et al., 2012), rainfall conditions (Jacinthe et al., 2004), topography (Le Bissonnais et al., 2005; Armstrong et al., 2011), and land use (Leys et al., 2007). Furthermore, given the inherent complex interactions between soil properties and erosion process, variation between replicates may also inevitably compromise the reliability of soil and SOC erosion data as input to erosion models. In addition, these SOC erosion models are often too specialized in SOC loss prediction to incorporate the partial replacement of lost SOC by inputs of decomposing plants into calculations (Figure 1-2).

Harden et al. (1999), after comparing soil samples from undisturbed slopes and slopes cropped for 100 years, stated that soil erosion amplifies both SOC loss and SOC recovery. On one hand, soil erosion decreases soil productivity by reducing available water capacity, decreasing effective rooting depth, and reducing water and nutrient use efficiencies (Lal, 2003). Declined productivity then reduces the amount of plant residues, thus less organic SOC is returnable to the soil, which could have partially replaced the lost SOC. This ultimately depletes SOC stock on eroding sites (Figure 1-2). On the other hand, the removal of topsoil material from eroded sites exposing subsoil material can also lead to rapid SOC replacement

through roots and litter input in the soil (hereafter termed as dynamic replacement) (Figure 1-2) (Stallard, 1998; Harden et al., 1999; Berhe et al., 2007). This is because many mineral surfaces in the deeper layers of the soil profile are under-saturated with SOC, as little SOC input from plants occurs in these deeper layers (van Oost et al., 2012). However, the magnitude of dynamic replacement rates reported in the literature varies largely. For instance, Smith et al. (2001) assumed a steady state SOC content at eroding sites (i.e., 100% replacement of eroded SOC), when calculating the budgets of SOC erosion and deposition across United States. But van Oost et al. (2007) suggested that dynamic replacement of eroded carbon is limited to the active carbon pools, i.e. pools have relatively high average C/N ratios and short half-lives. These active carbon pools constitute on the order of 25% rather than 100% of the eroded carbon. Different replacement rates then result in widely varying CO_2 sink strength ranging from 1 to 0.12 $Pg \cdot yr^{-1}$ (Stallard, 1998; van Oost et al., 2007). The field investigation by Berhe et al. (2012) and the modeling results from Billings et al. (2010) both suggested that higher rates of plant productivity are needed to create and maintain a CO_2 sink in eroding watersheds. This at least in part is managed by adding artificial fertilizers. However, greenhouse gases generated during artificial fertilizers production potentially correspond to 15 to 30% of the organic carbon buried owing to soil erosion (Kuhn, 2010a). This would, to a certain extent, offset against the CO_2 sink effects potentially induced by soil erosion. Meanwhile, Billings et al. (2010) also stressed that the sink strength resulted from dynamic replacement of eroded SOC could be cancelled out by the fraction of eroded SOC oxidized during transport and burial. Therefore, it requires accounting for all the lateral and vertical fluxes of SOC during erosion, transport and deposition to accurately identify the contribution of soil erosion to global carbon cycling.

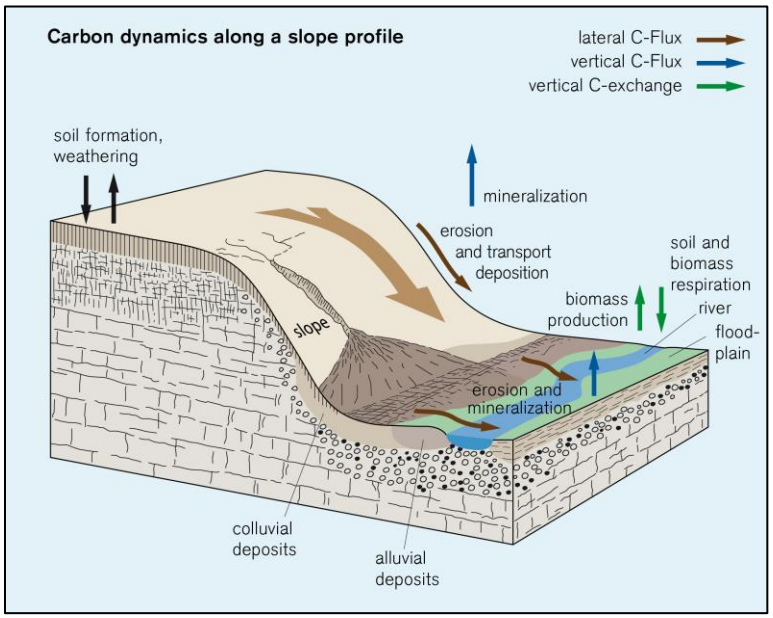

Figure 1-2 Carbon dynamics along a slope profile, showing interactions between biomass production, soil formation, erosion and deposition processes and their effects on lateral and vertical carbon fluxes on landscape scale in a terrestrial system with an adjacent aquatic environment. This figure is adopted from Kirkels et al. (submitted).

1.2.2. Carbon fate during transport

In-transit from eroding sites to depositional sites, eroded SOC will be gradually re-deposited after different transport distances (Figure 1-2). Understanding the fate of eroded SOC during transport is an essential component to close our carbon balances, but so far no compatible perception has been achieved on its significance. The re-distribution of eroded SOC during transport is not always uniform, but very often affected by preferential deposition (Kuhn et al., 2009; Hu et al., 2013a; Kuhn, 2013). The site of deposition is dependent on the transport distance of the sediment fraction containing a specific amount of SOC. The potential transport distances of sediment fractions are reflected by their settling velocities (Beuselinck et al., 1999a; Loch, 2001; Tromp-van Meerveld et al., 2008), as well affected by sediment discharge and hydraulic conditions (Beuselinck et al., 1998, 2000). Starr et al. (2000), after comparing stable aggregate size distribution in the runoff from plots and that in rivers in watersheds, inferred that more than 73% of eroded SOC is likely to be deposited on the landscape because it is associated with aggregates greater than 62 μm. Only 8% of eroded SOC has the highest likelihood to be lost from watershed soils to aquatic ecosystem with fine silt and clay domain. However, Wang et al. (2010), based on the aggregation index derived from dispersed mineral particle size distribution, found that the carbon delivery ratios out of the two small agricultural catchments in the Belgian Loess Belt ranged from 48.6 to 82.4%. These inconsistent observations, to a large extent, result from different assessments on transport distance of eroded sediment and the associated SOC.

The fate of SOC during transport is also determined by its susceptibility to mineralization. However, current investigations on the fate of eroded SOC are either deduced from SOC stock on eroding and depositional sites, or conducted after arbitrary transport distances, and thus cannot reflect the actual mineralization potential of SOC during transport. For instance, Jacinthe et al. (2004) only measured respiration rates of SOC collected from outlets at the end of each watershed, conveniently disregarding potential effects of various transport processes on accelerating SOC mineralization. In another case, Wang et al. (2014) monitored the in-situ respiration rates of SOC on different positions of a 3.75 m long flume, each time after it was subjected to simulated rainfall events. Even though this methodology is improved compared to that in Jacinthe et al. (2004), soil in Wang et al. (2014) only experienced arbitrary transport processes (certain slope gradient and length). Thus, observations from such experiments are of little relevance to predict the fate of eroded SOC in other erosion and transport scenarios. This requires an approach to effectively fractionate SOC according to transport distance to identify the mineralization potential of different SOC fractions during transport.

1.2.3. Carbon dynamics on depositional sites

Decomposition of SOC in the buried sediments of depositional basins is generally accepted to be slower than that in the source profiles on the eroding slopes (Figure 1-2). Deposition of eroded SOC

downslope is often accompanied with increased water content, reduced oxygen availability, compaction, and physical protection within inter-or intra-aggregates spaces. These conditions collectively can retard the decomposition rate of buried SOC (Berhe et al., 2007). Post-deposition remobilization and transformations are also reduced in wetter depositional basins, favoring SOC preservation over mineralization (Stallard, 1998; Harden et al., 1999; McCarty and Ritchie, 2002). However, other reports argued that SOC in depositional sites may be more biologically active than in erosional sites because of the accumulation of light and small particles (Gregorich et al., 1998; Fiener et al., 2012). Gregorich et al. (1998) reported that labile fractions of organic matter such as mineralizable carbon reflected the effects of soil re-distribution, with the lowest levels found at the mid-slope position and highest levels at the lowest slope position. Similarly, Fiener et al. (2012) observed a tendency that CO_2 effluxes at erosional sites were smaller than that at depositional sites in a small agricultural watershed subjected to water and tillage erosion processes. After a controlled experimental study, van Hemelryck et al. (2010) agreed that a significant fraction of eroded SOC was mineralized after deposition. However, they also pointed out that deposition produced a dense stratified layer of sediment that capped the soil surface, leading to a decrease in SOC decomposition in deeper soil layers. These diverging views highlight our limited knowledge of carbon dynamics at depositional sites, demanding great efforts in the future to enhance current understanding. However, even if carbon dynamics on depositional sites had been thoroughly investigated, because of the unaccounted SOC loss during transport, building up slope-scale carbon balances merely based on observations from depositional sites still bears great uncertainties. This, therefore, requires a comprehensive understanding of all the possible SOC fluxes during erosion, transport and deposition.

1.3. Four knowledge gaps in current studies of SOC erosion on hillslopes

1.3.1. Crusting and erosion-induced temporal variation of SOC erosion

Findings on SOC erosion reported in the literature discussed in section 1.2.1 have often been observed on a wide range of soils under relatively tight patterns of rainfall conditions (selected literature in Table 1-1), without adequately accounting for the potential effects of crusting over time. The results of such tests are useful, when comparing the reaction of a soil to a "standard" stress. But they provide only a snapshot out of all possible soil and rainfall scenarios. Such snapshots may therefore not be reliable to predict the reaction of soils to a wider range of naturally occurring rainfalls, let alone the rainfall scenarios of future climate and land use (Meyer, 1994). This problem extends to the quality of eroded sediments (Palis et al., 1990; Kinnell, 2012), particularly those from selective interrill erosion. Although on-site soil loss by interrill erosion is many times smaller than that from rill erosion when both occur at the same eroding site, it literally affects all arable land (globally, 14.2 million km^2) (Kuhn et al., 2009). Due to

limited raindrop kinetic energy and lack of concentrated runoff, interrill erosion is associated with selective entrainment and transport of sediment (Parson and Abrahams, 1992). As a consequence, fine and / or light particles and associated substances (e.g., soil organic carbon, phosphorus and nitrogen) are entrained and transported away from eroding sites in greater proportions than their concentration in the source soil suggests. The eroded sediment is thus generally enriched in substances, such as SOC (Sharpley, 1985), phosphorous (Quinton et al., 2001), nitrogen (Teixeira and Misra, 2005) and clay (Warrington et al., 2009), when compared to the source soil. Overall, between 0.57 and 1.33 Pg C yr^{-1} may be affected by interrill erosion, potentially influencing global carbon cycling (Kuhn et al., 2012). The delivery of SOC-enriched sediments into wetlands and water courses can also have profound off-site impacts (Lal, 2003). However, most of the recently published data on selective interrill erosion (reviewed by Kuhn and Armstrong, 2012) show only snapshots of SOC enrichment in eroded sediment, namely reactions to a particular rainfall out of complete crust formation. While most studies report a positive enrichment of SOC in interrill sediment, the enrichment ratios of SOC (ER_{SOC}) varies largely in the literature, ranging from 1.0 to 6.2 (Kuhn, 2007; Polyakov and Lal, 2004b; Schiettecatte et al., 2008; Sharpley, 1985). Discrepancies are attributed to soil properties, such as texture, aggregation, initial SOC content or initial soil moisture (Darboux and Le Bissonnais, 2007; Heil et al., 1997; Kuhn and Armstrong, 2012; Kuhn and Bryan, 2004; Ramos et al., 2000), as well as to rainfall intensities, kinetic energy, duration (Jacinthe et al., 2004; Martínez-Mena et al., 2012; Palis et al., 1990) and, finally, to diverse local micro-topography and deposition processes (Le Bissonnais et al., 2005; Kuhn, 2010b).

Table 1-1 Selection of literature studying enrichment ratio of soil organic carbon (ER_{SOC}), and the rainfall and slope conditions used in these investigations.

Literature	Soil type	Rainfall intensity ($mm\ h^{-1}$)	Rainfall duration (min)	Slope gradient (%)	Slope length (m)	ER_{SOC} in sediment
Jacinthe et al., 2004	Silt loam	Natural rainfall	Natural rainfall	Not reported	Not reported	1.2 to 2.9
Kuhn 2007	Silt	45	120	10	1	1.2 to 1.49
Polyakov and Lal, 2004	Silt loam	80	90	1 to 8	1 to 4	1 to 1.70
Polyakov and Lal, 2008	Clay loam	Natural rainfall	Natural rainfall	4 to 10	10 to 30	1.10 to 1.89
Kuhn and Armstrong, 2012	Sandy loam	25, 45	120, 180	10	1	0.77 to 1.46
Wang et al., 2010	Loess	45	Not reported	< 10	0.85	1.2 to 3.0
Wang et al., 2014	Silty loam	42	18	2 to 15	1.75 to 2	0.94-1.67

Apart from the factors identified above, some of the uncertainties on SOC erosion prediction are introduced by extrapolating constant or average SOC enrichment ratio to long-term or large-scale SOC erosion. The practical limitations of using one enrichment value for SOC in sediment are questioned from

a theoretical point of view: conservation of mass dictates that perpetual enrichment is not possible. Polyakov and Lal (2004b), Schiettecatte et al. (2008), as well as Kuhn and Armstrong (2012) observed decreasing ER_{SOC} in sediment after certain rainfall durations. This is in accordance with the conservation of mass, which dictates that the observed enrichment of particles must be a non-steady-state phenomenon (Kinnell, 2012). Failure to recognize this among other factors may lead to overestimating the loss of organic carbon, fine mineral particles, nutrients and other chemicals when soil is eroded by interrill processes (Kinnell, 2012; Kuhn and Armstrong, 2012). Ignoring crust-induced temporal variation of ER_{SOC} is also likely to introduce systematic variability when comparing SOC erosion observed from rainfall events of distinct durations. However, such systematic variability has not been adequately accounted for in current erosion models.

1.3.2. Inter-replicate variability induced by the inherent complexity of interrill erosion

The second knowledge gap identified in this study is the potential variability between replicates, which also questions the accuracy of using an average ER_{SOC} to assess SOC erosion. Major variability between replicates caused by differences in soil properties, rainfall conditions or plot set-up has been extensively discussed (Agassi and Bradford, 1999). The interrill erosion processes are also very sensitive to minor interactions between the impact angle, speed, and size of individual raindrops (Agassi and Bradford, 1999), the characteristics of particle units resulting from aggregate breakdown (Le Bissonnais, 1990), the changes of surface roughness (Anderson and Kuhn, 2008), as well as initial soil moisture (Le Bissonnais et al., 1995; Heil et al., 1997). Uncertainties coming from these sources are inherent in erosion processes, which are impossible or very difficult to eliminate even under ideal experimental conditions (Bryan and Luk, 1981; Nearing et al., 1999; Wendt et al., 1986). Such uncertainties hereafter are termed as inter-replicate variability. In addition, the significance of inter-replicate variability on runoff rates has been reported to differ from that on soil erosion rates, respectively up to 75% and 35% in Luk and Morgan (1981), while up to 105% and 173% in Rüttimann et al. (1995). This may imply a different extent of variability on SOC erosion rates than on runoff or soil erosion rates, as SOC erosion involves more factors, such as SOC distribution in eroded sediment and mineralization during crusting. However, the significance of inter-replicate variability on SOC erosion has not yet been systematically investigated.

1.3.3. Aggregation effects onto the likely transport distance of eroded SOC

As discussed in section 1.2.2, no compatible perception has been achieved on the fate of eroded SOC during transport. The major difficulty is to acquire the re-distribution pattern of eroded SOC, which is strongly related to the transport distance of the sediment fraction where the SOC is stored. Under given overland flow conditions, the transport distances of displaced soil particles are strongly related to their settling velocities (Dietrich, 1982; Kinnell, 2005, 2001). The settling velocity of mineral particles is determined by their size, density and shape (Dietrich, 1982). But soil particles are mostly eroded in the

form of aggregates rather than as mineral particles (Walling, 1988; Slattery and Burt, 1997; Beuselinck et al., 2000). For eroded soil particles composed of aggregates, settling velocities generally do not correspond to the average or median mineral grain size, because aggregates differ in size, density and shape from mineral particles (Johnson et al., 1996; Tromp-van Meerveld et al., 2008). Hence, the third knowledge gap identified for this study is the potential effects of aggregation onto the likely transport distance of eroded SOC on hillslopes.

The distribution of settling velocities based on mineral particle size classes has already been included in some erosion / deposition models (Aksoy and Kavvas, 2005; Fiener et al., 2008a; Morgan et al., 1998; van Oost et al., 2004). However, inconsistencies such as over-prediction of clay in sediment fractions or under-prediction of sand and silt in sediment samples are often present in their results (Beuselinck et al., 1999b; van Oost et al., 2004). This is because soil particles are mostly eroded in the form of aggregates rather than as mineral particles (Walling, 1988; Slattery and Burt, 1997; Beuselinck et al., 2000). The average or median mineral particle size can be the same for a range of soils, but the aggregate size distribution can differ, especially when clay enhances the formation of aggregates. Furthermore, SOC is more likely to be accumulated in macro-aggregates (Tisdall and Oades, 1982; Cambardella and Elliott, 1994), which probably have different settling velocities from individual mineral particles. This implies that aggregation can potentially change the settling velocities of individual mineral particles that are clued into aggregates, and thus alter the likely transport distance of the associated SOC. As a consequence, aggregation can lead to aggregate specific, rather than mineral grain specific SOC distribution across a landscape by preferential deposition (Kuhn, 2007; Kuhn and Armstrong, 2012). However, potential effects of aggregation on the likely transport distance of eroded SOC on hillslopes have not yet been investigated.

1.3.4.Mineralization of eroded SOC during transport

The fourth knowledge gap identified for this study is the mineralization of eroded SOC during transport. Many reports had described accelerating SOC mineralization during the detachment and transport of eroded soils, because structural aggregates are broken down, thereby exposing the previously protected SOC to microbial processes (Six et al., 2002; Lal and Pimentel, 2008; van Hemelryck et al., 2010). Lal (2003) estimated that with 20% mineralization of the displaced carbon, erosion-induced emission may be 0.8 – 1.2 Pg C yr^{-1} on the earth. Therefore, Lal and his colleagues proposed that SOC mineralization during transport should be included in SOC erosion models (Jacinthe and Lal, 2001; Jacinthe et al., 2004; Polyakov and Lal, 2004a). But other reports argued that large loads of sediment are moved during rapid transport, thus SOC loss by mineralization during transport is of minor importance, and hence could be ignored when calculating carbon balances (van Oost et al., 2007; Quinton et al., 2010). To solve these discrepancies, it is required to identify the quality of eroded SOC of different transport

distances. As discussed in section 1.3.3, under given overland flow conditions, the transport distance of eroded SOC is strongly related to the settling velocity of sediment fraction that carries the SOC. Therefore, in this study, the quality of eroded SOC can be identified by fractionating sediment according to settling velocity and measure the mineralization potential of fractionated sediment.

1.4. Objectives of this study

After identifying the four knowledge gaps in section 1.3, the two main aims of this study can be identified as: 1) to evaluate the potential impact of the temporal variation of SOC erosion on estimating slope-scale SOC loss; 2) to investigate the influence of the potential spatial variation of deposition onto the fate of eroded SOC. Six objectives were formulated in order to address the two aims:

1. To capture the crusting and erosion-induced temporal variation of SOC enrichment ratio in eroded sediment;
2. To assess the potential risk of bias estimation induced by crusting-induced systematic variability in SOC erosion prediction;
3. To examine the significance of inherent variability of runoff, soil and SOC erosion rates;
4. To establish an approach to effectively fractionate aggregated soils according to their likely transport distances;
5. To examine the potential effects of aggregation on the likely transport distance of eroded SOC;
6. To detect the susceptibility of eroded SOC to mineralization during erosion and transport.

1.5. Experiments rationale

All the above-listed objectives were investigated in this study by a series of experiments (Table 1-2). The first three objectives of this study, namely crusting and erosion-induced temporal variation of SOC enrichment ratio in eroded sediment, the potential risk of systematic variability in SOC erosion prediction, and the significance of inter-replicate variability of runoff, soil and SOC erosion rates, were investigated by the *SOC-Variability* experiment. The fourth objective, to establish an approach to efficiently fractionate aggregated soils according to their likely transport distances, was addressed by building a settling tube apparatus in the *SOC-Settling* experiment. The fifth and sixth objectives to examine the potential effects of aggregation on the likely transport distance and the mineralizability of eroded SOC were investigated in the *SOC-Aggregation 1 and 2*. In order to exclusively monitor the specific variations during SOC erosion, transport and deposition (i.e., temporal, systematic, inter-replicate and spatial variation), which otherwise

might be disguised or interfered by complex situations on natural field, all the experiments in this study were carried out under controlled laboratory conditions. Field investigations will be carried out in the future research, once all the presumed variations of SOC erosion have been detected in laboratory experiments.

In the *SOC-Variability* experiment, simulated rainfalls were applied for six hours on two silty loams of different tillage managements. Small round flumes each with an opening in the center were chosen to limit the effect of increasing flow depth and transport process on interrill erosion, as well to ensure a sufficiently large area to generate sediment for sampling and further analysis. Simulated rainfalls were on purpose prolonged to six hours to ensure the completion of crust formation. On one hand, this enabled the occurrence of temporally varying SOC enrichment ratios in eroded sediment; on the other hand, six hours of rainfall allowed the possibility to divide the entire event into several collective sub-events, and hence to investigate the potential of crusting-induced duration-related systematic variability. In addition, the *SOC-Variability* experiment was repeated for ten times under the most achievably uniform conditions, which also offers a possibility to evaluate the significance of the inter-replicate under ideally controlled conditions.

Table 1-1 An overview on the aims, experiment rationale, objectives and chapter structure of this study.

Aim	Experiment	Objective	Chapter
Potential temporal variation of SOC erosion	SOC-Temporal Variability	To capture the crusting and erosion-induced temporal variation of SOC enrichment ratio in eroded sediment	2
	SOC-Systematic Variability	To assess the potential risk of crusting-induced systematic variability in SOC erosion prediction	3
		To quantify the significance of inter-replicate variability of runoff, soil and SOC erosion rates	
Potential spatial variation of SOC deposition	SOC-Settling Velocity	To establish an approach to efficiently fractionate aggregated soils according to their likely transport distances	4
	SOC-Aggregation Effects 1	To examine the potential effects of aggregation on the likely transport distance of eroded SOC	5
	SOC-Aggregation Effects 2	To detect the susceptibility of eroded SOC to mineralization during erosion and transport	6

In order to reflect the actual settling behavior of aggregated fractions, rather than rely on bias estimation derived from mineral particle size distribution, a settling tube apparatus was designed in the *SOC-Settling* experiment to fractionate aggregated soils according to their settling velocities. This offered an opportunity to assess the quality of soil fractions of different likely transport distances. The distinct distributions of SOC by aggregate size and by mineral particle size illustrate that aggregation effects can facilitate the settling velocity of individual particle, and thus reduce the likely transport distance of the associated SOC. Assuming similar effects would also occur to eroded sediment fractions, this settling tube

apparatus was then applied in the *SOC-Aggregation 1* experiment to fractionate eroded loess generated from a 1.5 m long flume. A flume of this length was chosen to generate sufficient runoff to initiate non-selective erosion, meanwhile to limit the effects of transport process onto preferential deposition of eroded sediment. Key results show that aggregate effects can reduce the transport distance of eroded SOC and thus potentially skew the re-deposition of eroded SOC towards the terrestrial system. Based on the findings of the *SOC-Aggregation 1*, the *SOC-Aggregation 2* aimed at assessing the likely fate of SOC eroded from two types of soils with different textures, structures and SOC contents. The susceptibility of eroded SOC to mineralization was also determined by measuring the long-term mineralization potential of fractionated SOC.

1.6. Thesis structure

The remaining part of this thesis consists of six chapters, which are outlined as in the following:

Chapter 2 presents the first part results observed from the *SOC-Variability* experiment: the temporal variation of SOC enrichment from two silty loams. This chapter was published as an article in *Agriculture (Agriculture* 2013, 3, 726-740; doi:10.3390/agriculture3040726).

Chapter 3 is a manuscript describing the second part results observed from the *SOC-Variability* experiment: the significance of inter-replicate variability and crusting-induced systematic variability of SOC erosion. This manuscript is planned to submit to *Journal of Soils and Sediments*.

Chapter 4 describes the design and operation rationale of a settling tube apparatus in the *SOC-Settling* experiment. Different distributions of SOC between aggregates fractionated by the settling tube apparatus and mineral particles dispersed by ultrasound were then compared to examine the efficiency of such fractionation approach. This chapter was published as a technique note in *Geomorphological Techniques (Online Edition)* (Hu et al., 2013. Section 1.1.1: Particle size analysis. In: Clarke, L.E & Nield, J.M. (Eds.) Geomorphological Techniques (Online Edition). British Society for Geomorphology; London, UK. ISSN: 2047-0371).

Chapter 5 presents the results from the experiment *SOC-Aggregation 1*. It mainly discusses the effects of aggregation to reduce the likely transport distance of SOC, and the potential of such reducing effects to skew the re-deposition of eroded SOC into the terrestrial system. This chapter was published as a research article in *Biogeosciences*, 11, 6209-6219, 2014.

Chapter 6 is a manuscript presenting the results from the experiment *SOC-Aggregation 2*. As an extension of the *SOC-Aggregation 1*, this experiment compares the skewing effects of different

aggregation degrees onto the spatial re-distribution of eroded SOC. It also focuses on the long-term mineralization potential of eroded SOC. This manuscript is planned to submit to *Global Biogeochemical Cycles*.

Chapter 7 summaries the primary results observed from each experiment, and evaluates if all the knowledge gaps identified in Chapter 1 are properly addressed. General conclusions are then drawn to stress the contribution of this study to current understanding of erosion-induced carbon sink or source effects. At the end, potential research opportunities in the future are discussed.

Chapter 2

Temporal Variation of SOC Enrichment from Interrill Erosion over Prolonged Rainfall Simulations

Yaxian Hu, Wolfgang Fister and Nikolaus J. Kuhn

Published in *Agriculture*, 3(4), 726–740, 2013

Abstract: Sediment generated by interrill erosion is commonly assumed to be enriched in soil organic carbon (SOC) compared to the source soil. But the reported SOC enrichment ratios (ER_{SOC}) vary widely. It is also noteworthy that most studies reported that ER_{SOC} is greater than unity, while conservation of mass dictates that ER_{SOC} of sediment must be balanced over time by a decline of SOC in the source area material. Although the effects of crusting on SOC erosion have been recognized, a systematic study on complete crust formation and interrill SOC erosion has not been conducted so far. The aim of this study was to analyze the effect of prolonged crust formation and its variability on the ER_{SOC} of sediment. Two silty loams were simultaneously exposed to a rainfall simulation for 6 hours. ER_{SOC} in sediment from both soils increased at first, peaked around the point when steady state runoff was achieved and declined afterwards. The results show that crusting plays a crucial role in ER_{SOC} development over time, and in particular, that the conservation of mass applies to ER_{SOC} of sediment as a consequence of crusting. A "constant" ER_{SOC} of sediment is therefore possibly biased leading to an overestimation of SOC erosion. The results illustrate that potential off-site effects of selective interrill erosion require considering the crusting effects on sediment properties in the specific context of the interaction between soil management, rainfall and erosion.

Keywords: *interrill erosion; SOC enrichment ratio; temporal variation; crust formation; prolonged rainfall duration*

2.1. Introduction

Although the on-site soil loss by interrill erosion is many times smaller than that from rill erosion, it literally affects all arable land (globally 14.2 mil. km^2) (Kuhn et al., 2009). Due to the limited raindrop kinetic energy and lack of concentrated runoff, interrill erosion is associated with selective entrainment and transport of sediment (Parson and Abrahams, 1992). As a consequence, fine and/or light particles and associated substances (e.g. soil organic carbon, phosphorus and nitrogen) are entrained and transported away from eroding sites in greater proportions than their concentration in the source soil suggests. The eroded sediment is thus generally enriched in substances such as soil organic carbon (SOC) (Sharpley, 1985), phosphorous (Quinton et al., 2001), nitrogen (Teixeira and Misra, 2005) and clay (Warrington et al., 2009) when compared to the source soil. Interrill erosion may therefore play a great role as source of non-point pollution for rivers and lakes (Lal, 2003). In addition, a potentially significant amount of between 0.6 to 1.3 Pg·-of organic carbon is affected annually by interrill erosion processes including aggregate breakdown, crust formation, rainsplash and rainwash (Kuhn et al., 2009). The susceptibility of soil organic carbon in interrill sediment to mineralization (van Hemelryck et al., 2010) also emphasizes the necessity to improve our understanding of the role of interrill erosion and the associated crust formation onto interrill SOC enrichment.

The reported SOC enrichment in sediment compared to source area soil, expressed as enrichment ratio (ER_{SOC}), varies largely in the literature, ranging from 0.74 to 6.2 (Kuhn, 2007, 2010b; Polyakov and Lal, 2004b; Rodríguez Rodríguez et al., 2004; Schiettecatte et al., 2008; Wang et al., 2010). Discrepancies are attributed to soil properties such as texture, aggregation, initial SOC content, or initial soil moisture (Darboux and Le Bissonnais, 2007; Heil et al., 1997; Kuhn and Armstrong, 2012; Kuhn and Bryan, 2004; Ramos et al., 2000), as well as to rainfall intensities, kinetic energy and duration (Jacinthe et al., 2004; Martínez-Mena et al., 2012; Palis et al., 1990), and finally to diverse local micro-topography and deposition processes (Le Bissonnais et al., 2005; Kuhn, 2010b). ER_{SOC} also varies during an erosion event as a consequence of selective erosion and crust formation (Hairsine et al., 1999; Palis et al., 1990; Walker et al., 1978). While most papers report ER_{SOC} in sediment greater than unity, Polyakov and Lal (2004), Schiettecatte et al. (2008) as well as Kuhn and Armstrong (2012) observed decreasing ER_{SOC} in sediment after certain rainfall durations. This is in accordance with conservation of mass, which dictates that the observed enrichment of particles must be a non-steady state phenomenon (Kinnell, 2012), particularly on the eroding site where no repletion comes from adjunctive areas (e.g. slope shoulder). Failure to recognize this among other factors may lead to overestimating the loss of organic carbon, fine mineral particles, nutrients and other chemicals when soil is eroded by interrill processes (Kinnell, 2012; Kuhn and Armstrong, 2012).

The enrichment and subsequent depletion of SOC in interrill sediment is attributed to crust formation as well as the duration of erosion (Kuhn, 2010b). Chen et al. (1980) developed a three-stage conceptual model of crust formation by interrill erosion processes: at the beginning of an erosion event, the formation of a structural crust is initiated by the aggregate slaking and micro-cracking. Patches of depositional crust are formed by displaced small stable particles composed of minerals (Kuhn and Armstrong, 2012) or aggregates (Le Bissonnais, 1996; Slattery and Bryan, 1992), the latter of which are often enriched in SOC. As rainfall proceeds, the loose depositional material is removed by raindrop-impacted flow and structural crust grows, progressively covering the soil surface. Its cohesive surface reduces the erodibility of the soil surface, but also increases runoff and thus flow erosivity (Le Bissonnais, 1996). After achieving steady state runoff, the equilibrium between crust formation and removal is achieved for the given rainfall and runoff conditions (Moore and Singer, 1990b). Achieving the dynamic balance between soil erodibility and runoff erosivity is thus highly likely to cause changes in ER_{SOC} of sediment. As long as rainfall and runoff have not produced a steady state crust, the increasing runoff transport capacity and abundant erodible SOC-rich particles easily lead to a ER_{SOC} of sediment greater than unity (Kuhn et al., 2012). Once the crust formation has reached a steady state, ER_{SOC} of sediment should develop towards unity between crust and sediment because the amount of easily erodible particles enriched in SOC has declined (Kuhn and Armstrong, 2012). Apart from the few studies on declining sediment SOC cited above, the effect of crust completion on ER_{SOC} of sediment has not been investigated systematically. Therefore, this study aims to analyze the effect of prolonged crust formation and its variability on the ER_{SOC} of sediment.

2.2. Experimental Section

2.2.1. Soil samples and preparation

Two silty loams from Möhlin (47˚ 33’ N, 7˚ 50’ E) near Basel, Switzerland, one from the conventionally managed (CS) Bäumlihof Farm and the second from the organically managed (OS) Eulenhof Farm, were used in this study. Soils of A-horizons (about 100 kg for each) from a gentle shoulder slope (< 5 %) were sampled in April 2010 on each farm. Previous research conducted in the region of Möhlin showed that the silty loams used in this study are of structural stability and prone to form crusts (Hu and Fister, 2011). The two soils were of almost identical texture (wet-sieving after dispersion by 1% Sodium hexametaphosphate), but different in SOC content (LECO RC 612 at 550 ˚C), aggregate stability (method adapted from (Nimmo and Perkins, 2002)) and tillage management (Table 2-1).

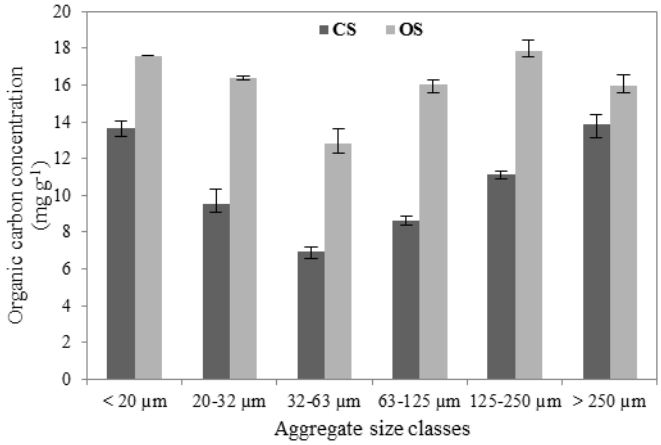

Figure 2-1. Distribution of soil organic carbon concentration in aggregate size classes of conventionally farmed (CS) and organically farmed (OS) silt loams. Aggregates were fractionated by settling velocities following the method described in Hu et al. (2013c). Error bars indicate the minimum and maximum values observed during three replicate measurements.

In addition, SOC was not equally distributed in aggregate classes, but -more concentrated in small particles (< 20 µm) and macro-aggregates (> 250 µm) than in other classes (Figure 2-1). Similar distribution, but less SOC concentration in macro-aggregates (> 250 µm), was also observed in aggregate fractions of eroded sediment (Hu and Kuhn, 2014). Their similarity in texture, but different aggregation was considered suitable to observe the differences on crusting and thus ER_{SOC} in eroded sediment, as well as to ensure that during the rainfall simulation the presumed decline of ER_{SOC} in eroded sediment would occur. After sampling, the soils were dried at 40 ˚C until constant dry weight was reached and then sieved to 1 to 8 mm. On one hand, this resembled the seedbed conditions on the field. On the other hand, excluding over-sized clods largely reduced the variation of surface roughness both within each flume and between replicates, ensuring the dominance of interrill erosion processes rather than the differences in initial roughness in the results.

Table 2-1 Texture, percentage of stable aggregates greater than 250 µm, soil organic carbon concentration (SOC), and tillage management of conventionally farmed (CS) and organically farmed (OS) silt loams. Different superscripted letters in each column indicate significant differences (T-test, $P \leq 0.05$). The subscripted numbers after each average value show the standard deviations (n=10).

	Clay (%)	Silt (%)	Sand (%)	Stable aggregates greater than 250 µm (%)	SOC ($mg \cdot g^{-1}$)	Tillage operation	Rotation	Fertilizer
CS	$16.80^{a}{}_{1.38}$	$71.47^{a}{}_{1.76}$	$11.50^{a}{}_{1.00}$	$66.85^{a}{}_{0.47}$	$10.9^{a}{}_{0.05}$	Plowing (at least once a year) together with other tillage operations	Maize, rape, wheat, grass	Chemical fertilizer and manure
OS	$14.39^{b}{}_{0.52}$	$75.84^{b}{}_{0.56}$	$9.77^{b}{}_{0.38}$	$77.76^{b}{}_{1.87}$	$16.9^{b}{}_{0.10}$	Non-plowing, harrowing	Pumpkin, carrot, salad, pea, bean	Sheep manure, horn shavings

Dry soils were placed in a round flume (Figure 2-2a) with an outside diameter of 50 cm and a center opening of 10 cm (Figure 2-2b). These flumes were designed to limit the effect of increasing flow depth on interrill erosion, as well to ensure a sufficiently large area to generate sediment for sampling and further analysis. To assist drainage, the floor of the flume was perforated, covered by a fine cloth and a layer of sand (~ 2 cm). The soils were placed on the sand and molded into a straight slope of 10% between the outer and inner rim. Preliminary tests had shown that to achieve a complete crust, indicated by constant runoff rates, required more rainfall than that could be feasibly applied during one day. Therefore, a 30 min rainfall corresponding in intensity to the one used for the actual test (described below) was applied one day prior to the simulation event. This short pre-wetting, on one hand, enabled the observation of the effects of aggregate breakdown during crusting process; on the other, an initial crusting and soil settling was induced, which facilitated the faster runoff development during the actual test.

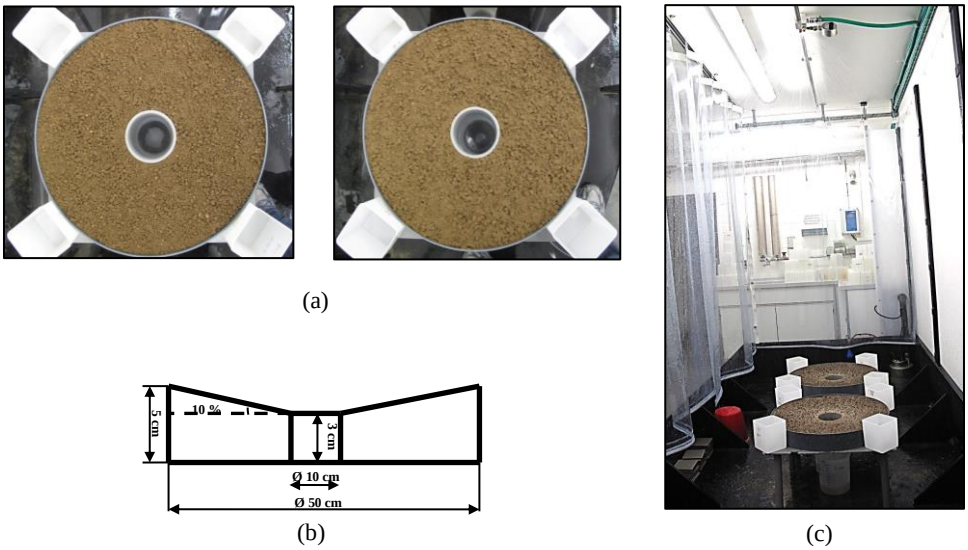

(a) (b) (c)

Figure 2-2. Conventionally farmed soil (CS) and organically farmed soil (OS) in round flumes were simultaneously subjected to rainfall simulation. (a) Two round flumes filled with soils; (b) the cross-section profile of the round flume; (c) the layout of rainfall simulation experiment. The white containers were used to monitor the rainfall intensity.

2.2.2. Rainfall simulation

Two flumes, one of each filled with CS and OS, were exposed to a rainfall of 30 $mm \cdot h^{-1}$ for 6 hours simultaneously (180 mm rain in total) (Figure 2-4c). An event precipitation of 180 mm is not a frequent phenomenon in Basel region. The monthly precipitation during April, May and June (corresponding to periods with bare soil after tillage) varied widely over the past three decades, ranging from 6 to 241 mm (MeteoSwiss, 2013). Preliminary tests and field observations had shown that the two silty loams used in this study required between 90 and 120 mm rainfall (i.e. 180 and 240 min) to complete crust formation, and roughly 180 mm rainfall (i.e. 360 min) to develop the presumed decreasing SOC

erosion rates (Hu and Fister, 2011). The return frequency of such monthly rainfall is 0.65 years for 90 mm, 1 year for 120 mm, and 7 years for 180 mm. The selected rainfall therefore suited the objective of this study to observe the effect of prolonged crust formation on ER_{SOC} using rainfall intensity and kinetic energy as well as an amount that can be experienced by the soil in Basel region. This therefore leads to a quasi-natural sequence of crust formation, except for the effect of drying between rainfall events. Drying is likely to rejuvenate the granular structure of the crust (Kuhn and Bryan, 2004); however, the effects of drying on ER_{SOC} are unknown. Ignoring the drying effect does not limit the objective of this study, which aimed at testing the sensitivity of ER_{SOC} to crust formation in principle.

A FullJet nozzle (¼ HH14WSQ), installed 2 m above the soil surface, was used to generate multiple-sized raindrops (D_{50} of 2.3 mm). Kinetic energy of raindrops was detected by a Joss-Waldvogel-Distrometer (average energy of 113.9 $J \cdot m^{-2} \cdot h^{-1}$). Tap water was used for each rainfall. The electric conductivity of tap water was 2220 $\mu s \cdot cm^{-1}$, which was five times higher than the rainwater in Basel (462 $\mu s \cdot cm^{-1}$). In general, increased electric conductivity of tap water enhances dispersion during rainfall simulation tests (Borselli et al., 2001). A comparative aggregate stability test (Wet Sieving Apparatus, Eijkelkamp, Netherlands) using tap water and rainwater from Basel had shown that tap water had only a minor effect on aggregates greater than 250 µm after 20 min of continuous oscillating movement (67.24 % in rainwater and 73.59 % in tap water for CS, while 70.60 % and 68.84 % for OS). Therefore, the use of tap water was considered acceptable. During the simulation event, runoff and sediment were sampled in intervals of 30 minutes and all runoff and sediment generated during the interval were collected. Sampling at intervals of 30 min produced enough runoff and sediment for further analysis and still enabled to record the temporal changes of erosional response. In addition, no supplement was applied to replenish the on-site soil and SOC loss, which although unlike natural conditions (i.e. with vegetation or litter input or upland deposition), served our purpose well to observe the potential of ER_{SOC} varying against time. The rainfall simulation tests were repeated 10 times for each soil (two pairs of flumes used for 5 times) to generate a data set that would enable the statistical analysis of the variability of the erosional response.

2.2.3. Soil and sediment analysis

The runoff samples were weighed immediately after collection to acquire the amount of discharge. Sediment transported by splash was not considered relevant in this study, since a preliminary test revealed that its effect was negligible to merit carrying out further measurements. After the simulation events, sediment in all runoff samples was allowed to settle for more than 48 hours. The supernatant was then decanted off and the sediment was dried at 40 ˚C and weighed. Surface roughness was used as an index of crust formation. Twenty-centimeter transects from the outside rim to the center of the flume were scanned stepwise at a 1 mm resolution by a laser scanner before and after each rainfall simulation. The scanner was controlled by Stepper Motor Controller CSD 315 (Isel Automation, Germany) and

programmed using MatLab 2007. The surface relative roughness was expressed as the standard deviation of the differences between the actual height of the individual point and its theoretical height along a straight slope. The flumes were also dried at 40 ˚C until constant dry weight was obtained. Loose aggregates left on the dry soil surface were swept and collected by a vacuum pump. A 1 - 2 mm layer of dry crust was carefully scratched off the soil surface. The thickness of crust, as a secondary source of confirmatory information, was measured using a ruler. Soils below the crusts were also collected for each replication, for use as a reference to the original soils. Soil organic carbon concentration of the original soils, eroded sediment, loose aggregates on surface, and crusts were measured by LECO RC 612 at 550 ˚C. Enrichment ratios were calculated between SOC concentration of the eroded sediment and the original soil, between the crust and the original soil, and between the soils below the crust and the original soil. The grain size distributions of sediments and crusts were measured with a Mastersizer 2000 (Malvern, Germany) after dispersion with 4 ml of sodium hexametaphosphate and ultrasound at 9 $J \cdot ml^{-1}$ (i.e. energy = output power 30 W × time 300 s / suspension volume 1000 ml). Statistical analyses were calculated using Microsoft Excel 2010 and SPSS.

2.3. Results

2.3.1. Erosional response during rainfall time

Both CS and OS showed a similar temporal pattern of runoff and erosion (Figure 2-3). However, CS responded more rapidly and significantly pronounced than OS (T-test, $P \leq 0.05$). The runoff of CS started after 60 min and kept increasing until a steady state was achieved at 180 min (Figure 2-3a), indicating the completion of structural crust formation(Chen et al., 1980; Moore and Singer, 1990b). The runoff on OS started 60 min. later than for CS, and reached a steady state after 240 min of rainfall, but with a relatively lower runoff rate than CS (Figure 2-3a). By the end of the 6 hour rainfall simulation, the runoff coefficients of CS and OS were on average 29.4 % and 18.1 %. Soil erosion from CS was also higher than from OS. The temporal pattern of soil erosion rates for both soils corresponded with their runoff rates (Figure 2-3b). The slight decline of soil erosion rates on CS implies the depletion of erodible materials. The sediment concentration of CS and OS roughly stayed constant after runoff reached steady state conditions (Figure 2-3c). Due to limited amount of soil erosion at the beginning of the tests, the sediment concentration could not be calculated accurately and is therefore not shown here. The inter-replicate variations of runoff and soil erosion rates (indicated by the error bars in Figure 2-3a, b and standard deviation in Table 2-2) were between 10 and 38% after reaching runoff steady state. This is mostly due to the unavoidable inherent variability of erosion process (Bryan and Luk, 1981; Wendt et al., 1986). However, the temporal patterns of runoff, soil erosion rates and ER_{SOC} of each replicate

corresponded with each other (detailed data shown in (Hu et al., In preparation)). Meanwhile, the erosional response for CS significantly differed from that for OS in almost all the cases (Table 2-2). The erosion data observed in our study is, therefore, considered capable of drawing representative conclusions on the effect of crusting on ER_{SOC}. Detailed erosional responses during the 360 min rainfall simulation are summarized in Table 2-2.

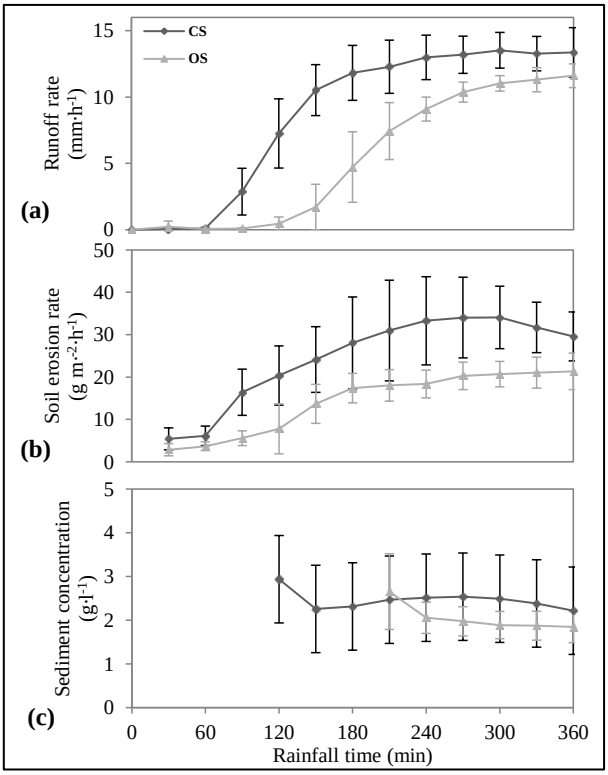

Figure 0-1. Development of (a) runoff rate, (b) soil erosion rate and (c) sediment concentration of conventionally farmed soil (CS) and organically farmed soil (OS) over 360 min of rainfall time. Error bars indicate the standard deviation. n=10.

2.3.2. Temporal variation of ER_{SOC} in sediment during rainfall time

ER_{SOC} in sediment changed for both CS and OS during the simulated rainfall (Figure 2-4). On both soils, ER_{SOC} in sediment initially increased, peaked around the time when steady state runoff was achieved and thereafter declined. Maximum ER_{SOC} in CS sediment was 1.86 and occurred between 120 and 150 min., while the peak ER_{SOC} of OS sediment was only 1.37 and occurred around 240 to 270 min. At the end of the simulated rainfall, the CS ER_{SOC} of 7 out of 10 replicates approached unity. Enrichment of SOC in sediment < 1 compared to the original source soil was observed for the remaining three replicates. Overall, the total amount of eroded SOC was 369.1 mg for CS and 326.0 mg for OS, which were not significantly different from each other (t-test, $P > 0.05$, n=10). Detailed data on SOC erosion are shown in Table 2-2.

Table 2-2. Summary of erosional responses of conventionally farmed soil (CS) and organically farmed soil (OS) over 360 min of rainfall time (average of 10 replicates). The erosion area is 1884.96 cm^2. Different superscripted letters in each column indicate the significant differences (T-test, $P \leq 0.05$). The subscripted numbers after each average value show the standard deviation (n=10).

Soil	Steady state				Total runoff (mm)	Runoff coef. (%)	Total soil erosion (g)	Soil conc. in runoff ($mg \cdot mm^{-1}$)	Total SOC erosion (mg)	SOC conc. in runoff ($mg \cdot mm^{-1}$)
	Time (min)	Runoff rate ($mm \cdot h^{-1}$)	Erosion rate ($g \cdot m^{-2} \cdot h^{-1}$)	Sediment conc. ($g \cdot l^{-1}$)						
CS	180	$12.9^{a}{}_{\pm 0.2}$	$31.7^{a}{}_{\pm 2.5}$	$2.4^{a}{}_{\pm 0.2}$	$55.6^{a}{}_{\pm 9.1}$	$29.4^{a}{}_{\pm 5.0}$	$27.4^{a}{}_{\pm 7.6}$	$484.7^{a}{}_{\pm 69.1}$	$369.1^{a}{}_{\pm 85.1}$	$6.6^{a}{}_{\pm 0.6}$
OS	240	$10.7^{b}{}_{\pm 0.2}$	$20.3^{b}{}_{\pm 0.5}$	$1.9^{b}{}_{\pm 0.02}$	$34.1^{b}{}_{\pm 6.0}$	$18.1^{b}{}_{\pm 3.0}$	$16.1^{b}{}_{\pm 3.0}$	$476.1^{a}{}_{\pm 57.7}$	$326.0^{a}{}_{\pm 59.1}$	$9.6^{b}{}_{\pm 1.0}$

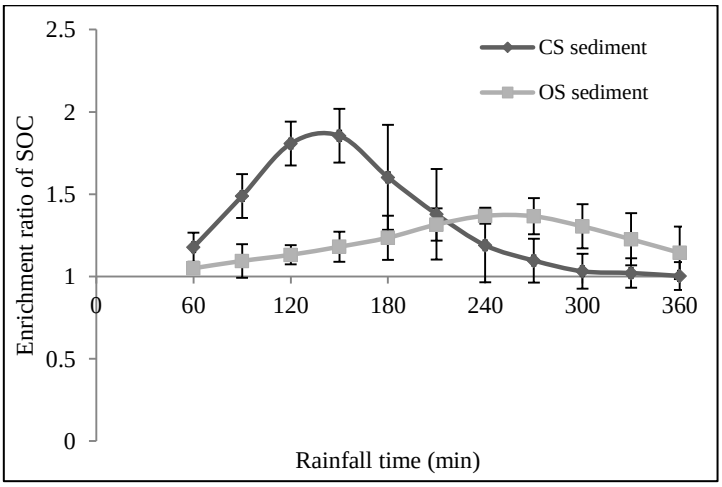

Figure 2-4 Development of enrichment ratio for soil organic carbon (ER_{SOC}) in eroded sediment from a conventionally farmed soil (CS) and organically farmed soil (OS) over 360 min of rainfall time. Error bars indicate the standard deviation (n=10).

2.3.3. Interrill erosional response and SOC erosion

The relationship between runoff and soil erosion rates differed noticeably for CS and OS (Figure 2-5a, b): soil erosion rates for the CS increased rapidly from 20 to 50 $g \cdot m^{-2} \cdot h^{-1}$ after runoff rates exceeded 10 $mm \cdot h^{-1}$, while the soil erosions rate for OS stabilized around 20 $g \cdot m^{-2} \cdot h^{-1}$ for runoff rates ranging from 2 to 14 $mm \cdot h^{-1}$. The power regression between runoff and soil erosion rate also showed that CS was more sensitive to runoff erosivity (exponent 0.34 vs. 0.28) and soil erodibility (constant factor 12.12 vs. 10.27) than OS (Figure 2-5a, b). In addition, the constant relationship for OS and cloud above the tail of the power regression line of the CS imply that the erosion was non-selective (Figure 2-5a). There was no consistent relationship between ER_{SOC} of sediment and runoff rate or erosion rate for either soil (Figure 2-5c, d, e, f), indicating that there must be some other factors (e.g. duration or stage of crust formation (Kuhn and Armstrong, 2012; Kuhn, 2010b)) affecting the ER_{SOC} of sediment than just the runoff erosivity or soil erodibility.

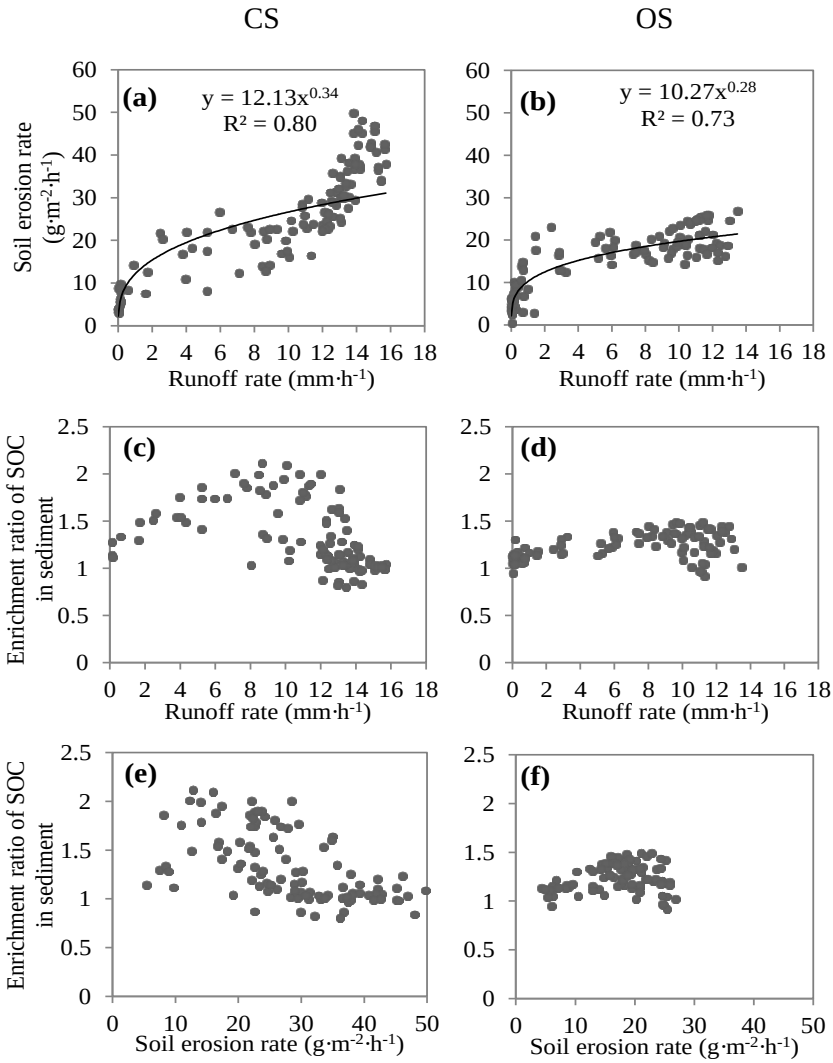

Figure 2-5. Correlation of soil erosion rate with runoff rate (a, b), correlation of ER_{SOC} with runoff rate (c, d) and correlation of ER_{SOC} with soil erosion rate (e, f) of conventionally farmed soil (CS) and organically farmed soil (OS). Data from all 10 replicates are presented.

2.3.4. Crust formation and surface properties

Both soils experienced the formation of distinct crust features during the simulation. After 6 hours of rainfall, only a limited amount of large aggregates remained embedded on the CS, surrounded by a coherent depositional crust (Figure 2-6). In contrast, the extent of the structural crust on the OS was much greater than CS and the depositional crust also contained visibly distinguishable aggregates (Figure 2-6). This indicates that the crusting process on CS progressed further than that on OS. A typical pattern of surface roughness changes is shown in Figure 2-7. The difference in surface relative roughness before and after all rainfall events was significant (Mann-Whitney Test, $P \leq 0.05$) for the CS, but not for the OS. This result reflects the progressed crusting on the CS, which generated a stronger elevation contrast between flat extended depositional crusts and embedded crumbs. On the OS, the soil surface was still interspersed

by more coarse aggregates and a smaller area was covered by depositional crust. A similar effect of crusting on roughness was observed by Anderson and Kuhn (2008). The texture of sediments and crusts was similar to the original soil, which indicates non-selective erosion. The SOC content in the crust after 6 hours of rainfall was not significantly different from that in their original source for either soil (P = 0.47 for CS and P = 0.08 for OS) (Figure 2-8).

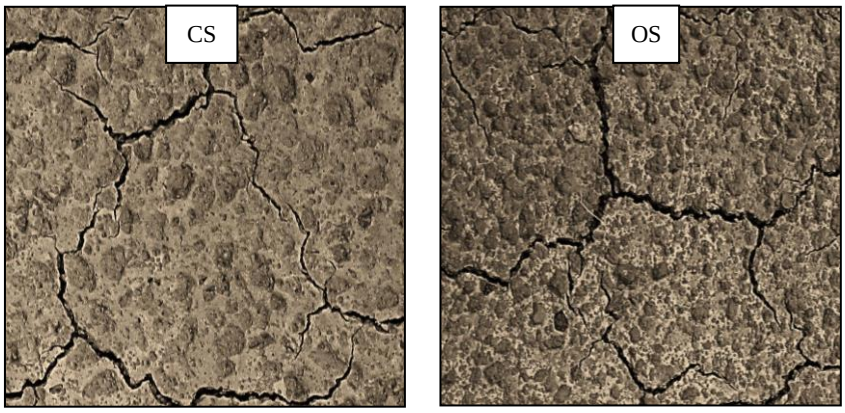

Figure 2-6. Soil surface after 6-hour rainfall on conventionally farmed soil (CS) on the left and organically farmed soil (OS) on the right. On both soils, the dark patches are formed by structural crust consisting of degraded crumbs. Light-colored areas are depositional crusts consisting of fragments detached from structural crust by raindrop impact and wetting. (Picture size: 10 cm × 10 cm).

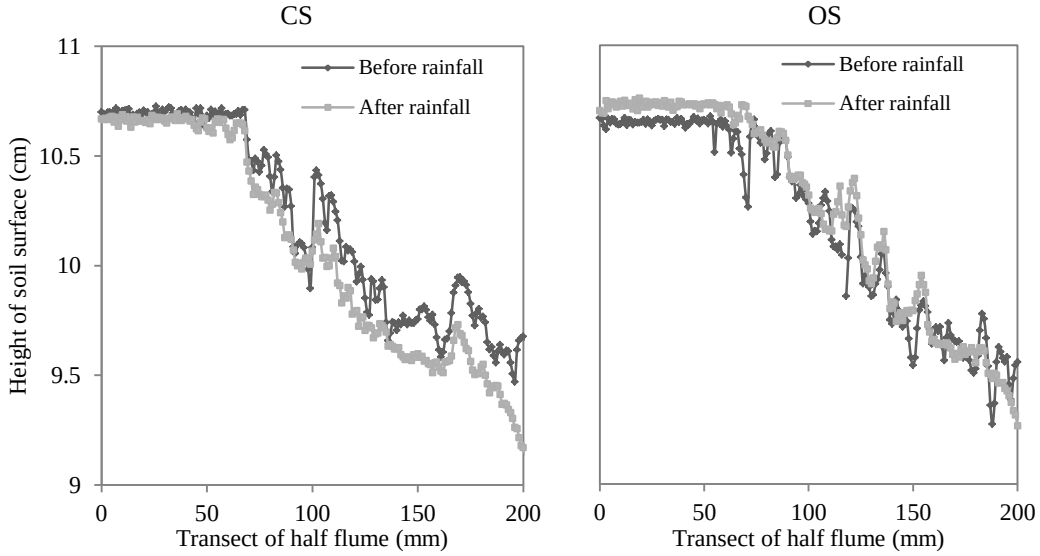

Figure 2-7. Typical pattern of surface roughness on the flume transects before and after rainfall. The 10th replicate from conventionally farmed soil (CS) on the left and organically farmed soil (OS) on the right are shown here as an example.

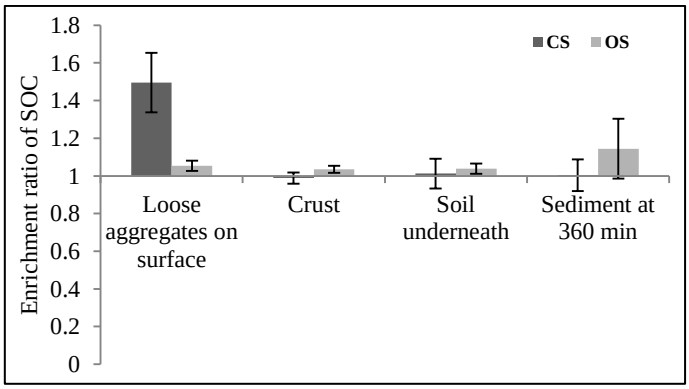

Figure 2-8. Enrichment ratio of soil organic carbon (SOC) in soils below the crust, depositional crust and eroded sediment at 360 min. from a conventionally farmed soil (CS) and from an organically farmed soil (OS) compared to their initial SOC contents. Error bars indicate the standard deviation. n=10.

2.4. Discussion

Our results confirm the a priori rationale that ER_{SOC} is influenced by crusting. For both soils used in this study, a cohesive structural crust and a depositional crust were formed (Figure 2-6). This pattern of crust formation follows the model developed by Chen et al. (1980). The loose particles forming the depositional layer were eroded once runoff started. This leads to a distinct pattern of soil erodibility during the simulation event: increasing until shortly after the runoff rate reaches maximum, and declining when the depositional layer is removed (Figure 2-3). The erodibility peaks shortly after the steady state runoff is achieved, because runoff becomes more competent and the preceding destruction of aggregates has produced a temporally unlimited supply of particles that can be eroded by raindrop impacted flow. The erodibility peak was less pronounced and delayed on the OS compared to the CS (Figure 2-3). Such differences are attributed to the greater aggregate stability of the OS (Table 2-1), which leads to slower aggregate breakdown (Figure 2-8), less erodible particles, slower crusting, and less runoff (Barthes and Roose, 2002; Le Bissonnais et al., 2005; Singer and Le Bissonnais, 1998).

The ER_{SOC} showed a similar pattern: increased first, peaked around when steady state runoff conditions were obtained, and declined afterwards (Figure 2-4). We attribute this pattern to the depletion of SOC in source soil induced by the effect of crusting on selectivity of erosion. At the end of the rainfall event, texture and SOC content of the soil and sediment did not differ for CS (Figure 2-8). This indicates that erosion was non-selective, and therefore soil and sediment also had the same SOC content, i.e. ER_{SOC} of 1. Schiettecatte et al. (2008) also observed ER_{SOC} equal to 1 on a silt loam when unit sediment discharge exceeded a certain rate (1.7 $g \cdot s^{-1} \cdot m^{-1}$). They attributed this to the decreasing selectivity of the erosion process at greater sediment transport rates. We speculate that in our study at the beginning of

interrill erosion the soil surface consisted of a mixture of aggregates of various sizes, promoting selective erosion of small and light particles. As indicated by the high SOC concentration in small-sized aggregates in the original soils (e.g. < 20 μm in Figure 2-1) as well as in eroded sediment (data not published), sediment enriched in small-sized aggregates was also likely enriched in SOC. This explanation is consistent with the observation by Schiettecatte et al. (2008).

Kuhn and Armstrong (2012) also reported selective erosion of fine particles from a sandy soil. However, in their study a non-erodible sandy layer was developed on the surface, armoring the lower lying soil, and thus preventing the achievement of non-selective erosion. In the end, provided no supplement from adjacent areas or litter input, interrill soil and SOC erosion eventually declined to zero. On the soils used in this study, aggregate destruction continued as the rainfall proceeded. Therefore, the particles forming the depositional crust became finer, while erosivity increased with higher runoff. As a consequence, erosion was increasingly non-selective and ER_{SOC} declined over time again. This declining trend suggests that the ER_{SOC} in sediment must be balanced over time by a decrease of SOC in the source area material. It further implies that scaling the ER_{SOC} obtained from short rainfall events up to overall SOC erosion may be misleading. Similar declining pattern of ER_{SOC} over time was also observed by Polyakov and Lal (2004b) on both the erosional and depositional positions on a 4 m long slope. Although the temporal variation of ER_{SOC} observed in our study apply, in strict sense, only to laboratory conditions (without effects of drying, vegetation growth and pronounced roughness elements), they point to the necessity of assessing the degree of crust formation in the field, so as to determine the relevance of crusting for ER_{SOC} under more complex natural conditions.

The effect of soil management practices on crusting also affected SOC. The SOC concentration in the runoff of the OS was greater than on the CS (9.6 vs. 6.6 $mg \cdot mm^{-1}$, Table 2-2). While such a difference in concentration reflects the SOC of the two soils (16.9 $mg \cdot g^{-1}$ of CS vs. 10.9 $mg \cdot g^{-1}$ of OS, Table 2-1), it does not correspond to the observed total soil erosion of 16.1 g from OS and 27.4 g from CS (Table 2-2). . As a consequence, total SOC loss from the OS (326.0 mg) was only slightly lower than from the CS (369.1 mg) (Table 2-2). Overall, the loss of SOC from the OS is greater than its lower soil erodibility would suggest, highlighting the necessity to include the effect of crusting, which is often ignored in current SOC erosion modeling, into the assessment of SOC erosion. We attribute the difference in erosional response of CS and OS to the stronger aggregation on the OS, which delayed the crust formation. This reduced, but stretched the peak of ER_{SOC} compared to the CS (Figure 2-4).

2.5. Chapter conclusion

Interrill erosion, due to its universal occurrence, location at the soil-atmosphere interface and the assumed preferential erosion of SOC, potentially plays a great role in global carbon cycling (Kuhn et al., 2009). The enrichment of SOC in interrill sediment observed in several studies is thus a potentially crucial parameter to assess soil-climate interaction, as well as off-site impacts of interrill erosion to water courses. However, ER_{SOC} of sediment is temporally variable as a consequence of crust formation and erosion. Conservation of mass also questions the use of a quasi-constant average (annual) value of ER_{SOC} of sediment to estimate the carbon erosion for a prolonged erosion time. ER_{SOC} of sediment must be balanced over time by a decline of SOC in the source area material. Therefore, extrapolation of enrichment ratios of organic carbon (ER_{SOC}) obtained from short rainfall events up to overall SOC erosion may bear non-ignorable errors. The results of this study confirm these risks by illustrating that ER_{SOC} is closely related to the duration of rainfall events and the associated extent of crust formation and erosion.

While the prolonged rainfall (6 hours) applied here is very limited in its feasibility under natural conditions, the temporal variation of ER_{SOC} of sediment proves that ER_{SOC} is dependent on the degree of crust formation and interrill erosion during the period when the soil is vulnerable to erosion by raindrop impacted flow. Comparing our results with other observations (Kuhn and Armstrong, 2012; Polyakov and Lal, 2004b; Schiettecatte et al., 2008) on ER_{SOC} dynamics caused by crusting, we observe two basic patterns: 1) particles at the surface eventually become small enough for non-selective transport due to continuous aggregate breakdown, so that ER_{SOC} will achieve unity; or 2) The erosion remains selective and a non-erodible layer (e.g. armored by crust or by over-sized particles) is formed at the surface. In this case, provided that no supplement from adjacent areas occurs, interrill and SOC erosion will eventually decline to zero. For both scenarios, a "constant" ER_{SOC} of sediment is biased, leading to an overestimation of SOC erosion unless ER_{SOC} was determined for the entire crust formation. This conclusion applies in strict sense only to laboratory conditions without effects of drying, vegetation growth and pronounced roughness elements. Observations in the field are now required to determine the relevance of crusting for ER_{SOC} under more complex natural conditions. Nonetheless, the results of our study show the need for assessing the degree of crust formation in the field, both to ensure that rainfall simulation in the field reflects a typical degree of crust formation under given natural rainfall conditions and that monitoring covers the entire crusting process.

Chapter 3

Inter-Replicate Variability and Crusting-Induced Systematic Variability in Organic Carbon Erosion Modeling

Manuscript in preparation, planned to submit to *Journal of Soils and Sediments*

Abstract: Sediment generated by interrill erosion processes is often reported to be enriched in soil organic carbon (SOC). To assess SOC loss by erosion, the amount of eroded sediment is often multiplied with the average organic carbon content in the eroding soil and the average enrichment ratio of SOC in sediment. However, the complex interaction between rainfall, runoff and soil crusting renders SOC erosion is highly variable over time. Apart from the inherent variability of crust formation and soil erosion that may affect SOC enrichment, conservation of mass dictates that the enrichment ratio of SOC in sediment must be balanced over time by a decline of SOC in the source area material. The use of average enrichment values or values from short erosion events is therefore likely to generate a great uncertainty in estimating SOC loss over longer events. Similar errors are also likely to occur if applying SOC erosion data based on current rainfall characteristics to estimate SOC loss in the future with changing rainfall magnitudes.

To evaluate the relevance of inherent variability, crusting evolvement over time and the accordingly derived systematic variability to soil and SOC erosion, two silty loams were subjected to a simulated rainfall of 30 mm h^{-1} for 360 min. Runoff and soil erosion rates were recorded every 30 min. The whole rainfall event was repeated 10 times to enable statistical analysis of the variability of the erosional response. Two-step erosion models were developed based on the infiltration, runoff and soil erosion data obtained from six selected event durations: 60, 120, 180, 240, 300 and 360 minutes. The results show that: i) the enrichment ratios of SOC dropped to unity or even below 1 during prolonged crusting, confirming that preferential erosion is limited by depletion of SOC on the eroding soil surface; ii) the inter-replicate variability of runoff and soil erosion rates considerably declined over rainfall time. Yet, even after maximum runoff and erosion rates were reached, the inter-replicate variability still remained between 15 and 39%, indicating the existence of significant inherent variability; and iii) the increasingly improved predictions with extending event durations suggested that observations from short events cannot be directly extrapolated to predict soil and SOC loss over longer events, and vice versa.

Keywords: *interrill erosion, soil organic carbon enrichment, inherent variability, systematic variability*

3.1. Introduction

Soil erosion by water is strongly influenced by rainfall characteristics and thus potentially affected by climate change (Moore and Singer, 1990a; Parson and Abrahams, 1992; Wang et al., 2012; Wan et al., 2013). Runoff and erosion generally occur within the domain of one or two processes: non-concentrated and raindrop-impacted sheet flow, or concentrated flow with sufficient shear forces to incise into rills. Both processes, in sequence, involve the effects of raindrop impact, wetting, soil resistance to erosion (erodibility) and the erosivity of the flow (Govers and Poesen, 1988; Kimaro et al., 2008). During a rainfall event, the soil surface is affected by the temporal pattern of infiltration, runoff erosivity and soil erodibility. One of the most obvious changes of a soil surface during a rainfall event is the crusting process. Crust formation not only alters the surface roughness, infiltration, runoff speed and runoff erosivity (Moore and Singer, 1990a; Kuhn et al., 2003), but also affects the abundance of depositional particles, selective entrainment and transport of depositional particles, as well as the SOC erosion over rainfall time (Kuhn and Armstrong, 2012; Hu et al., 2013a). In this study, all the processes influencing soil surface changes are summarized as crusting. However, current findings on soil and SOC erosion in the literature discussed above have often been observed on a wide range of soils under relatively tight patterns of rainfall conditions, without adequately accounting for the potential effects of crusting over time (Bryan and de Ploey, 1983; Agassi and Bradford, 1999; Iserloh et al., 2013). The results of such tests are useful, when comparing the reaction of a soil to a "standard" stress. But they provide only a snapshot out of all possible soil and rainfall scenarios. Such snapshots may therefore not be reliable to predict the reaction of soils to a wider range of naturally occurring rainfalls, let alone the rainfall scenarios of future climate and land use (Meyer, 1994).

The problem of inadequately accounting for the potential effects of crusting over time also extends to the quality of eroded sediments (Palis et al., 1990; Kinnell, 2012), particularly those from selective interrill erosion. Although on-site soil loss by interrill erosion is many times smaller than that from rill erosion when both occur at the same eroding site, it literally affects all arable land (globally, 14.2 million km^2) (Kuhn et al., 2009). Due to limited raindrop kinetic energy and lack of concentrated runoff, interrill erosion is associated with selective entrainment and transport of sediment (Parson and Abrahams, 1992). As a consequence, fine and / or light particles and associated substances (e.g., soil organic carbon, phosphorus and nitrogen) are entrained and transported away from eroding sites in greater proportions than their concentration in the source soil suggests. The eroded sediment is thus generally enriched in substances, such as SOC (Sharpley, 1985), phosphorous (Quinton et al., 2001), nitrogen (Teixeira and Misra, 2005) and clay (Warrington et al., 2009), when compared to the source soil. Overall, between 0.57 and 1.33 Pg C yr^{-1} may be affected by interrill erosion, potentially influencing global carbon cycling (Kuhn et al., 2012). The delivery of SOC-enriched sediments into wetlands and water courses can also

have profound off-site impacts (Lal, 2003). However, most of the recently published data on selective interrill erosion (reviewed by Kuhn and Armstrong, 2012) show only snapshots of SOC enrichment in eroded sediment, namely reactions to a particular rainfall out of complete crust formation. While most studies report a positive enrichment of SOC in interrill sediment, the enrichment ratios of SOC (ER_{SOC}) varies largely in the literature, ranging from 1.0 to 6.2 (Sharpley, 1985; Polyakov and Lal, 2004b; Kuhn, 2007; Schiettecatte et al., 2008). Discrepancies are attributed to soil properties, such as texture, aggregation, initial SOC content or initial soil moisture (Heil et al., 1997; Ramos et al., 2000; Kuhn and Bryan, 2004; Darboux and Le Bissonnais, 2007; Kuhn and Armstrong, 2012), as well as to rainfall intensities, kinetic energy, duration (Palis et al., 1990; Jacinthe et al., 2004; Martínez-Mena et al., 2012) and, finally, to diverse local micro-topography and deposition processes (Le Bissonnais et al., 2005; Kuhn, 2010b).

Apart from the influences of soil properties, rainfall properties and local micro-topography, some of the uncertainties on SOC erosion prediction are introduced by extrapolating constant or average SOC enrichment ratio to long-term or large-scale SOC erosion. The practical limitations of using one enrichment value for SOC in sediment are questioned from a theoretical point of view: conservation of mass dictates that perpetual enrichment is not possible. Polyakov and Lal (2004b), Schiettecatte et al. (2008), as well as Kuhn and Armstrong (2012) observed decreasing ER_{SOC} in sediment after certain rainfall durations. This is in accordance with the conservation of mass, which dictates that the observed enrichment of particles must be a non-steady-state phenomenon (Kinnell, 2012). Failure to recognize this among other factors may lead to overestimating the loss of organic carbon, fine mineral particles, nutrients and other chemicals when soil is eroded by interrill processes (Kinnell, 2012; Kuhn and Armstrong, 2012). Ignoring crust-induced temporal variation of ER_{SOC} is also likely to introduce systematic variability when comparing SOC erosion observed from rainfall events of distinct durations. However, such systematic variability has not been adequately accounted for in current erosion models.

The potential variability between replicates also questions the accuracy of using an average ER_{SOC} to assess SOC erosion. Major variability between replicates caused by differences in soil properties, rainfall conditions or plot set-up has been extensively discussed (Agassi and Bradford, 1999). The interrill erosion processes are also very sensitive to minor interactions between the raindrop impact angle, speed, and size of individual raindrops (Agassi and Bradford, 1999), the characteristics of particle units resulting from aggregate breakdown (Le Bissonnais, 1990), the changes of surface roughness (Anderson and Kuhn, 2008), as well as initial soil moisture (Le Bissonnais et al., 1995; Heil et al., 1997). Uncertainties coming from these sources are inherent in erosion processes, which are impossible or very difficult to eliminate even under ideal experimental conditions (Bryan and Luk, 1981; Wendt et al., 1986; Nearing et al., 1999; Hu et al., 2013a). Such uncertainties hereafter are termed as inter-replicate variability. In addition, the

significance of inter-replicate variability on runoff rates has been reported to differ from that on soil erosion rates, respectively up to 75% and 35% in Luk and Morgan (1981), while up to 105% and 173% in Rüttimann et al. (1995). This may imply a different extent of variability on SOC erosion rates than on runoff or soil erosion rates, as SOC erosion involves more factors, such as SOC distribution in eroded sediment, SOC characteristics in the particle units resulting from aggregate, and availability of SOC fractions during crusting. However, the significance of inter-replicate variability on SOC erosion has not yet been systematically investigated.

The aims of this paper are therefore: 1) to capture the temporal variation of SOC erosion, and then evaluate the effects of the accordingly derived systematic variability onto SOC erosion prediction; 2) to identify the significance of the inherent complexity of interrill erosion processes onto the inter-replicate variability of SOC enrichment in eroded sediment; and 3) to assess the risk of linearly scaling models developed from current rainfall characteristics up to predict the SOC erosion under climate conditions in the future.

3.2. Materials and Methods

3.2.1. Soil samples and preparation

Two silty loams from Möhlin (47˚ 33’ N, 7˚ 50’ E) near Basel, Switzerland, one from the conventionally managed (CS) Bäumlihof Farm and the second from the organically managed (OS) Eulenhof Farm, were used in this study. The conventionally managed farm has planted crops over decades, and has been applied chemical fertilizer and plowed at least once a year (Table 3-1). Meanwhile, the organically managed farm mainly plants vegetables and applies only organic fertilizer (Table 3-1). Soil of A-horizon (about 100 kg for each) from a gentle shoulder slope (< 5%) was sampled in April 2010 on each farm. Previous research conducted in the region of Möhlin showed that the silty loams used in this study are likely to experience non-selective erosion, as raindrop-impacted flow is sufficiently competent to remove all the transportable materials (Hu and Fister, 2011). The two soils were of almost identical texture (wet-sieving after dispersion by 1% Sodium hexametaphosphate), but different in SOC content (LECO RC 612 at 550 ˚C), and aggregate stability (method adapted from (Nimmo and Perkins, 2002)). Therefore, their similarity in texture but unalike aggregation was thus considered suitable to observe the differences on crusting, as well as to ensure that during the rainfall simulation the presumed decline of ER_{SOC} in eroded sediment would occur (Hu et al., 2013a).

Table 3-1 Texture, percentage of stable aggregates greater than 250 µm, soil organic carbon concentration (SOC), and tillage management of conventionally farmed (CS) and organically farmed (OS) silt loams. Different superscripted letters in each column indicate the significant differences (P <= 0.05, T-test). The subscripted numbers after each average value show the standard deviation (n=10).

	Clay (%)	Silt (%)	Sand (%)	Stable aggregates greater than 250 µm (%)	SOC ($mg \cdot g^{-1}$)	Tillage operation	Rotation	Fertilizer
CS	$16.80^{a}{}_{1.38}$	$71.47^{a}{}_{1.76}$	$11.50^{a}{}_{1.00}$	$66.85^{a}{}_{0.47}$	$10.9^{a}{}_{0.05}$	Plowing (at least once a year) together with other tillage operations	Maize, rape, wheat, grass	Chemical fertilizer and manure
OS	$14.39^{b}{}_{0.52}$	$75.84^{b}{}_{0.56}$	$9.77^{b}{}_{0.38}$	$77.76^{b}{}_{1.87}$	$16.9^{b}{}_{0.10}$	Non-plowing, harrowing	Pumpkin, carrot, salad, pea, bean	Sheep manure, horn shavings

After sampling, the two soils were dried at 40 ˚C until constant dry weight was reached and then sieved to 1 to 8 mm. Excluding over-sized clods largely reduced the variation of surface roughness both within each flume and between replicates, ensuring the dominance of interrill erosion processes in the results rather than the differences in initial roughness. Then, dry soils were placed in a round flume with an outside diameter of 50 cm and a center opening of 10 cm. These flumes were designed to limit the effect of increasing flow length and thus depth on interrill erosion, as well as to ensure a sufficiently large area to generate sediment for sampling and further analysis. The soils rested on the sand and were molded into a straight slope of 10% between the outer and inner rim. Preliminary tests had shown that slight soil compaction/settlement via pre-wetting was necessary to ensure that once subjected to rainfall, soils would not to sink below the center rim and hence block the transportation path. Besides, preliminary tests also indicated that achieving a crust with constant runoff on such dry silt loams required more rainfall than that could feasibly be applied during one day. Therefore, a 30 min rainfall of 30 mm h^{-1}, corresponding to the intensity used for the actual test, was applied one day prior to the simulation event. This short pre-wetting, on one hand, enabled the observation of the effects on aggregate breakdown during crusting process; on the other, induced an initial crusting and soil settling, which facilitated the faster runoff development during the actual test.

3.2.2.Rainfall simulation

Two flumes, one of each filled with CS and OS (Figure 3-1), were simultaneously exposed to a simulated rainfall of 30 $mm \cdot h^{-1}$ for 360 min (in total about 180 mm of rainfall). An event precipitation of 180 mm is not a frequent phenomenon in the region of Möhlin. The monthly precipitation during April, May and June (corresponding to periods with bare soil after tillage) varied widely over the past three decades (Figure 3-2), ranging from 6 to 241 mm (MeteoSwiss, 2013). Preliminary tests and field observations had shown that the two silty loams used in this study required between 90 and 120 mm rainfall (i.e. 180 and 240 min) to complete crust formation, and roughly 180 mm rainfall (i.e. 360 min) to develop the presumed decreasing SOC erosion rates (Hu and Fister, 2011). The return period of such

monthly rainfall is 0.65 years for 90 mm, 1 year for 120 mm, and 7 years for 180 mm. The selected rainfall, therefore, was suitable to observe all the potential effects of prolonged crust formation onto the variability of erosional response that would possibly be experienced by the soil in the region of Möhlin, except for the effects of drying between rainfall events. Drying is likely to rejuvenate the granular structure of the crust (Kuhn and Bryan, 2004); however, the effects of drying on ER_{SOC} are unknown. Ignoring the drying effect does not limit the objective of this study which aimed at testing the sensitivity of ER_{SOC} to inter-replicate and systematic variability in principle (likewise stated in Hu et al., 2013a).

Figure 3-1 Conventionally farmed soil (CS) and organically farmed soil (OS) in round flumes were simultaneously subjected to simulated rainfall. The white boxes were used to monitor the rainfall intensity. This picture was also presented in (Hu et al., 2013a).

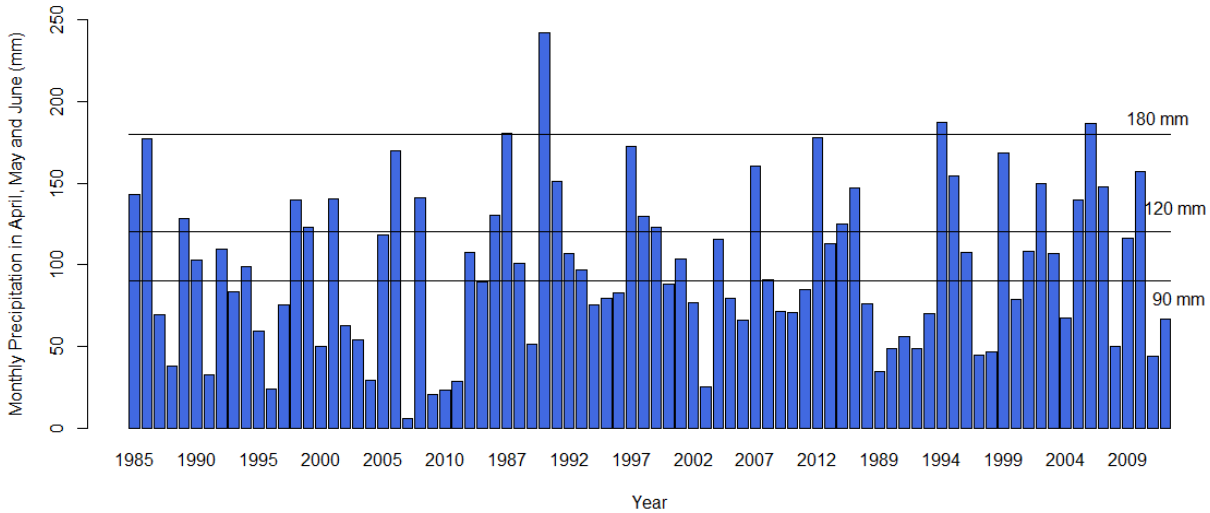

Figure 3-2 Monthly total precipitation during April, May, and June in the region of Möhlin over the past 28 years. Three lines mark the monthly precipitation of 90 mm, 120 mm and 180 mm, respectively. Data source: Station Arisdorf (47°30' N, 7°46' E, the closest climate station near Möhlin, Switzerland), MeteoSwiss, Federal Office of Meteorology and Climatology, Zürich, Switzerland.

A FullJet nozzle (¼HH14WSQ), installed 2 m above the soil surface, was used to generate multiple-sized raindrops (D_{50} of 2.3 mm). The rainfall intensity was measured every 30 minutes by monitoring the rainfall amount collected in four gauges (area: 0.1 m × 0.1 m) that were placed on the four corners of each flume (Figure 3-1). Kinetic energy of raindrops was detected by a Joss-Waldvogel-Distrometer (average energy of 113.9 $J \cdot m^{-2} \cdot h^{-1}$). The preliminary tests had showed that the nozzle used in this experiment was by nature apt to produce spatially varying raindrop distribution. Therefore, the two soils were alternatively placed on the left and right positions for five times (positions as noted in Figure 3-3). This manner ensured that the any distinct patterns observed in erosional responses were reflecting the actual differences in soil properties between CS and OS, rather than being misled by the persistent spatial variation of rainfall properties. However, doing so may, as a side effect, introduce extra inter-replicate variation within each soil. In order to minimize such variation, strict operations were carried out with greatest care, such as identical preparation for each replicate, application of the rainfall with accurate pressure, and precise installation of the cleaned and dried nozzle with the same orientation. Numerically, the spatial variability of the rainfall intensity within each flume was ≤ 5%, and that of the kinetic energy was about 15%. Such spatial variability persisted in the same pattern between different replicates, leading to low inter-replicate variability of rainfall intensity and kinetic energy on the same position (Figure 3-3, Table 3-2). Moreover, in order to provide the most constant conditions practicably achievable in laboratory, all the experiments were conducted by the same operator using the same flumes.

3.2.3. Soil and sediment analysis

During the simulation events, all the runoff and sediment discharges were sampled in intervals of 30 min. Sampling at intervals of 30 min produced enough runoff and sediment for further analysis and also enabled to record the temporal changes of the erosional response. The runoff samples were weighed immediately after collection to record the amount of discharge. After the simulation events, sediments in all runoff samples were allowed to settle for 48 h. The supernatant was then decanted off, and the sediments were dried at 40 ˚C and weighed. Soil organic carbon concentration of original soils and eroded sediment were measured by a LECO RC 612 at 550 ˚C. The enrichment ratio of SOC (ER_{SOC}) was calculated between the SOC concentration of eroded sediment and original soil (as described in Hu et al., 2013a).

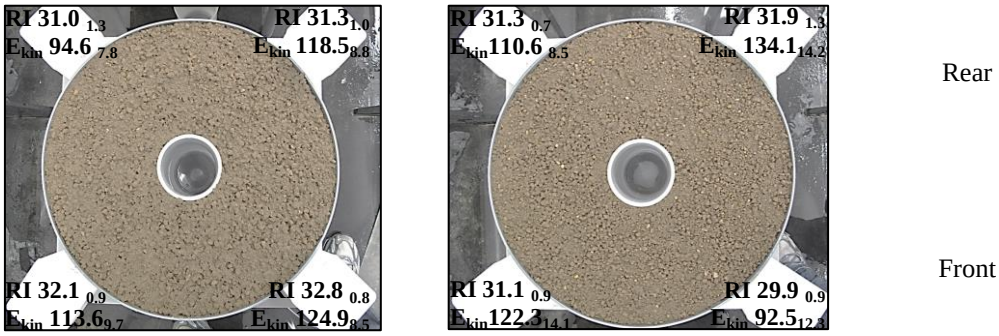

Figure 3-3 The spatial distribution of rainfall intensity (RI, $mm \cdot h^{-1}$) and kinetic energy (E_{kin}, $J \cdot m^{-2} \cdot h^{-1}$) in the area of the two round flumes centered by the position of nozzle. Lower base numbers indicate the standard deviation at each corner between 10 replicates.

Table 3-2 The correlations of runoff and erosion rates with the spatial distribution of rainfall intensity (RI) and kinetic energy (E_{kin}). Values in the table represent the Pearson product-moment correlation coefficient (*r*). For conventionally farmed soil (CS), only runoff and erosion rates after 180 min were processed (n = 70), and accordingly the critical value of *r* is 0.235 at significance level of 0.05 for a two-tailed test. For organically farmed soil (OS), only runoff and erosion rates after 240 min were processed (n = 50), and accordingly the critical value of *r* is 0.279 at significance level of 0.05 for a two-tailed test. The shaded values indicate the significant correlations at significance level of 0.05 for a two-tailed test.

Correlation coefficient (*r*) of Pearson product-moment		**Rainfall intensity (RI)**					**Kinetic energy (E_{kin})**				
		Front Left	**Front Right**	**Rear Left**	**Rear Right**	**Average of four corners**	**Front Left**	**Front Right**	**Rear Left**	**Rear Right**	**Average of four corners**
CS (n=70)	Runoff	0.123	0.403	-0.078	-0.183	0.127	0.420	0.497	-0.414	-0.142	0.319
	Soil Erosion	0.245	0.501	-0.060	-0.309	0.165	0.233	0.658	-0.478	-0.381	0.159
OS (n=50)	Runoff	0.426	0.531	-0.058	0.045	0.503	-0.419	0.520	-0.509	-0.458	-0.121
	Soil Erosion	0.158	-0.018	-0.031	0.118	0.078	0.381	-0.062	0.166	0.080	0.335

3.2.4. Variability analysis

Analysis of inter-replicate variability by ten replicates

The whole rainfall simulation experiment was repeated 10 times (two pairs of flumes used for 5 times) to generate a large enough data set to enable the statistical analysis of the variability of erosional response. Generally, greater numbers of replicates improve the accuracy of erosion data, especially when erosion loss is relatively small (Nearing et al., 1999). Ten replicates were thus considered as a compromise between being sufficient to obtain reliable statistics and being feasible to be conducted (Bryan and Luk, 1981; Rüttimann et al., 1995). The coefficient of variation (CV), i.e., the standard deviation divided by the mean value, was applied to evaluate the inter-replicate variability of rainfall intensity, kinetic energy, runoff rates, erosion rates and ER_{SOC}. Since the coefficient of variation (CV) is independent of

measurement units, the inter-replicate variability (i.e., CV) of the above-mentioned parameters can be directly compared.

Analysis of systematic variability of soil erosional response by erosion modeling

In order to assess the relevance of crusting-induced systematic variability to predict erosional response and SOC erosion, the entire rainfall event (360 min) was divided into six sub-events with increasing durations: 60, 120, 180, 240 and 360 min. Erosion data from the beginning (i.e. 0 min) up to the end of each of the six sub-events were used to develop models for runoff, soil erosion and SOC erosion. Six sets of models were then respectively extrapolated to estimate the erosional response of the entire 360 min event. All the modeling and statistical analyses were carried out by R Studio software packages (R version 2.15.1).

The modeling comprises two steps (Figure 3-4): first, an infiltration model was developed based on the regression between the measured runoff and rainfall time (Eq. 3-1).

$$\boldsymbol{I_t = a * e^{-dt}} \quad \text{Eq. (3-1)}$$

Where, I_t = infiltration rate (mm·h^{-1}) at time t, t = erosion time (min), a = constant value depending on the initial and final infiltration rate, d = infiltration decay factor. The best-fitted exponential curve (Eq. 3-1) from each sub-event was then applied to predict infiltration and in turn runoff rates over the entire 360 min event: Afterwards, *r* was used to represent the coefficient of determination of the infiltration model from each sub-event. *R* indicates how well the predicted runoff rates match the measured values by pairwise comparison.

The second step involved developing a model for soil erosion based on the regression between the measured runoff and measured soil erosion rates during each sub-event (Figure 3-4).

$$\boldsymbol{q_{soil} = k * q_{runoff}^{\ s}} \quad \text{Eq. (3-2)}$$

Where, q_{soil} = soil erosion rate (g·m^{-2}·h^{-1}), q_{runoff} = runoff rate (mm·h^{-1}), k = constant factor for erodibility, s = constant factor for runoff erosivity. The best-fitted power function from each sub-event (Eq. 3-2) was driven by the previously predicted runoff rates (from Eq. 3-1) to predict the soil erosion rates over the entire 360 min event. The same as for runoff rates, *r* was used to represent the coefficient of determination of erosion model from each sub-event, and *R* was to indicate how well the predicted soil erosion rates match the measured values by pairwise comparison.

Analysis of systematic variability of SOC erosion by erosion modeling

The SOC erosion rates were computed by multiplying the predicted soil erosion rates with the measured ER_{SOC} and the soil original SOC content at each runoff collection interval (Figure 3-4). The total SOC losses from the entire rainfall events were calculated by summing up the SOC loss from all intervals.

The systematic variability of SOC erosion induced by crusting evolvement over time can then be evaluated by comparing the measured SOC erosion with the SOC erosion predicted by models developed from the six sub-events (Figure 3-4). Such modeling approach (Figure 3-4), although not exquisite, serves well enough to capture the relevance of crusting-induced systematic variability to soil and SOC erosion. Where other erosion scenarios are of interest, different models should be developed accordingly (Agassi and Bradford, 1999).

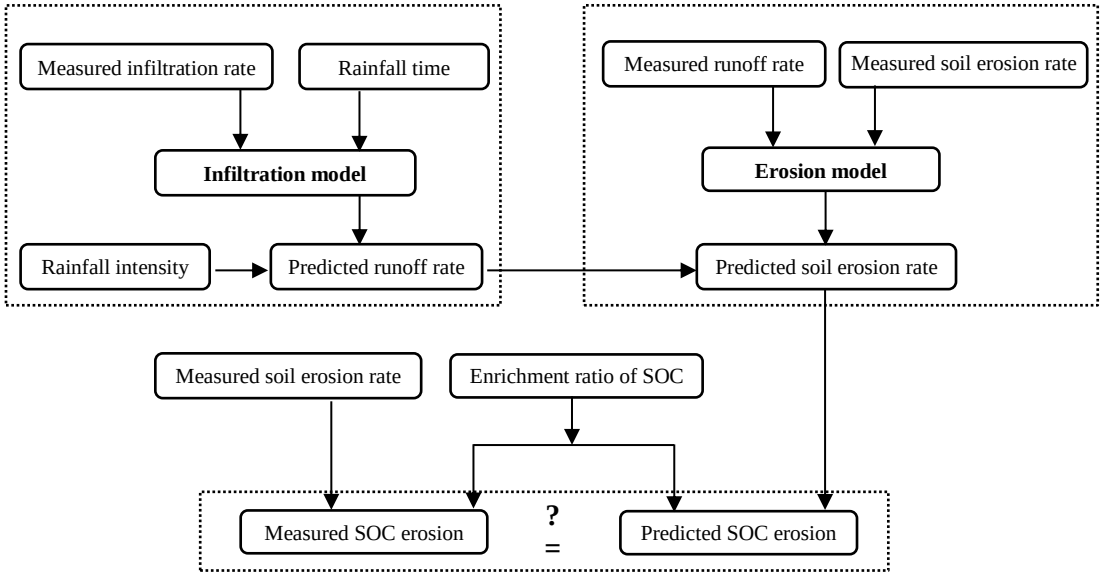

Figure 3-4 Flow chart of the modeling procedure. The box on upper left represents the package of the infiltration model. The dash-lined box on upper right represents the package of the erosion model. The dash-lined box at bottom represents the outcomes of the whole modeling process.

3.3. Results

3.3.1. Soil erosional responses over rainfall time

Runoff and soil erosion on the conventionally managed soil (CS) responded more pronounced and rapidly than on the organically managed soil (OS) (Figure 3-5a, b, c, d). The runoff started after 60 min for the CS and 120 min for the OS, then increased and achieved steady state after 180 min for the CS and 240 min for the OS (Figure 3-5a, b). The soil erosion rates for the CS peaked around runoff steady state and slightly decreased afterwards (Figure 3-5c), whilst the soil erosion rates for the OS roughly maintained steady until the end of the rainfall event (Figure 3-5d). The declining trend of soil erosion rates on the CS from 300 to 360 min (Figure 3-5c), as opposed to the steady runoff rates (Figure 3-5a), reflects the depletion of erodible materials. The ER_{SOC} on both soils increased at first, peaked around the achievement of runoff steady state, and declined afterwards (Figure 3-5e, f). This indicates that preferential erosion of SOC depends on the extent of crusting and the associated aggregate breakdown

over rainfall time (Hu et al., 2013a). It also highlights the deficiency of applying one average or annual ER_{SOC} to assess SOC erosion over longer events.

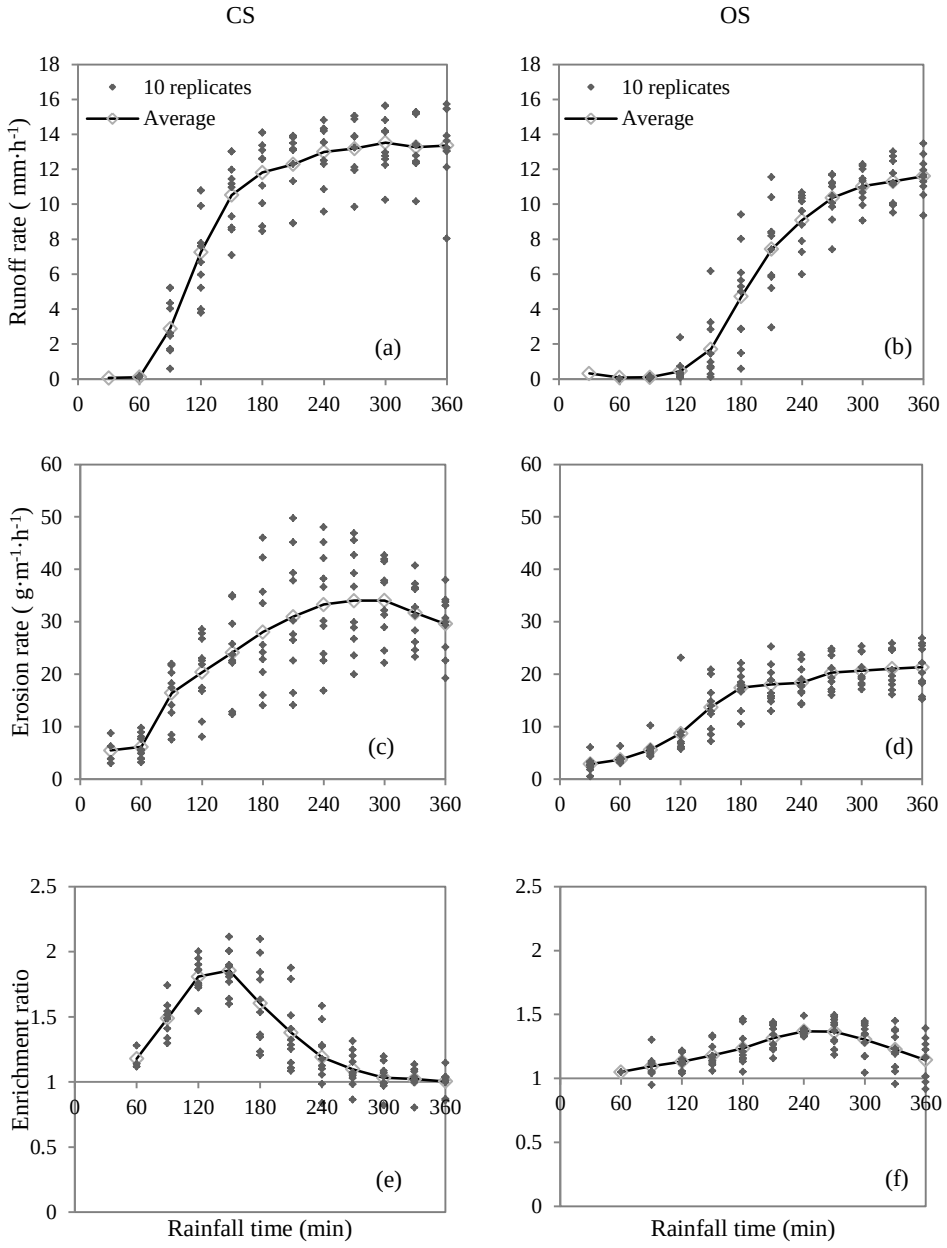

Figure 3-5 Comparisons between conventionally farmed soil (CS) and organically farmed soil (OS) over 360 min of rainfall in terms of runoff rates of 10 replicates and their average (a, b), erosion rates of 10 replicates and their average (c, d) and ERSOC of 10 replicates and their average (e, f).

3.3.2. Inter-replicate variability

The inter-replicate variability (coefficient of variation, CV) of runoff rates as well as soil erosion rates considerably decreased with rainfall time for both the CS and the OS (Figure 3-6a, b). At the beginning of the rainfall events, the inter-replicate variability of the runoff rates was high up to 82% for

the CS and 163% for the OS. But they kept declining to 18 and 17%, until the runoff rates reached maximum (around 180 min for the CS and 240 min for the OS) (Figure 3-6a, b). The inter-replicate variability of soil erosion rates experienced a similar trend but with smaller differences, decreasing from 48 to 39% for the CS, and from 51 to 18% for the OS (Figure 3-6a, b). However, even with 10 replicates under the most ideally controlled laboratory conditions, the lowest achievable inter-replicate variability of runoff rates and soil erosion rates in this study still remained as high as 12 to 19% for the CS, and 9 to 15% for OS (Figure 3-6a, b). Relatively, the inter-replicate variability of ER_{SOC} did not vary that much over time (Figure 3-6a, b), ranging between 8 and 20% for the CS, 7 and 27% for the OS.

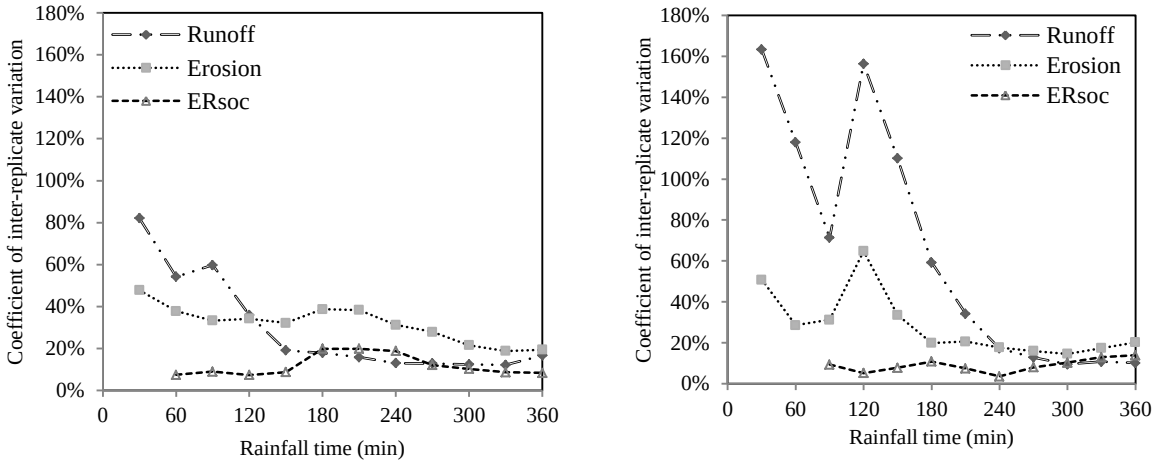

Figure 3-6 Variability (coefficient of variation) of runoff rates, variability of erosion rates and variability of ER_{SOC} of (a) conventionally farmed soil (CS) and (b) organically farmed soil (OS) over 360 min of rainfall.

3.3.3. Prediction of erosional response by models

Results of the infiltration and erosion models are presented in Table 3-3 and Table 3-4. The infiltration decay factors (d) for the CS increased first when the sub-events extended from 60 to 180 min, and then declined when the sub-event durations prolonged from 180 to 360 min (Table 3-3). Similar, but delayed and a lesser extent pattern, was also observed for the infiltration decay factor d on the OS (Table 3-3). In addition, the erodibility factor k increased with extending durations for both the CS and the OS (Table 3-4). A similar pattern was also observed for the runoff erosivity factor s (Table 3-4), illustrating the relevance of crusting evolvement over time to predict erosional response. Both the erodibility factor k and the erosivity factor s for the CS were greater than that for the OS for almost all the sub-events (Table 3-4).

In both the infiltration and erosion models, the r^2 (coefficient of determination of the modeling) increased with prolonging sub-event durations (Table 3-3 and 3-4), illustrating the improved modeling

efficiency. The R^2 of the pairwise comparison between the predicted and measured values also increased (Table 3-3 and 3-4), showing that the quality of model predictions was also improved with extending sub-event durations. However, even the best R^2 of soil erosion rates for the CS was rather low (only 0.257 from sub-events of 360 min) (Table 3-4), implying the existence of other elements than event durations affecting erosional response (e.g., the counterbalance between runoff erovisity and soil erodibility). Hu et al. (2013a) explained that the loose particles forming the depositional layer were eroded once runoff started, leading to a peak in soil erodibility shortly after the steady-state runoff was achieved. With the removal of the depositional layer, soil erodibility declined as runoff speed and thus erosivity increased.

Table 3-3 Parameters of infiltration models developed from six sub-events of different durations for the conventionally farmed soil (CS) and the organically farmed soil (OS). The r^2 represent the coefficient of determination of the infiltration models, and n mean the sample size for modeling. The R^2 indicate the coefficient of determination by pairwise comparison between the predicted and measured runoff rates, and N mean the sample size for pairwise comparison.

Duration of sub-events	CS					OS				
	Modeling			Pairwise comparison		Modeling			Pairwise comparison	
	Infiltration decay factor d	r^2	n	R^2	N	Infiltration decay factor d	r^2	n	R^2	N
60 min	1.9×10^{-5}	-0.056	20	-0.305	120	3.8×10^{-5}	-0.056	20	-0.698	120
120 min	2.9×10^{-3}	0.545	40	0.741	120	2.3×10^{-5}	-0.026	40	-0.675	120
180 min	3.5×10^{-3}	0.781	60	0.680	120	8.5×10^{-4}	0.298	60	-0.135	120
240 min	2.9×10^{-3}	0.790	80	0.726	120	1.7×10^{-3}	0.649	80	0.780	120
300 min	2.4×10^{-3}	0.762	100	0.719	120	1.9×10^{-3}	0.800	100	0.646	120
360 min	1.9×10^{-3}	0.702	120	0.596	120	1.7×10^{-3}	0.839	120	0.791	120

Table 3-4 Parameters of erosion models developed from six sub-events of different durations for the conventionally farmed soil (CS) and the organically farmed soil (OS). The r^2 represent the coefficient of determination of the erosion models, and n mean the sample size for modeling. The R^2 indicate the coefficient of determination by pairwise comparison between the predicted and measured soil erosion rates, and N mean the sample size for pairwise comparison.

Duration of sub-events	CS						OS					
	Modeling				Pairwise comparison		Modeling				Pairwise comparison	
	Erodibility factor k	Erosivity factor r	r^2	n	R^2	N	Erodibility factor k	Erosivity factor r	r^2	n	R^2	N
60 min	10.809	0.268	0.305	20	-0.471	120	2.296	-0.106	-0.002	20	-0.526	120
120 min	11.464	0.292	0.793	40	-0.296	120	6.281	0.123	0.045	40	-0.755	120
180 min	11.602	0.305	0.802	60	-0.175	120	10.264	0.282	0.512	60	0.733	120
240 min	11.907	0.325	0.788	80	0.066	120	10.176	0.279	0.644	80	0.716	120
300 min	12.114	0.339	0.792	100	0.230	120	10.233	0.281	0.703	100	0.731	120
360 min	12.130	0.342	0.796	120	0.257	120	10.269	0.283	0.729	120	0.739	120

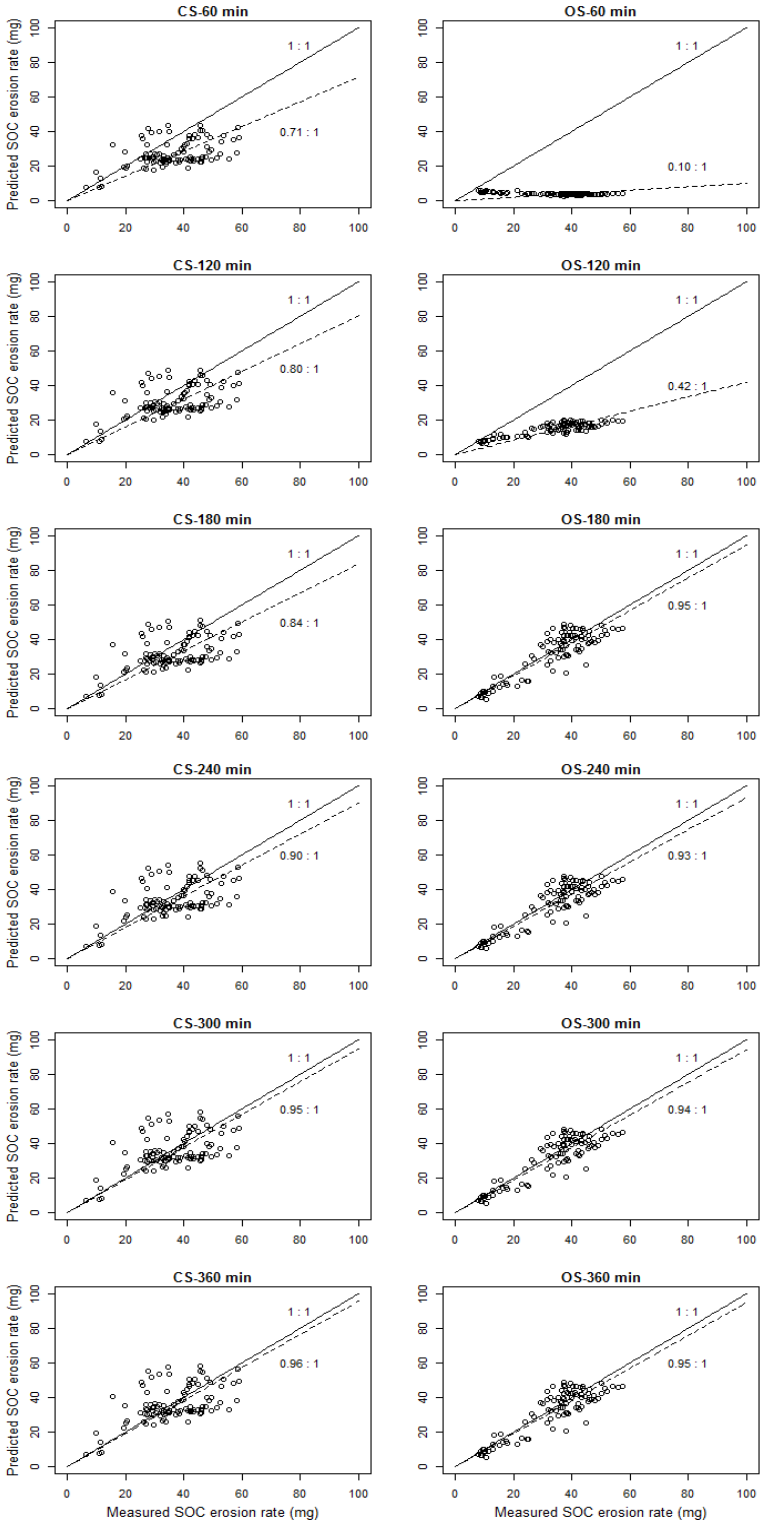

Figure 3-7 Comparison between the measured amounts of soil organic carbon (SOC) eroded from the entire event (360 min) and the amounts predicted by models based on six sub-events (60 min, 120 min, 180 min, 240 min, 300 min and 360 min) from conventionally farmed soil (CS) on the left and the organically farmed soil (OS) on the right. The black line right through the diagonal of each figure implies the 1:1 ratio of the predicted values to the measured values. The other dashed line represents the aspects of the regression lines (y intercept = 0) formed by the predicted values and the measured values.

3.3.4.Prediction of SOC losses by models

The quality of the prediction of SOC erosion rates was progressively improved with increasing sub-event durations (Figure 3-7). If the models were built on the data from the sub-events of 60 min, the SOC erosion rates would have been under-predicted by 30% for the CS, and even by 90% for the OS (see the aspects of the dash lines in Figure 3-7a and b). Considerable improvement on SOC erosion prediction occurred when the durations of sub-events exceeded 120 min for the CS (Figure 3-7c). Similar patterns were observed for the OS when the durations of sub-events were longer than 180 min (Figure 3-7). Similar to the measured ER_{SOC}, the predicted SOC erosion rates for the CS and the OS also showed temporal patterns over rainfall time (Figure 3-8a, b): increased first, peaked around the achievement of runoff steady state (after 180 min for the CS, and 240 min for the OS), and declined afterwards. Overall, the total amount of SOC losses predicted from six prolonging sub-event was progressively advancing towards the total amount of measured SOC losses (Table 3-5).

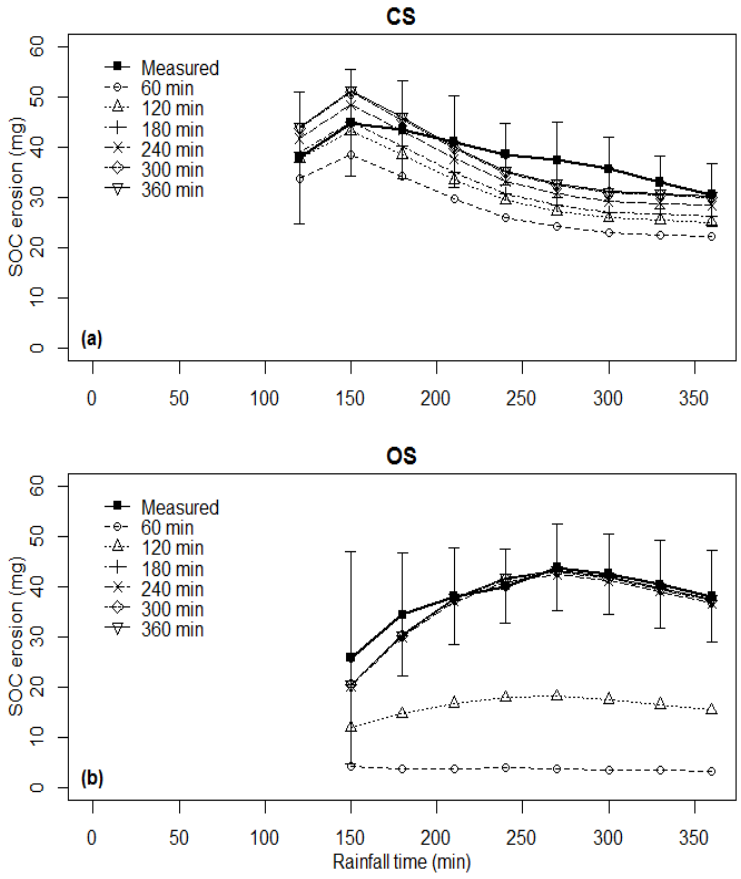

Figure 3-8 Comparison between the temporal pattern of the measured amounts of soil organic carbon eroded over the entire rainfall events (360 min), and the temporal pattern predicted by models based on six sub-events (60 min, 120 min, 180 min, 240 min, 300 min and 360 min). Figure on the left is from the conventionally farmed soil (CS) and figure on the right is from the organically farmed soil (OS). Error bars on the line of "Measured" indicate the standard deviations of 10 replicates.

Table 3-5 The comparison between measured total soil organic carbon loss over entire 360 min rainfall and the predicted loss by models of six different durations (60 min, 120 min, 180 min, 240 min, 300 min and 360 min) for the conventionally farmed soil (CS) and the organically farmed soil (OS).

Soil	Total soil organic carbon loss (mg)						
	Measured	60 min	120 min	180 min	240 min	300 min	360 min
CS	342.67	254.50	286.35	298.64	321.78	338.72	341.66
OS	303.36	30.46	129.22	292.35	287.70	290.90	292.99

3.4. Discussion

3.4.1. Inter-replicate variability introduced by inherent complexity of interrill erosion

The existence of high inter-replicate variability of runoff and erosion rates clearly demonstrates the significance of the inherent variability in affecting interrill erosion (Figure 3-6). The inter-replicate variability declined over time primarily because the numerically increasing runoff and erosion rates (Figure 3-5) lead to a decreasing ratio of the standard deviation to the mean value. Therefore, as a result of the barely detectable runoff and erosion rates at the initial stage (Figure 3-5a, b, c, d), the inter-replicate variability of erosional response was fairly high before 90 min for the CS and 150 min for the OS (Figure 3-6). Nevertheless, even after runoff and erosion rates reached the maximum values (after 180 min for the CS and 240 min for the OS), the inter-replicate variability still remained 10 to 18% for runoff rates, and 15 to 39% soil erosion rates (Figure 3-6a, b). About 5 to 10% of such inter-replicate variability can be explained by the spatial and inter-replicate variation of the applied rainfall (Figure 3-4, Table 3-2). But there still remained 5 to 29% inter-replicate variability unexplained. Similar unexplained variability was also reported by Bryan and Luk (1981) and Wendt et al. (1986). They attributed it to the minor variables in interrill erosion process, such as changes aggregate size on the soil surface, micro-relief and aggregate stability. Armstrong et al. (2011) also reported that interrill soil erosion of a silt loam at low slopes is highly variable, and attributed it to variation in soil properties, variable surface sealing and connectivity controlled by the micro-topography. The relevant dominance of these factors is impossible or very difficult to determine, as they are interrelated and cannot be controlled independently. The high inter-replicate variability of erosional response in this study confirms such conclusion, and proves the existence of inherent complexity of interrill erosion processes even under sophisticated experiment conditions. Such inherent complexity could be even more significant on natural field, where far more complicated factors are involved to affect the inter-replicate variability in soil erosion data (Wendt et al., 1986; Rüttimann et al., 1995; Nearing et al., 1999).

3.4.2. Systematic variability induced by crusting development over rainfall time

The predictions of runoff, soil and SOC erosion rates were systematically improving with models developed from short to long sub-events (Table 3-3, 3-4, and 3-5, Figure 3-8 and 3-9). This illustrates the relevance of crusting evolvement and the accordingly derived systematic variability to predict soil erosional response and SOC erosion. However, even based on the data from the longest sub-event (360 min), the soil erosion rates for the CS were still poorly projected (R^2 from the pairwise comparison was only 0.257) (Table 3-4). This seems conflicting with the good prediction of total SOC loss for the CS (Table 3-5). It may result from two factors: 1) the failure of the erosion model to represent the rapidly increase of soil erosion rates after the runoff rates on the CS exceeded 10 mm h^{-1} (as discussed in Hu et al., 2013a). Therefore, the erosion model used in this study (Eq. 3-2), albeit best fitted, is apt to under-predict soil erosion at great runoff rates, while over-predict soil erosion at low runoff rates. 2) The temporal variation of ER_{SOC}, induced by crusting formation and thus the depletion of SOC on the eroding site over time, resulted in great values at low runoff rates and dropped to unity at great runoff rates (Figure 3-5). This means, the under-predicted soil erosion rates had ER_{SOC} of unity (Figure 3-5), while the over-predicted soil erosion rates featured high ER_{SOC} (Figure 3-5). As a consequence, the poor estimates introduced by the erosion model were cancelled out by the temporally varying ER_{SOC}, resulting in practicable predictions on SOC losses. This, therefore, gives a general precaution that crusting-induced systematic variability of soil erodibility, runoff erosivity and SOC availablity should be taken into account when interpreting erosion data from events of different durations.

3.4.3. Potential systematic variability to predict soil erosion in the future

Systematic variability is also likely to occur when extrapolating the models generated from current rainfall characteristics to predict soil and SOC loss under future conditions. As observed in this study, the return period of the critical monthly rainfall amount under current precipitation conditions in the region of Möhlin is quite high, i.e., 0.65 years for 90 mm to start crusting, and 1 year for 120 mm to complete crust formation. Therefore, soils in the region of Möhlin may experience different progressions of crusting during different tillage seasons. This renders the bare soils after tillage very sensitive to even minor differences in rainfall amount and intensity. In the future, further uncertainties may be brought about by the high likelihood of increase in the frequency, intensity, and/or amount of heavy precipitation (IPCC, 2014). These uncertainties may not only exacerbate the extent of soil and SOC erosion by heavier or more frequent precipitation, but may also alter the crusting processes by complicating the history of soil surface, e.g., different pre-wetting rates, aging durations, or drying cycles between storms (Le Bissonnais et al., 1989; Kuhn and Bryan, 2004; Levy et al., 1997). Without determining the dominance of soil surface changes during crusting, or the preceding history of the soil surface, erosion data may bear great systematic variability, and thus lead to biased estimation on soil and SOC erosion. Such biased estimation

on SOC losses, in further step, would mislead the assessment of the impact of SOC erosion on the aquatic system and global carbon cycling.

3.5. Chapter conclusion

This study aimed at evaluating the relevance of inherent variability, crusting formation over time and the accordingly derived systematic variability for soil and SOC erosion prediction. Two silty loams, of different structures and SOC contents, were subjected to a simulated rainfall of 30 mm h^{-1} for 360 min. The results show that the inter-replicate variability (coefficient of variation between ten replicates) of both runoff and soil erosion rates considerably declined over rainfall time. But even after runoff and soil erosion rates reached maximum values, the inter-replicate variability of soil erosional response still remained between 10 and 39%. This indicates the existence of inherent variability during interrill erosion process, and also points out that the complex interaction at the soil surface remains significant even under ideally controlled laboratory conditions.

The enrichment ratios of organic carbon dropped to unity or even below 1 during prolonged crusting, confirming that preferential erosion is limited by depletion of organic carbon on the eroding soil surface. While the continuous 360 min rainfall (more than 180 mm) applied in this study is very limited in reality under natural conditions, the progressively improved predictions with extending sub-event durations demonstrate the relevance of crusting evolvement and the accordingly derived systematic variability to soil and SOC erosion assessment. Similar variability may also occur when models built based on current rainfall characteristics are used to predict soil and SOC erosion loss in future events. Simple extrapolation of the parameters may not be sufficient to reflect the potential influence of ever-changing rainfall magnitudes and frequencies onto the soil and SOC loss in the future. The preceding history of the soil surface and the potential evolvement of crusting over time should also be accounted for, to accurately assess the on-site and off-site impacts of SOC erosion onto global carbon cycling.

Chapter 4

The Use of Equivalent Quartz Size and Settling Tube Apparatus to Fractionate Soil Aggregates by Settling Velocity

Yaxian Hu[1], Wolfgang Fister[1], Hans-Rudolf Rüegg[1], Peter A. Kinnell[2], Nikolaus J. Kuhn[1]

[1] Department of Environmental Sciences, University of Basel, Switzerland
[2] Institute of Applied Ecology, University of Canberra, Australia

Published in *Geomorphology Techniques (Online Edition)*, British Society for Geomorphology, section 1.1.1, 2013

Abstract: In a given layer of surface runoff, particle transport distance declines with increasing settling velocity. Settling velocity itself is determined by the size, density and shape of the particles. For sediment composed of aggregates, settling velocity does not only vary due to texture, but also due to aggregation, aggregate size and stability. Therefore, aggregation can strongly affect the transport distance of the sediment and the substance specific redistribution of the eroded material, such as organic matter. Understanding the effect of aggregation, for example, on redistribution of eroded organic matter is therefore essential for understanding local, regional and global carbon cycles. To capture and establish the relationship between aggregation, settling velocity and aggregate specific organic matter content, a settling tube apparatus, based on a previous design, was constructed and applied to fractionate soils by water stable aggregate size classes. To illustrate the effect of aggregation on settling velocity, the results were compared with mineral grain sizes after ultrasound dispersion. Five settling velocity classes were distinguished based on the Equivalent Quartz Size (EQS) of particles ≥ 250 µm, 125 to 250 µm, 63 to 125 µm, 32 to 63 µm, and ≤ 32 µm. Fractionation of a silty loam by settling tube illustrates that aggregation strongly affects settling velocities and should be considered in erosion models, as opposed to the texture of mineral grains. An analysis of sediment organic matter in the five settling velocity classes also showed that settling velocity is a suitable parameter to physically connect the redistribution of eroded soil organic matter to overland flow transport processes.

Keywords: *settling tube apparatus, settling velocity, transport distance, aggregate fractionation*

4.1. Introduction

Soil particles displaced by erosion experience selective deposition along their flow paths across watersheds (Walling, 1983). Understanding the effect of this selective deposition on the redistribution of particle-bound substances (e.g. soil organic carbon, phosphorous or other contaminants) within watersheds requires a discrimination of particles and their properties by their respective transport distances. The transport distances of displaced soil particles are related to their settling velocities (Dietrich et al., 1992; Kinnell, 2001, 2005) For eroded soil particles composed of aggregates, settling velocities generally do not correspond to the average or median mineral grain size, because aggregates differ in size, density and shape from mineral grains (Johnson et al., 1996; Tromp-van Meerveld et al., 2008). The average or median grain size can be the same for a range of soils, but the aggregate size distribution can differ, e.g. when clay enhances the formation of aggregates. The distribution of settling velocities therefore can provide more accurate information on the quality and behavior of eroded and aggregated sediment than just texture (Loch, 2001). The distribution of settling velocities based on grain size classes has already been included into some erosion / deposition models (Morgan et al., 1998; van Oost et al., 2004; Aksoy and Kavvas, 2005; Fiener et al., 2008b). However, inconsistencies such as over-prediction of clay fractions or under-prediction of sand and silt fractions in sediment samples are often present in their results (Beuselinck et al., 1999b; van Oost et al., 2004), because soil particles are mostly eroded as aggregates rather than as individual mineral grain (Walling, 1988; Slattery and Burt, 1997; Beuselinck et al., 2000). Aggregation potentially increases settling velocities and reduces transport distances. As a consequence, aggregation can lead to aggregate specific, rather than mineral grain specific, distribution of particle-bound substances across a landscape by selective deposition (Kuhn, 2007; Kuhn and Armstrong, 2012). The settling velocities of aggregates are therefore crucial to determine the effect of erosion on redistribution of substances (such as eroded soil organic carbon, phosphorous, nitrogen or metals) across landscapes, as well as their delivery into aquatic systems. By further identifying the lability of the eroded soil organic carbon, and quantifying the relative proportion mobilised into or out of different ecosystems, it also can substantially improve our understanding of the role of erosion / deposition on global carbon cycling.

The settling velocity of mineral particles is determined by their size, density and shape (Dietrich, 1982). For aggregated soils, their irregular shape, porosity, permeability, interaction with organic matter of low density, aggregation, and the relative fragility of wet aggregates (Le Bissonnais et al., 1989; Dietrich, 1982; Johnson et al., 1996; Tromp-van Meerveld et al., 2008) can all affect their settling velocities. Therefore, a conceptual approach based on Equivalent Quartz Sizes (EQS), modified from the equivalent sand size used by Loch (2001), is developed to address the effect of aggregation on the

potential redistribution of eroded soil organic matter across a hill-slope. EQS represents the diameter of a spherical quartz particle that would fall with the same velocity as the aggregated particle for which fall velocity is measured (Loch, 2001). Therefore, EQS represents an integrated index to indicate the settling behavior rather than to represent the specific size of the soil particles. In this manner, our current understanding of the effects of mineral grain size on sediment behavior can be applied to aggregated sediment particles based on the concept of EQS. Although the accurate size of aggregated particles needs to be validated by field data, the accuracy of soil erosion models can also be largely improved by applying the distribution of settling velocities based on EQS compared to grain size distribution.

4.2. Use of settling tubes to fractionate sediment particles

The settling tube (column) is a traditional technique used to measure the settling characteristics of aquatic solids (Droppo et al., 1997; Wong and Piedrahita, 2000; Rex and Petticrew, 2006), but the settling tubes used in river and marine environment are often short and with small openings. Consequently, they are unable to allow coarse particles to pass through, so they cannot be directly applied to fractionate sediment that is often in the form of aggregates. Settling tubes, such as the 20 cm long example used in (Johnson et al., 1996), cannot be used to fractionate the aggregated sediments either, because such a short settling distance is not capable of accurately distinguishing the velocities of fast settling particles.

In order to fractionate aggregated soils, Hairsine and McTainsh (1986) designed a top-entry settling tube apparatus (The "Griffith Tube"), which was adapted from the "Siltometer" developed by Puri (1934). In this design, soil samples were introduced into a 200 cm long vertical tube from the top by an injection barrel. After falling through the static water column by gravity, soil fractions were collected over predetermined time intervals into sampling dishes situated in a turntable under the widely-open bottom of the tube. This design was then improved by Kinnell and McLachlan (1988) using a more reliable injection barrel, and further by Loch (2001), who employed an electric motor to raise the tube and rotate the turntable. Unlike other physical fractionation methods, for instance, wet and dry sieving (Cambardella and Elliott, 1994; Christensen, 2001), where aggregates would inevitably experience abrasion, settling through a water column preserves fragile aggregates. However, such a technique has not been widely implemented, because the lack of details in describing the existing settling tube apparatus makes it very difficult to reconstruct one without detailed knowledge of their design specifications. Such information could only be obtained by personally contacting the authors, which is often not possible. In particular, measurements linked to modeling the redistribution of organic carbon and their implications on the carbon cycle are missing (Kuhn, 2013). It is also noteworthy that soil particles depositing through a column of static water neglects the potential effects of, for instance, flow turbulence during transport processes.

Other information (e.g. topography, and flow velocity) is required, therefore, in order to further calibrate the realistic transport distances of eroded soil particles.

4.3. Settling tube apparatus developed by Basel University

The settling tube apparatus built at Physical Geography and Environmental Change Research Group from Basel University consists of four components (Figure 4-1a): the settling tube, through which the soil sample settles (Figure 4-1b); the injection device, by which the soil sample is introduced into the tube (Figure 4-2); the turntable, within which the fractionated subsamples are collected (Figure 4-3); and the control panel, which allows an operator to control the rotational speed and resting / moving intervals of the turntable (Figure 4-4).

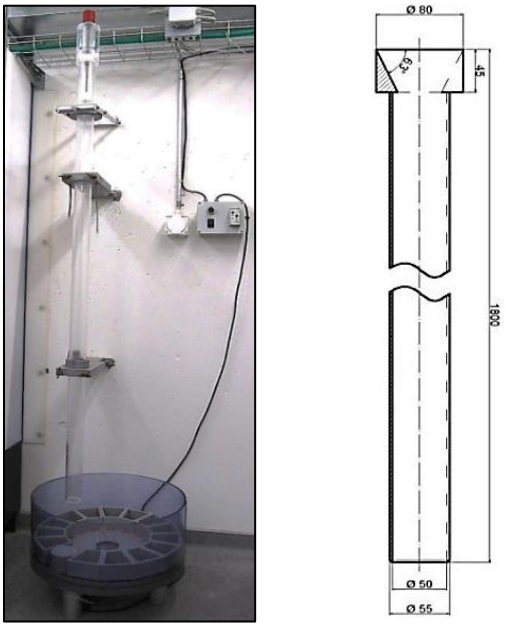

(a) (b)

Figure 4-1 (a) Overview of the complete setup of the Basel University settling tube apparatus; (b) The settling tube. Measurement units in mm.

4.3.1 The settling tube

The settling tube is made of transparent PVC, has a length of 180 cm and an internal diameter of 5 cm (Figure 4-1b). The tube can hold approx. 4 liters of water, through which the soil sample is free to settle. In most cases, the soil particles are smaller than 2 mm in diameter, so the diameter ratio of the tube (50 mm) to a particle (< 2 mm) is greater than 25 to 1. According to Loch (2001), such a ratio largely

eliminates concerns associated with edge effects and the variability introduced by wall effects is expected to be < 10%.

4.3.2 The injection device

An injection device is used to insert the soil sample into the top of the settling tube. It consists of a central chamber and a ca. 30 cm long metal rod connected to a Teflon cone at the lower end, a Teflon piston in the middle and a rubber plug attached to a handle at the upper end (Figure 4-2, based on the design of (Kinnell and McLachlan, 1988)).

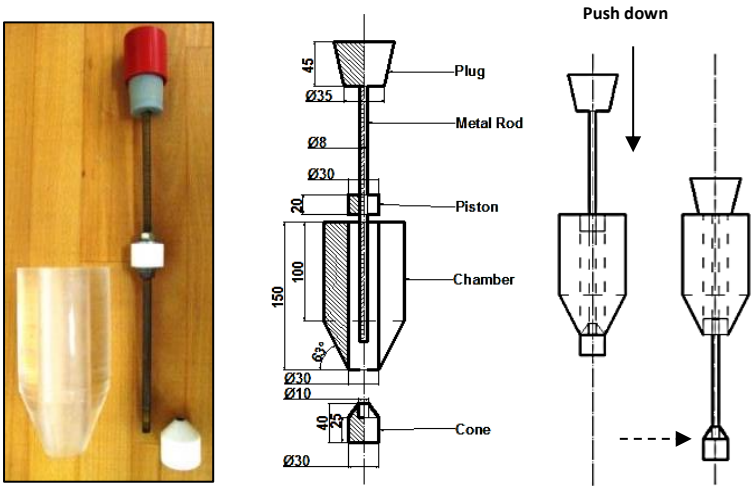

Figure 4-2 The injection device used in the Basel University settling tube apparatus. Measurement units in mm.

The soil sample is placed into the central chamber before injection, the 80 cm^3 capacity of which limits the mass of dry soil to 25 g. This leads to a soil concentration of approximately 6 g L^{-1} in the water column. Following Loch (2001), the concerns associated with particle interactions during settling are therefore minimal. The metal rod passing through the chamber opens the Teflon cone at bottom of the chamber, releasing the soil sample while the piston and plug keep the chamber sealed to prevent water flowing out at the bottom of the pipe. Kinnell and McLachlan (1988) used a pin inserted into the rod to prevent the piston from moving downwards before release. In our injection device the deformation of the Teflon is used to seal the chamber and prevent the movement of the piston (Figure 4-2). This design seals the chamber more effectively; however, it requires a much greater force to open it. A slow opening of the chamber can lead to inaccurate settling times. It is also noteworthy that the cone frequently represents an obstacle in the pathway of falling particles and small amounts (< 1 g) have been observed on the surface of the cone. Further improvements on the design of the injection device are required in order to solve this problem.

4.3.3 The turntable

The turntable is placed under the settling tube and is used to collect the soil fractions that settle out of the tube. It consists of a circular tank (Figure 4-3a, PVC transparent), and a set of sampling dishes (Figure 4-3b, PVC grey). The circular tank is 50 cm in diameter, 20 cm deep, and has a volume of 40 L. The net volume of each sampling dish is ca. 290 cm^3. When settling, the water level in the tank must be higher than the bottom opening of the tube to prevent the water from flowing out of the tube. The turntable tank rests on a layer of plastic ball bearings placed in a tray beneath the tank. This tray rests on three pillars (Figure 4-3c). An electric motor, affixed to the pillars, enables a timed and stepwise rotation of the turntable and thus places each respective sampling dish precisely underneath the settling tube, e.g. at time intervals corresponding to the settling times of the EQS. Where motor installation is not available, manual operation to replace the sampling dishes is also feasible.

4.3.4 The control panel

A plug-in time delay relay (© Comat, RS 122-H) is used to control the rotational speed and resting / moving intervals of the turntable (Figure 4-4). The control panel primarily consists of three parts: the main switch, the speed-control knob, and the interval-control buttons.

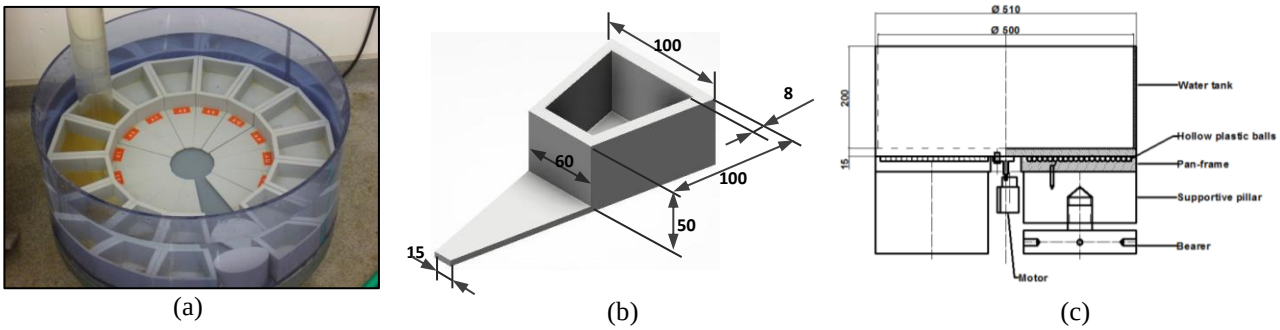

(a) (b) (c)

Figure 4-3 The turntable (a), the sampling dish (b), and the supporting frame (c) of the Basel University settling tube apparatus. Measurement units in mm.

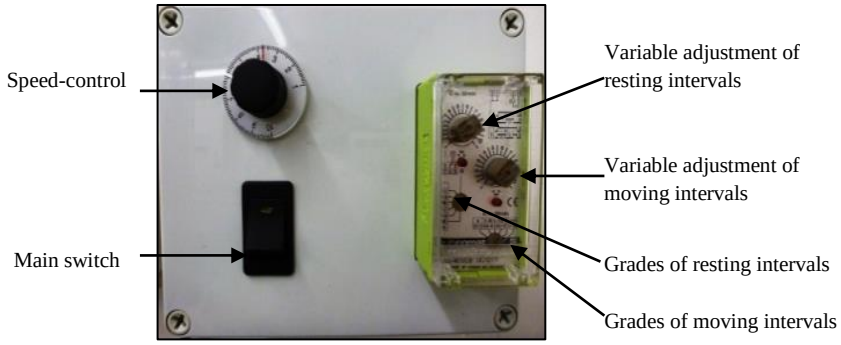

Figure 4-4 The control panel of the Basel University settling tube apparatus

4.4. Potential transport distance of eroded organic carbon based on texture and aggregation

4.4.1. Soil selection and preparation

A silty loam from Möhlin, northwest Switzerland (47˚ 33' N, 7˚ 50' E) was used to compare the differences between the potential transport distance of eroded organic carbon predicted based on soil texture and that predicted by aggregate fractionation. The soil was sampled from Bäumlihof Farm with a wheat-grass-maize rotation in August 2011. Sampling directly from the field, rather than from depositional sites after a certain extent of preferential transportation, provides an opportunity to evaluate the likely transport distance of all classes of eroded particles. Its total organic carbon concentration is 10.9 mg g^{-1}, and the aggregate stability (based on Nimmo and Perkins, 2002) is 66.85%. This degree of aggregation and organic carbon content were considered appropriate to investigate the effects of aggregation onto the potential redistribution of eroded soil organic carbon by deposition across the landscape.

4.4.2. Calculation of Equivalent Quartz Size

Stokes' Law covers the range of the mineral grain sizes dominating the silty loam used for this study. Their terminal settling velocities can be calculated by:

$$V = \frac{h}{t} = \frac{d^2 g(D_s - D_f)}{18\eta} \quad \text{(Eq. 4-1)}$$

Where: V = settling velocity ($m \cdot s^{-1}$), h = settling distance = 180 cm with this settling tube apparatus, t = settling time (s), d = diameter of settling particle (mm), g = gravitational force = 9.81 $N \cdot kg^{-1}$, η = viscosity of water at 20˚ C = 1×10^{-3} $Ns \cdot m^{-2}$, D_s = average density of the solid particles, for most soils = 2.65×10^3 $kg \cdot m^{-3}$, D_f = density of water = 1.0×10^3 $kg \cdot m^{-3}$.

The use of Stokes' Law to calculate EQS is, in the strictest sense, limited to particles < 0.07 mm (Rubey, 1933). For soils dominated by larger mineral grains, different relationships should be used (Ferguson and Church, 2004; Wu and Wang, 2006). Five size fractions were selected according to their likely transport distance once eroded (Starr et al., 2000): ≥ 250 µm, 125 to 250 µm, 63 to 125 µm, 32 to 63 µm, ≤ 32 µm (Table 4-1).

4.4.3. Soil fractionation by settling tube and wet sieving

The soil samples were dried at 40˚C until constant weight was achieved and then gently dry-sieved with an 8 mm sieve to avoid over-sized clods. Prior to settling / wet-sieving, 25 g of dry soil were immersed into 50 ml tap water for 15 min. This fast-wetting emphasizes slaking and slight clay dispersion and simulates the destruction of aggregates during an erosion event (Le Bissonnais, 1996). For all tests,

tap water was used. The electric conductivity of tap water was 2220 µs·cm^{-1}, which was five times higher than the rainwater in Basel (462 µs·cm^{-1}). In general, increased electric conductivity of tap water enhances dispersion during rainfall simulation tests (Borselli et al., 2001). A comparative aggregate stability test (Wet Sieving Apparatus, Eijkelkamp, Netherlands) using tap water and rainwater from Basel had shown that tap water only had a minor effect on aggregates greater than 250 µm after 20 min of continuous up-and-down movement (67.24% in rainwater, 73.59% in tap water). Therefore, the use of tap water was considered to be acceptable.

Table 4-1 Settling times and velocities of the Möhlin silty loam, based on the Equivalent Quartz Size (EQS) classes, and the likely transport distance of soil particles once eroded based on the conceptual function developed by Starr et al., 2000. The settling distance is 1.8 m.

EQS (µm)	Settling velocity (m·s^{-1})	Settling time (s)	Likely transport distance
> 250	$> 4.5 \times 10^{-2}$	< 40	Deposited across landscapes
125 - 250	1.5×10^{-2} - 4.5×10^{-2}	40 - 120	
63 - 125	3.0×10^{-3} - 1.5×10^{-2}	120 - 600	
32 - 63	1.0×10^{-3} - 3.0×10^{-3}	600 - 1800	Possibly transferred into rivers
< 32	$< 1.0 \times 10^{-3}$	> 1800	Likely transferred into rivers

A 25 g of fast-wetted soil sample was fractionated using the Basel University settling tube apparatus into five settling velocity classes (Table 4-1). A typical settling pattern of soil particles in the water column is shown in Figure 4-5. The finest particles correspond to those that remain in suspension after 1800 s of settling (i.e. EQS < 32 µm). Fractionated samples were dried at 40°C and dry weights as well as total organic carbon concentration (by Leco RC 612 at 550°C) were measured.

A second 25 g of fast-wetted soil sample was subjected to ultrasound using a Sonifier 250 from Branson, USA. The energy dissipated in the water / soil suspension was ca. 60 J·ml^{-1} (i.e. Energy = output power 70 W × time 85 s / suspension volume 100 ml) (North, 1976). According to Kaiser et al. (2012), although the aggregates were probably not thoroughly dispersed at this level of energy, the coarse mineral and organic particles (> 250 µm) were prone to be damaged if higher energy than 60 J·ml^{-1} was further applied. The dispersion energy level of 60 J·ml^{-1} was thus considered to be satisfactory, in the context of distinguishing the size distribution of aggregates from grains. The dispersed fractions were then wet-sieved into the five size classes corresponding to the five EQS classes used for the fractionation by settling tube. The weights and total organic carbon concentrations of each class were then measured in the same way as for the settling tube fractionated samples.

Figure 4-5. A typical settling pattern of soil particles through the water column: coarse particles settle fastest, while the fine particles stay suspension at upper part.

4.5. Effect of aggregation on settling velocity

The results of the two fractionation approaches are shown in Figure 4-6. The effect of aggregation on settling velocity is pronounced: 68.61% of the aggregated soil behaved like particles of EQS greater than 63 µm (Figure 4-6a). The mineral particle size distribution, on the other hand, shows that 89.65% of soil grains were smaller than 63 µm (Figure 4-6a). This difference between proportion of EQS and corresponding mineral grain size classes illustrates that aggregation has a great effect on the particle settling velocity of the silty loam tested in this study.

The relevance of this finding is further illustrated by the distribution of total organic carbon in aggregates and mineral grains. The distribution of total organic carbon concentration follows a similar pattern for both grain size and aggregate size classes (Figure 4-6b). However, multiplying the organic carbon concentration of each size class with its weight (Figure 4-6c) shows that 73% of the organic carbon stock is contained in particles > 63 µm, while 79% of the organic carbon stock was associated with grains < 32 µm. This implies that aggregation strongly affects the potential transport distance of the eroded organic carbon. Basically, the amount of deposition across the landscape would be tripled as the soil texture suggests. By contrast, the exportation of eroded organic carbon to watercourses would be reduced to a third. In consequence, the effect of aggregation on transport distances would fundamentally change our perspective on the environmental impact of eroded organic carbon as well as other nutrients and contaminants.

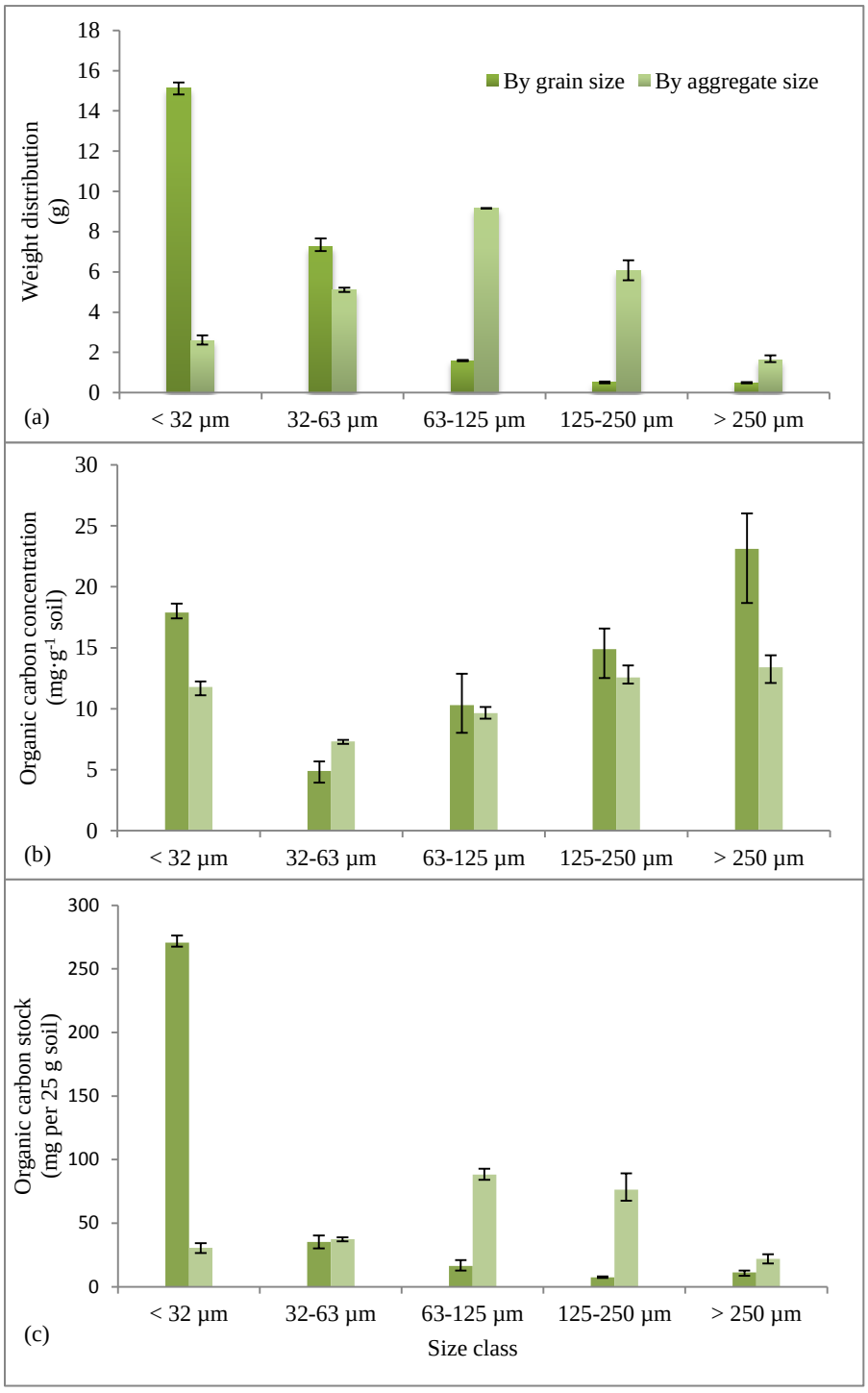

Figure 4-6 (a) Weight distribution, (b) organic carbon concentration distribution, and (c) organic carbon stock distribution of the Möhlin silty loam across aggregate size classes fractionated by the Basel University settling tube apparatus, and across grain size classes dispersed by ultrasound. Error bars indicate the range of minimum and maximum values. n=3.

4.6. Chapter conclusion

The settling tube fractionation provides settling velocity as a 'tool' to physically connect the redistribution of eroded soil organic carbon in an agricultural landscape with a soil transportability parameter used in current erosion models. While the initial test reported in this paper is very limited in its applicability to real erosion events, the results prove that a more accurate settling velocity of aggregated soil particles can be measured based on Equivalent Quartz Size than solely based on grain size distribution. The results also indicate that selective transport of aggregated sediment potentially has a great impact on the redistribution of eroded organic carbon in terrestrial ecosystems and its delivery to aquatic ecosystems. Such differentiation of sediment movement could, in turn, be highly significant for the effect of soil erosion on the global carbon cycle (Kuhn et al., 2009). As a consequence of the results of the settling velocity fractionation procedure presented in this study, we conclude that the settling tube apparatus can be further applied to determine the realistic settling velocities of eroded soil generated in the field. The application of a settling tube to fractionate sediment particles according to settling velocities makes a significant contribution to our understanding of local, regional and global geochemical fluxes within terrestrial ecosystems, and also of their interaction with atmospheric and aquatic systems.

Chapter 5

Aggregates Reduce Transport Distance of Soil Organic Carbon: Are Our Balances Correct?

Yaxian Hu, Nikolaus J. Kuhn

Published in *Biogeosciences*, 11, 6209-6219, 2014

Abstract: The effect of soil erosion on global carbon cycling, especially as a source or sink for greenhouse gases, has been the subject of intense debate. The controversy arises mostly from the lack of information on the fate of eroded soil organic carbon (SOC) whilst in-transit from the site of erosion to the site of longer-term deposition. Solving this controversy requires an improved understanding of the transport distance of eroded SOC, as this is principally related to the settling velocity of sediment fractions carrying SOC. Although settling velocity has already been included in some erosion models, it is often based on mineral particle size distribution. For aggregated soils, settling velocities are affected by their actual aggregate size rather than by mineral particle size distribution. Aggregate stability is, in turn, strongly influenced by SOC. In order to identify the effect of aggregation of source soil on the transport distance of eroded SOC and its susceptibility to mineralization after transport and temporary deposition, a rainfall simulation was carried out on a silty loam. Both the eroded sediments and undisturbed soil were fractionated into size different classes using a settling tube apparatus according to their settling velocities. Weight, SOC concentration and instantaneous respiration rates were measured for each of the six class fractions. Our results indicate that: 1) 41% of the eroded SOC was transported with coarse aggregates that would be likely re-deposited down eroding hill-slopes, rather than with fine particles likely transferred to water courses; 2) erosion was prone to accelerate the mineralization of eroded SOC and thus might contribute more CO_2 to the atmosphere than current estimates predict, as these often neglect the effects of aggregation of source soil on SOC transport distance; 3) the net erosion-induced carbon sink effect would be close to zero, if preferential deposition causes a reduction of SOC flux to the aquatic system and an increase of SOC flux into the terrestrial system.

Keywords: *eroded organic carbon, instantaneous respiration rate, transport distance, carbon source*

5.1. Introduction

The net effect of soil erosion as a source or sink of CO_2 in the global carbon cycle has been the subject of intense debate (Lal, 2003; van Oost et al., 2007; Quinton et al., 2010; Dlugoß et al., 2012; Doetterl et al., 2012). On one hand, erosion exposes the previously incorporated soil organic carbon (SOC), which may accelerate the mineralization of eroded SOC (Jacinthe et al., 2002a, 2004; Kuhn, 2007; Mora et al., 2007; Lal and Pimentel, 2008). On the other hand, deposition limits the decomposition of SOC upon burial, while inputs of decomposing plant material on the surface of eroding sites partially replaces the lost SOC (van Oost et al., 2007; Harden et al., 1999; Wang et al., 2010). So far, effects of erosion on CO_2 emissions have mostly been assessed by comparing SOC stocks at the assumed site of erosion and the site of colluvial deposition (Stallard, 1998; Berhe, 2011; van Hemelryck et al., 2011; Nadeu et al., 2012; van Oost et al., 2012). One underlying assumption associated with this approach is that the redistribution of eroded SOC across landscapes is non-selective. However, several recent publications showed (at least) temporary enrichment of SOC in sediment, as well as preferential deposition of aggregates with size distribution and SOC concentration that differ from original soils (Schiettecatte et al., 2008; Kuhn et al., 2009; Hu et al., 2013a; Kuhn, 2013). As a consequence, carbon balances drawn only from the SOC stocks on sites of erosion and colluvial deposition may not adequately consider the potential SOC re-deposition into terrestrial systems.

The SOC redistribution, regardless after selective or non-selective erosion, is strongly depending on the transport distance of eroded SOC. This is thus related to the respective settling velocities of sediment fractions carrying the eroded SOC (Dietrich, 1982; Kinnell, 2001, 2005). Although settling velocity has already been included in some erosion models, it is often based on mineral particle size distribution (Morgan et al., 1998; Beuselinck et al., 1999a; Flanagan and Nearing, 2000; van Oost et al., 2004; Aksoy and Kavvas, 2005). But for aggregated soils, settling velocities are affected by the actual size, irregular shape, porosity of soil fractions and their incorporation with light-dense SOC (Kinnell and McLachlan, 1988; Loch, 2001; Hu et al., 2013c). Hence, the mineral particle size classes, no matter how efficiently applicable in erosion models, are not the decisive factor that determines the actual settling behavior or movement of aggregates. Aggregation of original soil potentially increases the settling velocities of soil particles, and thereby likely reduces their transport distances after erosion (Hu et al., 2013c). This, in theory, would also reduce the transport distance of eroded SOC incorporated into soil aggregates.

The effect of aggregation of source soil may also affect the movement of SOC down eroding hill-slopes. Aggregation is related to SOC content, and SOC is often increased in both macro- and micro-aggregates (Tisdall and Oades, 1982; Cambardella and Elliott, 1994). The quality and stabilizing mechanisms of SOC in the soil matrix also vary with different aggregate conditions. For instance,

physically-stabilized SOC within macro- and micro-aggregates is protected from mineralization by forming physical barriers between microbes, enzymes and their respective substrates (Six et al., 2002). In turn, SOC is very susceptible to mineralization after aggregate break-up, as often occurs during erosion and transport (Starr et al., 2000; Lal and Pimentel, 2008; van Hemelryck et al., 2010). Therefore, erosion, either detaching aggregates from the soil matrix or disintegrating larger aggregates, may have diverse impacts on mineralization of eroded SOC (van Hemelryck et al., 2010; Fiener et al., 2012). In this study, as the first step to unfold the complex effects of aggregation onto SOC erosion, transport, and deposition, we aim to test the theoretical deductions made above by fractionating eroded loess sediments, generated during a laboratory rainfall simulation, according to their settling velocities, and then measure their SOC concentration and respiration rates.

5.2. Materials and Methods

5.2.1. Soil sampling and preparation

A silty loam from the conventionally managed Bäumlihof Farm in Möhlin (47˚33’ N, 7˚50’ E), near Basel in northwest Switzerland, was used in this study. The soil supports a maize-wheat-grass rotation. A-horizon material (top 20 cm) was sampled from a gentle shoulder slope (< 5%) in March 2012. Previous research on the same silty loam showed that aggregation increased the settling velocity of original soil fractions, particularly the medium sized fractions, in comparison with that expected based on the texture of the original soil (Hu et al., 2013b). The mineral particle specific SOC distribution, average SOC content (LECO RC 612 at 550°C), and aggregate stability of original soil (method adapted from Nimmo and Perkins, 2002), are shown in Table 1. The mineral particle size distribution was fractionated by wet-sieving, after dispersion by ultrasound using a Sonifier Model 250 from Branson, USA. The energy dissipated in the water/soil suspension was 60 $J \cdot ml^{-1}$ (i.e. Energy = output power 70 W × time 85 s / suspension volume 100 ml). The SOC mass proportions across mineral particle size classes were calculated only from average values of individual weight and SOC content. Although the ultrasound energy used in Hu et al. (2013b) was not enough to thoroughly disperse the original soil into real mineral particles (Kaiser et al., 2012), such extent of dispersion was notable enough to demonstrate the potential under-estimation of applying mineral particle size distribution to predict the settling velocity of eroded SOC. Hence, it is speculated that similar increasing effects would also occur to sediment fractions, and thus make the silty loam suitable to investigate the potential effects of aggregation of original soil on the transport distances of differently sized sediment fractions. While this study investigated only one soil, similar loess soils cover about 10% (ca., 14.9 million km^2) of the global land area (Sartori, 2000). This study was thus considered relevant as it generally reflects the erodible nature of similar loess soils under similar management regimes. In the future, more experiments with soils of different aggregation status

and various SOC contents will be carried out, once our theoretical deduction of aggregation effects on this silty loam has been verified.

Table 5-1 Mineral particle size distribution, soil organic carbon (SOC) concentration distribution across mineral particle size, general SOC concentration, and the percentage of stable aggregates greater than 250 µm in the silty loam used in this study.

	Mineral particle size (µm)[a]					General SOC ($mg \cdot g^{-1}$)[b]	Aggregates greater than 250 µm (%)[c]
	< 32	32-63	63-125	125-250	> 250		
Weight (%)	62.0 $_{\pm 0.3}$	29.1 $_{\pm 0.4}$	6.6 $_{\pm 0.3}$	1.2 $_{\pm 0.1}$	1.1 $_{\pm 0.1}$		
SOC ($mg \cdot g^{-1}$)	13.7 $_{\pm 0.7}$	3.0 $_{\pm 0.3}$	8.9 $_{\pm 2.6}$	21.9 $_{\pm 0.8}^{a}$	26.4 $_{\pm 1.3}^{a}$	10.8 $_{\pm 0.4}$	67.2 $_{\pm 6.9}$
SOC mass (%)[d]	80.8	8.3	5.6	2.5	2.8		

NOTE: a). It might be over-estimated due to the mixture of minute amount of residue or straw, which was previously incorporated into the aggregates but then released by dispersion and blended with coarse particles.
Lower case numbers indicate the range of minimum and maximum values (n = 3).

5.2.2. Rainfall simulation

The experiments consisted of three separate components: 1) rainfall simulation to sufficiently destroy aggregates, so as to ensure that the eroded sediments were less likely to experience further breakdown during the subsequent settling velocity measurements; 2) fractionation of the eroded sediments by a settling tube apparatus into six settling velocity classes; and 3) measurements of the instantaneous respiration rates of each settling class. The experiments were repeated three times in order to generate reliable erosion and respiration data.

Soils (0 - 5 cm depth) were placed in a 150 × 80 cm flume, which was pitched at a 15% gradient (Figure 5-1a). Preliminary tests revealed that a flume of this size could generate sufficient runoff to initiate non-selective erosion on this particular silt loam. The soil was sieved into aggregates of a diameter less than 10 mm and over-sized clods were excluded in order to reduce variations in surface roughness, both within the flume and between replicates. Levelling the surface also ensured that large roughness elements, in particular depressions, did not inhibit movement of aggregates across the flume and thereby prevent selective deposition on the soil surface. To assist drainage, the base of the flume was perforated and covered with a fine cloth and a layer of sand (c.a., 5 cm). A nozzle of FullJet ¼ HH14WSQ, installed 1.8 m above the soil surface, was used to generate rainfall (Figure 5-1). Soil of each replicate was then subjected to simulated rainfall at an intensity of 55 $mm \cdot h^{-1}$ for 3 h. The kinetic energy of the raindrops, detected by a Joss-Waldvogel-Disdrometer, was on average 200 $J \cdot m^{-2} \cdot h^{-1}$.

Natural precipitation events of 55 $mm \cdot h^{-1}$ are unlikely in the Möhlin region, where precipitation intensity is mostly less than 35 $mm \cdot h^{-1}$ (MeteoSwiss, 2013). But increased intensity is often considered necessary to compensate for the deficiency of kinetic energy associated with simulated rainfalls in order to recreate conditions that were as comparable as possible with natural rainfalls (Dunkerley, 2008; Iserloh et al., 2012, 2013). A previous study had shown that full crust formation on the Möhlin silty loam

(aggregates < 8 mm) requires a cumulative kinetic energy of about 340 $J \cdot m^{-2}$ (Hu et al., 2013a). This corresponds to natural precipitation of 35 $mm \cdot h^{-1}$ for 30 min (Iserloh et al., 2012). Therefore, a simulated rainfall of 55 $mm \cdot h^{-1}$ lasting for 3 h with a cumulative kinetic energy about 600 $J \cdot m^{-2}$ was chosen in this study to make sure that the aggregates (coarser than those in Hu et al., 2013a) would experience full crust formation to equilibrium conditions, i.e. resistance of crust against erosion equals the erosive force of raindrops and runoff.

Tap water, with an electric conductivity of 2220 $\mu s \cdot cm^{-1}$, which is five times higher than natural rainwater in Basel, was used during each rainfall simulation. In general, the increased electric conductivity associated with tap water increases soil dispersion during tests using simulated rainfall (Borselli et al., 2001). Despite this, however, comparative aggregate stability tests showed only a 7% difference between rainwater sampled in Basel and ordinary tap water; thus making it acceptable.

(a) (b)

Figure 5-1 The rainfall simulation flume (a), and the settling tube apparatus (b). The settling tube apparatus consists of four components: the settling tube, through which the soil sample settles; the injection device, by which the soil sample is introduced into the tube; the turntable, within which the fractionated subsamples are collected; and the control panel, which allows an operator to control the rotational speed and rest intervals of the turntable (operations see Hu et al., 2013c).

5.2.3. Sediment collection and fractionation by a settling tube apparatus

During each rainfall event, runoff and sediment were continuously collected over 30 min intervals. A 1.8 m settling tube (Figure 5-1b), which is described in detail in (Hu et al., 2013c) was used to fractionate the eroded sediment fractions according to their respective settling velocities. The injection device within this particular settling tube has a volume of 80 cm^3. As this limits the amount of sediment used during each test, only sediment collected during the first 10 min of each 30 min interval was used to determine settling velocities. Prior to being subjected to settling fractionation, the eroded sediment was allowed to settle for 1 h in collection beakers (height of 20 cm). Measurements confirmed that > 95% of the total mass settled after this pre-treatment. The supernatant and remaining suspended sediment (corresponding to EQS < 8 μm) was then decanted off and added to the < 20 μm fraction remaining in suspension in the settling tube (described as following).

Table 5-2 Six settling velocities based on the Equivalent Quartz Size (EQS) classes, and the likely fate of eroded fractions based on the conceptual model developed by Starr et al. (2000). The settling distance was 1.8 m.

EQS (μm)	Settling velocity ($m \cdot s^{-1}$)	Settling time (s)	Likely transport distance
> 250	$> 4.5 \times 10^{-2}$	< 40	Deposited across landscapes
125 - 250	1.5×10^{-2} - 4.5×10^{-2}	40 - 120	
63 - 125	3.0×10^{-3}- 1.5×10^{-2}	120 - 600	
32 - 63	1.0×10^{-3}- 3.0×10^{-3}	600 - 1800	Possibly transferred into rivers
< 32	$< 1.0 \times 10^{-3}$	> 1800	Likely transferred into rivers

Six particle size classes, based on the concept of Equivalent Quartz Size (EQS) described in (Hu et al., 2013c), were selected according to their likely transport distances after erosion (Table 5-2). The six EQS classes were converted to six settling velocities and corresponding settling times using Stokes' Law (Hu et al., 2013c). The use of Stokes' Law to convert EQS into settling velocity is, in the strictest sense, limited to particles < 70 μm (Rubey, 1933). From the perspective of terrestrial and aquatic systems, however, sediment fractions coarser than 63 μm are considered as one group that is likely to be re-deposited along hill-slopes. Hence, the potential error when using Stokes' Law to calculate the settling velocities of fractions of all sizes is considered rational. In addition, fine suspended fractions are considered as one group "export" out of the terrestrial system. Hence, with the current settling tube (length of 1.8 m), any fractions finer than 20 μm (settling time longer than 1.5 h) were not further fractionated to practically save the experiment time. Where settling tubes of different lengths are applicable, sediment fractions of distinct settling velocities should be separately treated. After fractionation, the six EQS classes were air-dried for 72 h in a dark environment at ambient temperature (20°C). Despite the possibility of biasing the mineralization SOC potential through the process of air-drying, as the first step to unwrap the

complex effects of aggregation onto SOC erosion, transport, and deposition, our aim was to produce quasi-natural sediments, i.e., subjecting to a single rainfall event, successively re-deposited after increasing transport distances and immediately dried afterwards. Further effects of multiple rainfall events, other soil moisture conditions (e.g., wet sediments) and long-term incubation will be investigated in future research, once the role of aggregation on eroded SOC has been studied.

5.2.4. Instantaneous respiration rate measurement

Instantaneous respiration rates were measured, based on the method described in Robertson et al. (1999) and Zibilske (1994). In brief, two grams (dry weight) of each EQS size fraction were placed into a 30 ml vial and re-wetted using distilled water in order to obtain a gravimetric moisture content equivalent to ca. 60%. Preliminary tests revealed that the gravimetric moisture of 60% represented a proper intermediate moisture level for sediment fractions of various surface areas, and thus exerted comparable effects on soil respiration rates (Xu et al., 2004; Bremenfeld et al., 2013). All the re-wetted fractions were then incubated over night at 25˚C (vials open). Two grams of original undisturbed soil were also prepared in the same way and used to generate reference measurements. Prior to soil respiration measurements, all vials were sealed using rubber stoppers. Gas from the headspace of each sealed vial was extracted by a 1 cc syringe at the beginning and end of the 1 h sampling period. Differences in CO_2 concentrations between these two measurements, as measured on a SRI8610C Gas Chromatograph (SRI Instruments, etc.), were used to calculate the instantaneous respiration rate.

5.2.5. Laboratory measurements and data analyses

Soil erosion rates for each 30 min interval were estimated by the mass of sediment samples both from the beginning 10 min (sum of the six EQS classes) and the late 20 min (not fractionated by the settling tube). Runoff samples collected during the late 20 min of each 30 min interval were allowed to settle for more than 48 h. The supernatant was then decanted off and the sediment was dried at 40°C and weighed. The SOC concentration of all the samples was measured by a LECO RC 612 at 550˚C. Data analysis was carried out using Microsoft Excel 2010 and R studio software packages (R version 2.15.1).

5.3. Results

Runoff began after 20 min. of rainfall and attained steady state conditions equivalent to 18 $mm \cdot h^{-1}$ after 120 min. Sediment discharge rates followed a similar pattern and reached steady state of 168.7 $g \cdot m^{-2} \cdot h^{-1}$. Detailed erosional responses are listed in Table 5-3.

Table 5-3 Summary of the erosional responses of Möhlin soil over 180 min of rainfall time. Subscripted numbers indicate the minimum and maximum range of the parameters (n=3).

Steady state (after 120 min)			Total runoff (kg)	Runoff coefficient (%)	Total sediment yield (g)
Runoff rate ($mm \cdot h^{-1}$)	Sediment discharge rate ($g \cdot m^{-2} \cdot h^{-1}$)	Sediment concentration ($g \cdot L^{-1}$)			
18.0 $_{\pm 0.9}$	168.7 $_{\pm 14.4}$	9.4 $_{\pm 0.1}$	40.7 $_{\pm 3.1}$	20.6 $_{\pm 1.6}$	475.8 $_{\pm 74.6}$

The fraction mass and SOC in the six EQS classes of sediment are presented in Figures 5-2 and 5-3. Preliminary data analysis had shown that the proportional composition of six EQS classes in each sediment collection interval did not significantly differ over rainfall time. Hence, each EQS class was considered to have 18 replicates (6 sediment collection intervals during each of the 3 rainfall events), and only proportional values (not absolute values) are presented. Nevertheless, the distribution of fraction mass and SOC concentration considerably differed across six EQS classes: about 61% of the sediment fractions were in EQS of 32 to 63 µm and 63 to 125 µm, containing about 65% of the SOC. Such aggregate specific SOC distribution in eroded sediment also contrasts against the association of SOC with mineral particles in the original soil (Table 5-1).

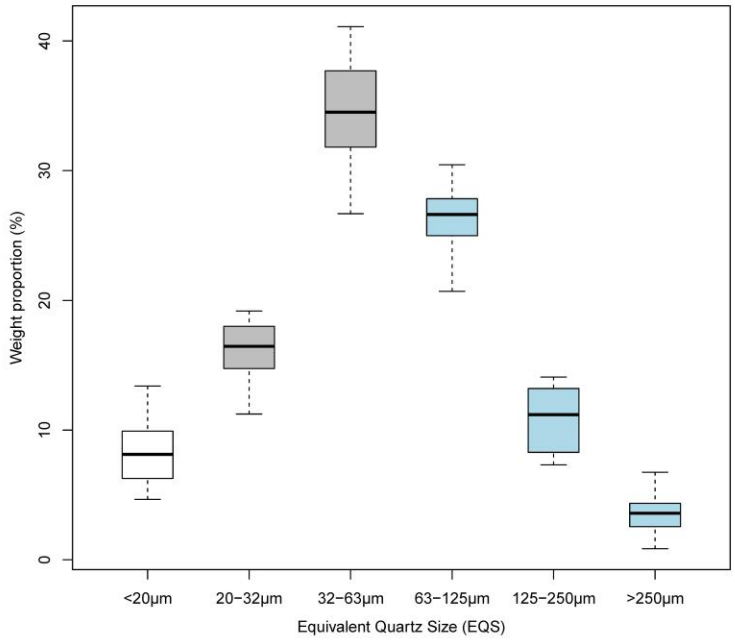

Figure 5-2 The weight distribution of the different Equivalent Quartz Size (EQS) classes of the sediment. Bars in the boxes represent median values. Whiskers indicate the lowest datum within 1.5 interquartile range of the lower quartile, and the highest datum within 1.5 interquartile range of the upper quartile (n = 18).

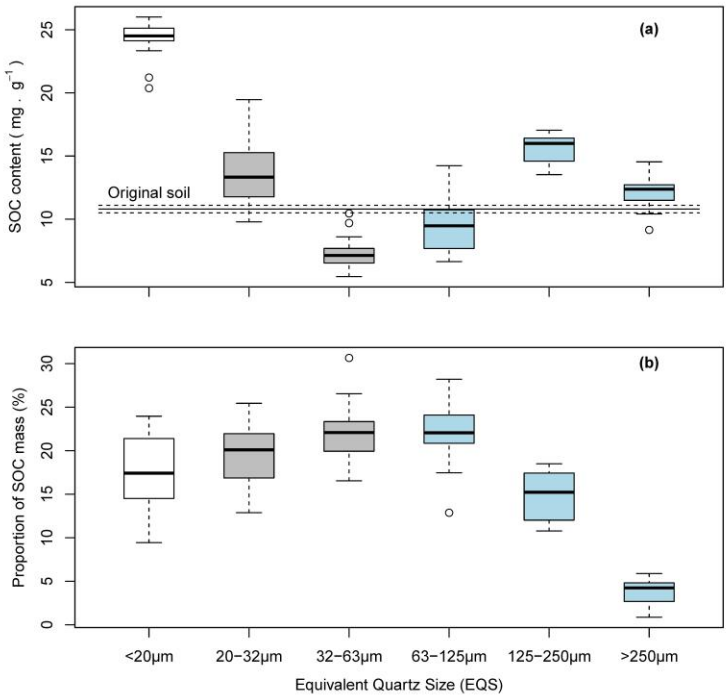

Figure 5-3 The distribution of soil organic carbon (SOC) concentration (a), and soil organic carbon (SOC) mass (b) in different Equivalent Quartz Size (EQS) classes of the sediment. The line in (a) denotes the average soil organic carbon (SOC) concentration of the original soil. Bars in the boxes represent median values. Whiskers indicate the lowest datum within 1.5 interquartile range of the lower quartile, and the highest datum within 1.5 interquartile range of the upper quartile (n = 18).

The instantaneous respiration rates from EQS classes of 32 to 63 μm and 63 to 125 μm were on average lower than that from other fractions (Figure 5-4a). However, after multiplying the respiration rate from each class with its fraction mass (Figure 5-2), EQS classes of 32 to 63 μm and 63 to 125 μm on average released even more amount of CO_2 than all other finer or coarser classes did (Figure 5-4b). The instantaneous respiration rates per gram of SOC also differ among different EQS classes. In EQS classes < 20 μm and 20 to 32 μm, the instantaneous respiration rates per gram of SOC were lower than that in the original soil (Figure 5-5). In contrast, all the other four EQS classes (> 32 μm) had higher instantaneous respiration rates per gram of SOC than the original soil (Figure 5-5). We attribute the increased respiration rates per gram of SOC in EQS classes > 32 μm to the detachment and transport of eroded soils, during which time the structural aggregates were broken down, thereby exposing the previously protected SOC to microbial processes (Six et al., 2002; Lal and Pimentel, 2008; van Hemelryck et al., 2010).

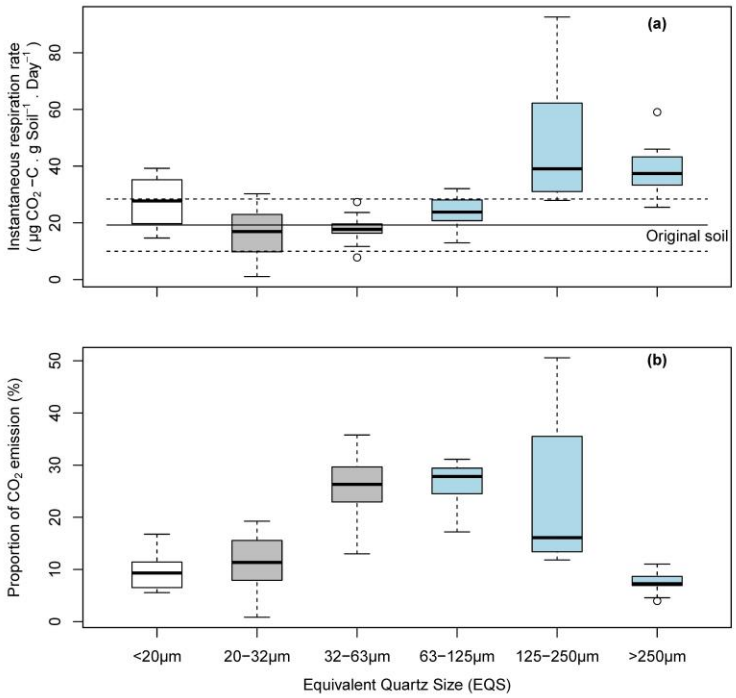

Figure 5-4 The distribution of instantaneous respiration rate (a); and potential CO_2 emission (b) in different Equivalent Quartz Size (EQS) classes of the sediment. The line in (a) denotes the average instantaneous respiration rate of the original soil (n = 18).

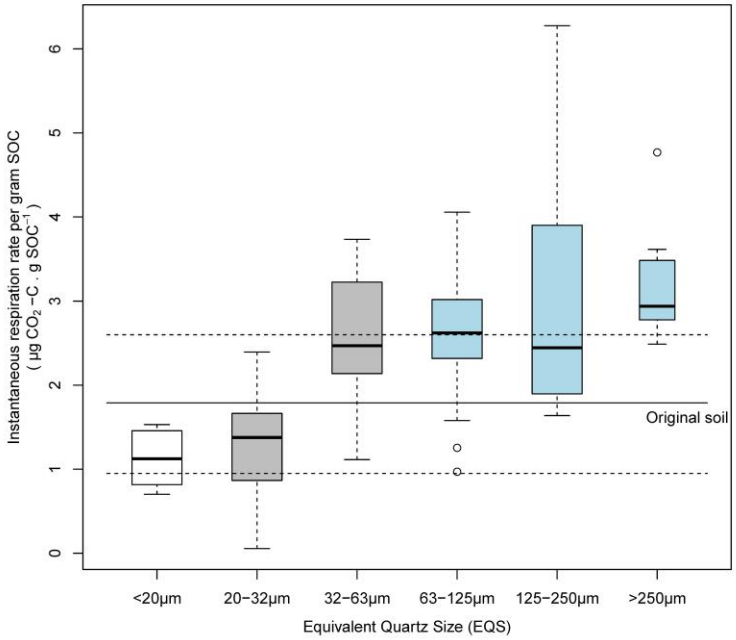

Figure 5-5 The distribution of instantaneous respiration rate per gram of soil organic carbon (SOC) in different Equivalent Quartz Size (EQS) classes of the sediment. The line denotes the average instantaneous respiration rate per gram SOC of the original soil (n = 18).

5.4. Discussion

5.4.1. Likely fate of eroded SOC in the terrestrial and aquatic system

Fractionation of eroded sediment by settling velocity shows that aggregation of source soil has a clear potential to affect movement of sediment fractions and thus the fate of associated SOC after erosion. According to the conceptual model developed by Starr et al. (2000) (Figure 5-6), the six EQS classes can be further grouped into three separate groups, each with a different likely fate: EQS < 20 µm would be likely remain suspended in runoff and hence, transferred to rivers, and all EQS > 63 µm would be re-deposited along eroding hill-slopes (Table 5-2). The intermediate EQS of 20 to 32 µm and 32 to 63 µm can have either fate, depending on localised flow hydraulics. In accordance with this model, approximately 41% of the eroded SOC from the silt loam used in this study would be re-deposited along eroding hill-slopes (Figure 5-7b). This proportion strongly contrasts against the approximately 11% SOC mass associated with coarse mineral particles > 63 µm in the original soil (Table 5-1), and is also contrary to the high SOC concentration (24.3 $mg \cdot g^{-1}$) in sediment fraction of EQS < 20 µm (Figure 5-3a). These results support our theoretical deduction that aggregation of source soil reduces the likely transport distance of eroded SOC. This would then decrease the likelihood of SOC being transferred from eroding hill-slopes to aquatic systems, but increase the amount of SOC being re-deposited into terrestrial systems. These findings are also consistent with those reported by Hu et al. (2013c), in which 79% of the SOC mass in a silty loam was associated with mineral particles of size < 32 µm, whereas 73% of the SOC mass was actually contained in aggregates of EQS > 63 µm. The distinct SOC distribution across aggregate size classes also agrees with the field investigation by Polyakov and Lal (2008), where the coarse aggregates (1 to 0.5 mm) fractionated by wet-sieving, contained up to 4.5 times more SOC than the finest fraction (< 0.05 mm). More experiments are in demand to verify the reducing effects on soils of different aggregation status and SOC contents.

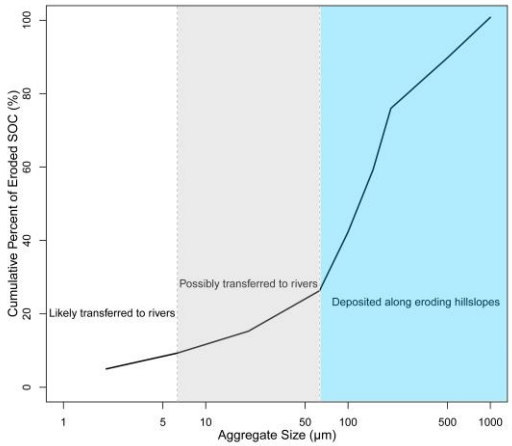

Figure 5-6 Likely fate of eroded soil organic carbon (SOC) as a function of aggregate size, re-drawn from the conceptual model developed by Starr et al. (2000). Two vertical dotted lines represent the aggregate sizes of 6.3 µm and 63 µm and represent convenient cut-off points to determine the likely fate of eroded SOC.

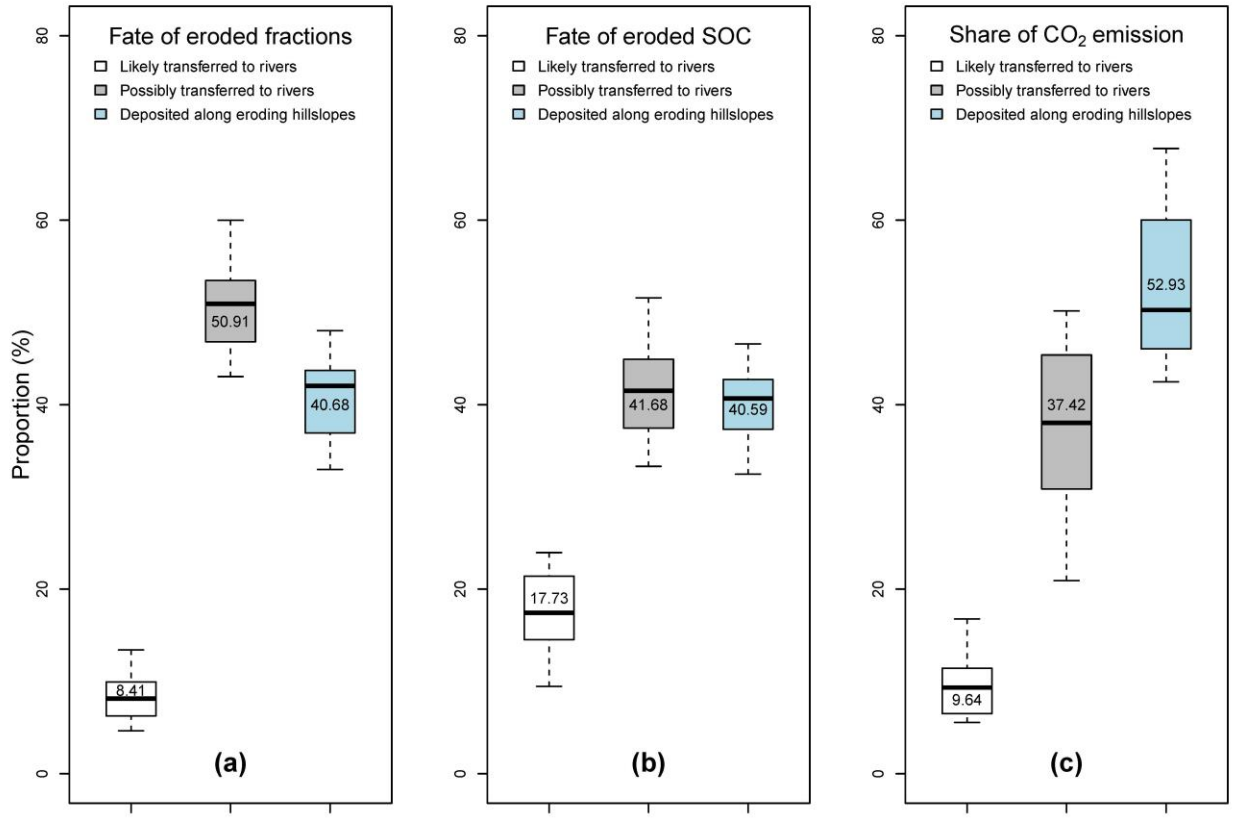

Figure 5-7 The likely fate of sediment fractions (a), eroded SOC (b), and potential share of CO_2 emission (c) by fractions that would have been likely transferred to rivers, possibly transferred to rivers, and deposited along eroding hill-slopes. The bar in box represents the median value, while numbers written in each box denote the average value. Whiskers indicate the lowest datum within 1.5 interquartile range of the lower quartile, and the highest datum within 1.5 interquartile range of the upper quartile (n = 18).

5.4.2.Erosion as a source of CO_2 flux

The effect of aggregation on the likely fate of SOC may also cast new light on understanding the effect of soil erosion on global carbon cycling. Based on the EQS specific SOC content (Figure 5-3), the potential SOC stock of a nominal 25 cm layer of topsoil on the foot-slope of a colluvial depositional site, assumingly composed of aggregates EQS > 63 µm, would be 5.1 kg·m-2 on average (Table 5-4). The potential SOC stock from the same 25 cm layer of original soil would be only 4.5 kg·m-2, or 15.5% lower than that on the foot-slope of a colluvial depositional site. Such a large difference implies that a combined model approach (Eq. 5-1), integrating the effects of aggregation on the likely fate of SOC, is demanded to adequately distinguish the proportion of SOC likely re-deposited along hillslopes from the portion potentially transferred to aquatic systems.

$$S_d \times C_d = S_e \times C_e - S_a \times C_a - C_{min} \quad \text{(Eq. 5-1)}$$

Where, S_d: mass of sediment likely to be re-deposited along hillslopes ; C_d: carbon content of sediment likely to be re-deposited along hillslopes ; S_e: mass of eroded soil; C_e: carbon content of eroded

soil; S_a: mass of sediment potentially to be transferred to aquatic systems; C_a: carbon content of sediment potentially to be transferred to aquatic systems; C_{min}:carbon mineralized during transport.

Table 5-4 Comparison between soil organic carbon (SOC) stock in top layer of 25 cm from a temporary depositional site which is theoretically composed of only three Equivalent Quartz Size (EQS) classes, and SOC stock of average original soil in the same top layer of 25 cm, as often applied in previous literature.

	EQS	SOC concentration ($mg \cdot g^{-1}$)	SOC stock ($kg \cdot m^{-2}$)[a]	Differences (%)[b]	Average SOC stock ($kg \cdot m^{-2}$)	Average differences (%)[b]
Re-distributed fractions	> 250	12.2	5.0	-11.1	5.1	-15.5
	125 - 250	15.7	6.5	-44.4		
	63 - 125	9.6	4.0	+11.1		
Original soil	NA	10.8	4.5	NA	4.5	NA

NOTE: a) Bulk densities for sediment fractions of different sizes are not available, so only particle density 1.65 $g \cdot cm^{-3}$ is applied here to have a preliminary comparison.

b) Minus (-) means underestimation compared to original soil; Plus (+) means overestimation compared to original soil.

In previous reports, C_{min} was considered to be a minor constituent in the overall carbon budget, and C_d was often assumed equivalent to the average of C_e (Stallard, 1998; Harden et al., 1999; Berhe et al., 2007; van Oost et al., 2007; Quinton et al., 2010). However, if presuming that C_e equals C_d observed in topsoil of colluvial depositional sites (e.g., in van Oost et al., 2012), then the C_d would lead to an overestimation of total SOC loss from eroding sites, because C_d is likely enriched by SOC-rich aggregates compared to C_e due to preferential deposition. Conversely, assuming C_d corresponds to C_e observed in topsoil at eroding sites (e.g., in Dlugoß et al., 2012), would neglect the potential enrichment of SOC in sediment fractions preferentially deposited on hillslopes. This would thus lead to an underestimation of C_{min} during transport. In both cases, SOC transferred to aquatic systems would be overestimated. The observed enrichment of SOC by 15.5% in sediment fractions composed only of EQS > 63 µm, indicates that the potential error of above-described estimates could be considerable. A 15.5% SOC enrichment of sediment re-deposited in the terrestrial system corresponds to the proportion of eroded SOC estimated to be deposited in permanent sinks (e.g., 0.12 Pg of SOC eroded per year by van Oost et al. 2007). While the effects of aggregation on SOC redistribution and subsequent fate cannot be assessed based on one experiment, most sediment is transported in form of aggregates (Walling, 1988; Walling and Webb, 1990). Ignoring the effect of aggregation on erosion and redistribution of SOC, therefore, bears the risk of overestimating the erosion-induced carbon sink effect. As a consequence, the behavior of aggregated sediment requires a reconsideration of existing approaches of sediment behavior in erosion models. Further study of different soil types, their aggregation and aggregate breakdown while moving through landscapes of varying topography during rainfall events of different intensity, frequency and duration, is required to assess the relevance of aggregation for SOC movement and fate identified in this study.

The risk of falsely estimating SOC losses during transport is further exacerbated by the observed instantaneous respiration rates. The instantaneous respiration rates probably merely represent a spike of SOC mineralization after erosion, and therefore, should not be extrapolated over longer periods of time. However, the 41% proportion of eroded SOC, which would likely be re-deposited along hillslopes, generated 53% of the entire instantaneous respiration (Figure 5-7c). This implies that the immediately deposited SOC is more susceptible to mineralization than both the mass of coarse sediment fractions and their SOC content would suggest. These findings are consistent with those observed by van Hemelryck et al. (2010), who reported that a significant fraction of SOC eroded from initially dry soil aggregates is mineralized after deposition. As a consequence, the preferentially deposited SOC could potentially generate a further error in the carbon source-sink balance. Such error would be particularly significant, when repeated erosion and deposition processes along hillslopes cause further disintegration of large aggregates (Kuhn et al., 2003; van Hemelryck et al., 2010). This would thereby result in additional SOC exposure and mineralization (Jacinthe et al., 2002; Six et al., 2002). Overall, as a result of preferential deposition of SOC-enriched sediment fractions and enhanced mineralization during transport, the carbon losses during transport, so far assumed to be small (van Oost et al., 2007; Quinton et al., 2010), would actually be underestimated.

5.5. Chapter conclusion

This study aimed to identify the effects of aggregation of source soil on the likely transport distance of eroded SOC and its susceptibility to mineralization after single-event transport and deposition. Our data show that 41% of the eroded SOC from a silty loam was incorporated into aggregates of EQS > 63 µm, and hence would likely be re-deposited into the terrestrial system rather than being transferred to the aquatic system. This proportion is much greater than the approximately 11% SOC mass associated with coarse mineral particles > 63 µm in the original soil (Table 5-1), and the high SOC content (24.3 $mg \cdot g^{-1}$) in sediment fraction of EQS < 20 µm would suggest. Respiration rates from sediment fractions of EQS > 63 µm also increased immediately after erosion and deposition. Both results indicate that aggregation of source soil and preferential deposition of SOC-rich coarse sediment fractions may skew the re-deposition of eroded SOC towards the terrestrial system, rather than further transfer to the alluvial or aquatic system. Consequently, a risk of overestimating lateral SOC transfer exists when mineral grain size rather than actual size of aggregated sediment is applied in erosion models. Our very limited data indicates that this error could be potentially within the same range as the current estimate of annual net erosion-induced carbon sink rate.

While based on a laboratory experiment and thus with very limited applicability to real landscapes, the potential effects of aggregation of source soil on reducing the transport distance of eroded

SOC appear to be considerable. This illustrates the need to integrate the effect of aggregation of source soil on SOC transport distance into soil erosion models (e.g., as a soil erodibility parameter), in order to adequately distinguish SOC likely re-deposited in the terrestrial system from the portion potentially transferred to aquatic systems, and further assess the implications to the global carbon cycle. Further research should, therefore, focus on the effects of preferential deposition of eroded aggregates and the fate of SOC in these aggregates whilst in-transit and during multiple rainfall events. More simulations as well as field experiments are also needed to examine the effects of various transport processes (such as slope length, slope gradients, field barriers) onto the mechanism of aggregate breakdown and aggregate specific SOC distribution. The effects of varying rainfall characteristics, crust formation, soil management and topography (e.g., Wang et al., 2008; Hu et al., 2013a) onto SOC transport should also be investigated.

Chapter 6

Different Degrees of Aggregation: How Diversely Do They Affect Likely Fate of Eroded SOC?

Manuscript in preparation, planned to submit to *Global Biogeochemical Cycles*

Abstract: During slope-scale erosion events, soil fractions and the associated soil organic carbon (SOC) are transported away from eroding sites mainly by overland flow. Eroded soil will be either gradually re-deposited along hillslopes or further transferred to river systems. Yet the re-distribution of eroded SOC during transport is not always uniform, but very often affected by preferential deposition. Under given flow conditions, the site of SOC deposition depends on the transport distances of sediment particles where SOC is stored. Very often, soil and SOC erosion risk is assessed by applying mineral particle specific SOC distribution to erosion models. However, soil is not always eroded as dispersed mineral particles, but mostly in form of aggregates. The aggregates possibly have settling velocity distinct from individual mineral particles. This may considerably change the transport distance of sediment fractions and the associated SOC. In addition, aggregation status differ SOC content in different aggregate fractions also differs from the average SOC content of original soil. Yet, little has been known about the potential effects of aggregation onto the movement and fate of eroded SOC.

In order to examine the potential effects of aggregation on the likely transport distance and the mineralizing susceptibility of eroded SOC, a simulated rainfall was applied to two soils of different texture, structure and SOC content. The eroded sediments were fractionated by a settling tube apparatus according to their likely transport distances. The mineralization potentials of the fractionated sediments were measured for 50 days. Our results show: 1) the re-deposition of eroded SOC into the terrestrial system was increased up to 64% compared to that suggested by the mineral particle specific SOC distribution. This indicates that using mineral particle specific SOC distribution, as often applied in current erosion models, would lead to under-estimation on terrestrial SOC re-deposition. 2) Over 50 days, the mineralization of SOC in the Möhlin sediment was increased by 114%, compared to the same amount of SOC in original Möhlin soil. The mineralization of the Movelier sediment was roughly equivalent to the original Movelier soil. This necessitates further investigation on the potential effects of different aggregation degrees onto the quality of eroded SOC. Overall, our results suggest that soil erosion is more likely to be a source of atmospheric CO_2.

Keywords: *erosion, aggregation, transport distance, fate of eroded SOC, carbon sink/source effects*

6.1. Introduction

During slope-scale erosion events, soil fractions and the associated soil organic carbon (SOC) are transported away from eroding sites mainly by overland flow. Afterwards, eroded SOC will be either re-deposited along hillslopes after increasing transport distances or further transferred to river systems (Starr et al., 2000; Walling, 1983). Very often, slope-scale soil and SOC erosion risk is assessed by comparing the SOC stock on eroding sites to that on colluvial depositional sites, or by applying mineral particle specific SOC distribution observed from either site to estimate the SOC stock of its counterpart (van Oost et al., 2007; Quinton et al., 2010; van Hemelryck et al., 2011; Dlugoß et al., 2012; van Oost et al., 2012). However, the re-distribution of eroded SOC during transport is not always uniform, but very often affected by preferential deposition (Kuhn et al., 2009; Hu et al., 2013b; Kuhn, 2013). The spatial variation of SOC re-distribution is strongly related to the transport distance of eroded SOC, which is dependent on the transport distances of sediment fractions. Apart from sediment discharge and hydraulic conditions (Beuselinck et al., 1998, 2000), the potential transport distances of sediment fractions are associated with their settling velocities (Beuselinck et al., 1999; Loch, 2001; Tromp-van Meerveld et al., 2008).

The distribution of settling velocities based on mineral particle size classes has been applied in some erosion / deposition models (Morgan et al., 1998; van Oost et al., 2004; Aksoy and Kavvas, 2005; Fiener et al., 2008). However, soil is not always eroded by dispersed mineral particles, but mostly in form of aggregates (Walling, 1988; Slattery and Burt, 1997; Beuselinck et al., 2000). For eroded soil particles composed of aggregates, settling velocities generally do not correspond to the average or median mineral grain size, because aggregates differ in size, density and shape from mineral particles (Johnson et al., 1996; Tromp-van Meerveld et al., 2008). Furthermore, SOC is more likely to be accumulated in macro-aggregates (Tisdall and Oades, 1982; Cambardella and Elliott, 1994), which probably have distinct settling velocities from individual mineral particles. This implies that aggregation may potentially change the settling velocities of individual mineral particles that are incorporated into aggregates, and thus alter the transport distance of the associated SOC. As a consequence, aggregation can lead to aggregate specific, rather than mineral grain specific SOC distribution across landscapes (Kuhn, 2007; Kuhn and Armstrong, 2012). Ignoring the effects of aggregation to the likely transport distance of eroded SOC would have a risk of miscalculating carbon source/sink balances (Hu and Kuhn, 2014).

The mineralization of eroded SOC during transport may add a further error to current carbon source/sink balances (Billings et al., 2010). Many reports had described accelerating SOC mineralization upon detachment or during transport of eroded soils (Jacinthe et al., 2004; Jacinthe and Lal, 2001; Polyakov and Lal, 2004). They mostly attributed it to structural breakdown of aggregates, thereby exposing the previously protected SOC to microbial processes (Six et al., 2002; Lal and Pimentel, 2008;

van Hemelryck et al., 2010). Therefore, Lal and his colleagues proposed that SOC mineralization during transport should be included in SOC erosion models (Jacinthe et al., 2004; Jacinthe and Lal, 2001; Polyakov and Lal, 2004). But other reports argued that large loads of sediment are moved during rapid transport, thus SOC loss by mineralization during transport is of minor importance, and hence could be ignored when calculating carbon balances (van Oost et al., 2007; Quinton et al., 2010). To solve these discrepancies, it is required to identify the quality of eroded SOC that has different transport distances.

Our previous studies (Hu et al., 2013b; Hu and Kuhn, 2014; Xiao et al., submitted), after examining the SOC content in sediment fractions of different likely transport distances, had found that 41% of the eroded SOC would be likely re-deposited down eroding hillslopes with coarse aggregates. The results also show that erosion and transport tend to accelerate the mineralization of eroded SOC immediately after erosion. While their findings confirm the necessity to account for the mineralization of eroded SOC during transport when calculating slope-scale carbon balances, the results were observed with only one type of soil after instantaneous mineralization potentials. Long-term monitoring on a wider range of soil is required to examine the effects of different degrees of aggregations, so as to quantify the potential contribution of eroded SOC to atmospheric CO_2. Therefore, this study, as a follow-up experiment to previous studies (Hu et al., 2013b; Hu and Kuhn, 2014), aims to examine the potential effects of different degrees of aggregation onto the likely transport distance of eroded SOC, as well to examine the long-term mineralization potential of eroded SOC during transport.

6.2. Materials and Methods

6.2.1. Soil sampling and preparation

Two Luvisols, a sitly loam from Möhlin (47˚ 33’ N, 7˚ 50’ E) and a silty clay from Movelier (47˚ 24’ N, 7˚ 18’ E), near Basel in northwest of Switzerland, were used in this study. Both soils were sampled from farmlands in December, 2012, and were immediately air-dried after sampling. They had distinct mineral grain size distribution, SOC content (LECO RC 612 at 550°C) and aggregate stability (method adapted from Nimmo and Perkins, 2002) (Table 6-1). The mineral particle size distribution was fractionated by wet-sieving, after dispersion by ultrasound using a Sonifier Model 250 from Branson, USA. The energy dissipated in the water/soil suspension was 60 $J \cdot ml^{-1}$ (i.e. Energy = output power 70 W × time 85 s / suspension volume 100 ml). The SOC mass proportions across mineral particle size classes were calculated only from average values of individual weight and SOC content. Previous studies on the same Möhlin soil had shown that aggregation potentially facilitates the settling velocities of individual mineral particles and thus reduces the likely transport distance of the associated SOC (Hu et al., 2013c; Hu and Kuhn, 2014). Hence, it is speculated that similar effects would also occur to other types of soil,

provided SOC is the dominant binding agent to form aggregates. This thus makes the silty loam from Möhlin and the silty clay from Movelier suitable to investigate the potential effects of different aggregate degrees onto the fate of eroded SOC.

Table 6-1 Selected properties of the original Möhlin and Movelier soil

		Mineral Particle Size (µm)					General SOC ($mg \cdot g^{-1}$)	Aggregates > 250 µm (%)
		<32	**32-63**	**63-125**	**125-250**	**>250**		
Möhlin	Weight (%)	$60.6_{\pm 1.3}$	$29.1_{\pm 1.6}$	$6.4_{\pm 0.1}$	$2.0_{\pm 0.2}$	$1.9_{\pm 0.1}$		
	SOC ($mg \cdot g^{-1}$)	$17.9_{\pm 0.7}$	$4.9_{\pm 1.0}$	$10.3_{\pm 2.6}$	$14.9_{\pm 2.4}$	$23.1^{a}{}_{\pm 4.4}$	$14.0_{\pm 0.2}$	$67.24_{\pm 7.9}$
	SOC mass (%)	79.3	10.3	4.8	2.2	3.3		
Movelier	Weight (%)	$62.2_{\pm 1.5}$	$12.7_{\pm 0.5}$	$9.8_{\pm 1.8}$	$4.5_{\pm 0.7}$	$10.7_{\pm 1.0}$		
	SOC ($mg \cdot g^{-1}$)	$46.8_{\pm 6.3}$	$42.0_{\pm 9.7}$	$47.3_{\pm 1.9}$	$68.0_{\pm 5.4}$	$30.3^{a}{}_{\pm 2.5}$	$42.8_{\pm 1.0}$	$91.37_{\pm 1.0}$
	SOC mass (%)	64.0	11.7	10.3	6.8	7.1		

NOTE: a) Might be over-estimated due to the mixture of minute amount of residue or straw, which was previously incorporated into the aggregates but then released by dispersion and blended with coarse particles. Lower case numbers indicate the range of minimum and maximum values (n = 3)

6.2.2. Rainfall simulation

The experiments consisted of three components (Figure 6-1): 1) rainfall simulation to generate sediments; 2) fractionation of the eroded sediments by a settling tube apparatus into six settling velocity classes; and 3) incubation of each settling class for 50 days to observe their long-term mineralization potentials. The experiments were repeated three times in order to generate reliable erosion and respiration data.

Two parallel halves of a 150 × 80 cm^2 flume (40 cm wide for each half) were pitched at a 15% gradient (Figure 6-1). One of each half was filled with the Möhlin and Movelier soil (depth of 5 cm). To assist drainage, the base of the flume was perforated and covered with a fine cloth and a layer of sand (c.a., 5 cm). Preliminary tests had revealed that a flume of this size could generate sufficient runoff to initiate non-selective erosion on the two soils. The soils were sieved into aggregates of a diameter less than 5 mm. Over-sized clods were excluded in order to reduce variations in surface roughness, both within the flume and between replicates. Leveling the surface was also managed to ensure that large roughness elements, in particular depressions, did not inhibit movement of aggregates across the flume and thereby prevent selective deposition on the soil surface.

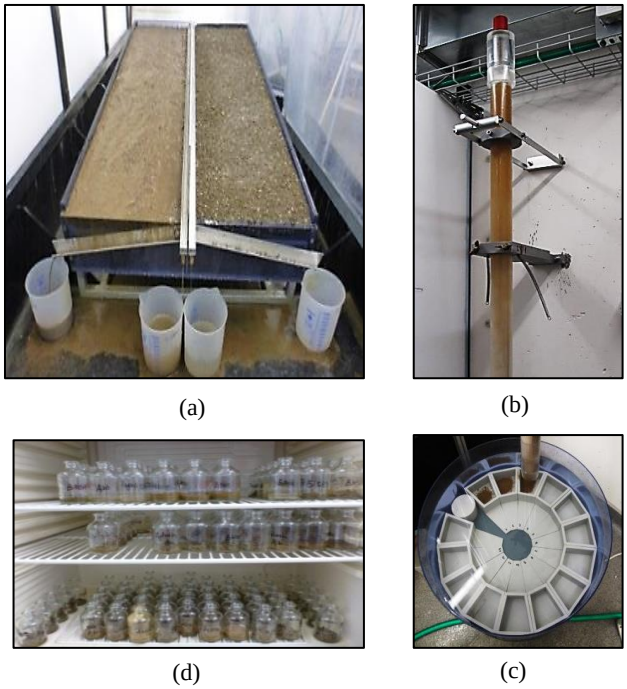

(a) (b)

(d) (c)

Figure 6-1 The experimental set-up: the rainfall simulation flume (a), the settling tube apparatus (b), the turntable to collect the fractionated sediment (c), and the incubation of the fractionated sediments (d).

A FullJet nozzle of ½ HH 50WSQ, installed 2 m high above the soil surface, was used to simulate the rainfalls (Figure 6-1a). The simulated rainfalls had an intensity of 200 mm h^{-1}. Previous studies on the same Möhlin soil had shown that it required about 90 mm of rainfall to develop non-selective erosion (Hu et al., 2013a). Hence, the simulated rainfalls lasted for 30 min for the Möhlin soil, and the runoff (and sediment) samples were collected every 2 min. For the Movelier soil, given its much greater aggregate stability (Table 1), the same simulated rainfalls were lasted for 2 h. The runoff (and sediment) samples from the Movelier soil were collected every 10 min. A rainfall of intensity 200 mm h^{-1} and lasting for 30 min or 2 h is unlikely in either Möhlin and Movelier region, where precipitation intensity is around 35 mm h^{-1} (MeteoSwiss, 2013). But increased intensity is often considered necessary to compensate for the deficiency of kinetic energy associated with simulated rainfalls, so as to create comparable conditions to natural rainfalls (Dunkerley, 2008; Iserloh et al., 2013). Therefore, the simulated rainfall used in this study was particularly chosen to sufficiently destroy aggregates, so that the eroded sediments were less likely to experience further breakdown during the subsequent settling velocity fractionation.

Tap water, with an electric conductivity of 2220 $\mu s \cdot cm^{-1}$, which is five times higher than natural rainwater in Basel, was used during each rainfall simulation. In general, the increased electric conductivity associated with tap water increases soil dispersion during tests using simulated rainfall (Borselli et al., 2001). Despite this, however, comparative aggregate stability tests showed only a 7% less for the Möhlin

soil and 1% less for the Movelier soil between rainwater sampled in Basel and ordinary tap water, thus making tap water acceptable.

6.2.3. Sediment fractionation by a settling tube apparatus

The sediment fractionation was conducted with a 1.8 m long settling tube apparatus (Figure 6-1b). The settling tube apparatus consists of four components: the settling tube, through which the soil sample settles; the injection device, by which the soil sample is introduced into the tube; the turntable (Figure 6-1c), within which the fractionated subsamples are collected; and the control panel, which allows an operator to control the rotational speed and resting/moving intervals of the turntable. Detailed descriptions about the settling tube apparatus can refer to Hu et al. (2013b). To control the number of subsamples under practical size, during each rainfall event, only the sediment samples collected at 6 min, 16 min and 30 min from the Möhlin soil, and those collected at 20 min, 60 min, and 120 min from the Movelier soil, were used to carry out settling fractionation. Sediments collected in such manner were assumed representative to reflect the sediment compositions over simulated rainfalls. After collected from the eroding flume, these sediments were allowed to settle for 1 h in collection beakers (height of 20 cm), before fractionated by the settling tube apparatus. The supernatant and remaining suspended sediment (corresponding to EQS < 8 μm) was then decanted off and added to the < 20 μm fraction remaining in suspension in the settling tube (described as following). Previous measurements confirmed that > 95% of the total mass settled after this pre-treatment (Hu and Kuhn, 2014).

Table 6-2 The six settling velocities based on the Equivalent Quartz Size (EQS) classes, and the likely fate of eroded fractions based on the conceptual model developed by Starr et al. (2000). The settling distance was 1.8 m.

EQS (μm)	Settling velocity ($m \cdot s^{-1}$)	Settling time (s)	Likely fate
> 250	$>4.5 \times 10^{-2}$	< 40	Landscape deposition
125 - 250	$1.5 \times 10^{-2} - 4.5 \times 10^{-2}$	40 - 120	
63 - 125	$3.0 \times 10^{-3} - 1.5 \times 10^{-2}$	120 - 600	
32 - 63	$1.0 \times 10^{-3} - 3.0 \times 10^{-3}$	600 - 1800	Possible transfer to rivers
20 - 32	$3.3 \times 10^{-4} - 1.0 \times 10^{-3}$	1800 - 5400	
< 20	$< 3.3 \times 10^{-4}$	> 5400	Likely transfer to rivers

Six particle size classes, based on the concept of Equivalent Quartz Size (EQS) described in Hu et al. (2013a), were selected according to their likely transport distances after erosion (Table 6-2). EQS represents the diameter of a nominal spherical quartz particle that would fall with the same velocity as the aggregated particle for which fall velocity is measured (adopted from Loch, 2001). The six EQS classes were converted to six settling velocities and corresponding settling times using Stokes' Law (Hu et al., 2013b). The use of Stokes' Law to convert EQS into settling velocity is, in the strictest sense, limited to particles < 70 μm (Rubey, 1933). From the perspective of terrestrial and aquatic systems (Starr et al.,

2000), all fractions of EQS > 63 µm are considered as one group that is likely to be re-deposited along hill-slopes (Table 6-2). Hence, the potential error when using Stokes' Law to calculate the settling velocities of fractions of all sizes is considered rational. In addition, with the current settling tube (length of 1.8 m), any fractions finer than 20 µm (settling time longer than 1.5 h) were not further fractionated to save time.

6.2.4. Sediment respiration rate measurement

After fractionation, the sediment samples were transferred into flasks (60 cm^3), and incubated at 20˚C (flasks open) (Figure 6-1d). Soil respiration rates of different sediment fractions were measured based on the method described in Robertson et al. (1999) and Zibilske (1994). Ten replicates of original undisturbed soils (about 10 g for each replicate) were also prepared and measured in the same way to generate references. Prior to respiration measurements, all flasks were sealed using rubber stoppers. Gas from the headspace of each sealed flask was extracted at the beginning and end of the 1 h sampling period. The differences of CO_2 concentrations between the two times were used to represent the soil respiration rate during the period of 1 h. Such respiration rate measurements were repeated at day 1, 2, 3, 6, 10, 18, 26, 34, 42, and 50. Concentrations of CO_2 were measured using a SRI8610C Gas Chromatograph (SRI Instruments, etc.). During the 50 days of incubation, the wet weight of each fraction was monitored every 3 days, and the variation of soil moisture was constrained within 1%.

6.2.5. Laboratory measurements

The sediment samples that were not used for settling fractionation were allowed to settle for 48 h. The supernatant was then decanted off, and the sediments were dried at 40°C and weighed. The SOC contents of the original soils, the fractions of six EQS, and the sediments samples were measured by a Leco RC 612 at 550˚C. The SOC mass of each settling class was calculated from its SOC content and weight. Data analysis was carried out using Microsoft Excel 2010 and R studio software packages (R version 2.15.1).

6.3. Results

6.3.1. Spatial distribution of eroded SOC

The SOC contents in six EQS classes of the sediment from both soils are shown in Figure 2. For the Möhlin sediment, the eroded fractions of EQS > 63 µm in general had equivalent SOC content to the original Möhlin soil (Figure 6-2a). Yet, in the Movelier sediment (Figure 6-2b), the SOC contents in EQS classes of 63 to 250 µm were much greater than that of the original Movelier soil. After multiplying the weight distribution of eroded fractions with their SOC contents, the likely re-distribution of eroded SOC

from the two soils is shown in Figure 6-3. Out of the total 5622 mg SOC eroded from the Möhlin soil, 63% was likely to be re-deposited along hillslopes, while only 6% was likely to be transferred into rivers (Figure 6-3a). For the Movelier sediment, the effects of aggregation to generate terrestrial re-deposition were even more pronounced (Figure 6-3b). Out of the total 3463 mg eroded SOC, 88% was potentially re-deposited along hillslopes, whereas only 4% likely transferred into rivers.

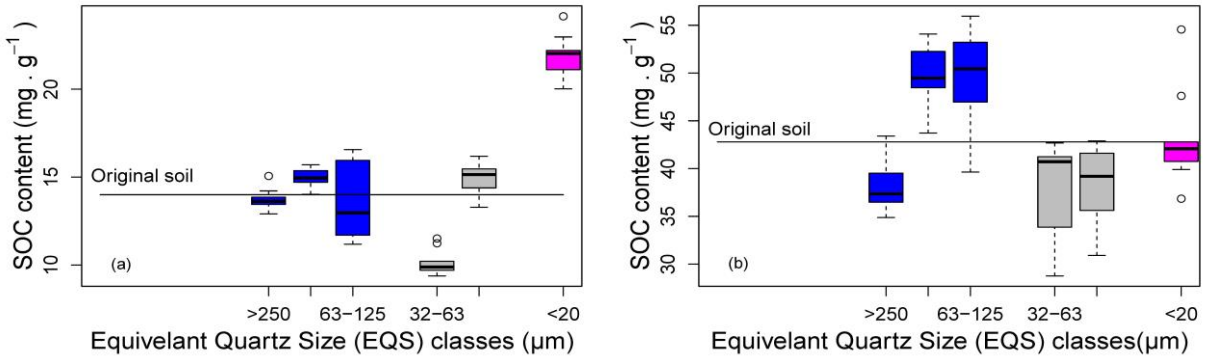

Figure 6-2. The soil organic carbon (SOC) content of different eroded fractions from the Möhlin (a) and Movelier soil (b). The two straight lines across the figure denote the SOC content of the original Möhlin and Movelier soil. The colors of the boxes correspond to their likely fate. See section 6.2.3 for the definition and explanation of the three manners of likely fate of sediment and eroded SOC (*n*=9).

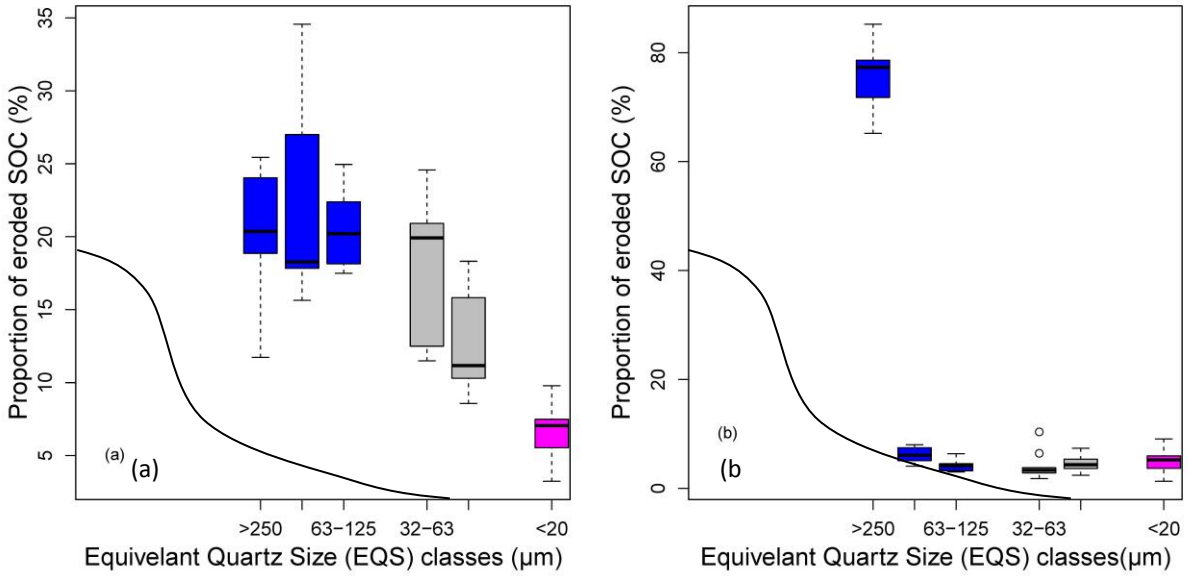

Figure 6-3. The likely spatial re-distribution of eroded soil organic carbon (SOC) from the Möhlin (a) and Movelier soil (b) after a slope-scale erosion event. The curves represent a hillslope profile, helping to visualize the likely transit of eroded sediment from the eroding site on the slope shoulder, to the colluvial depositional site on slope tail, and further to the alluvial or aquatic system. The colors of the boxes correspond to their likely fate. See section 6.2.3 for the definition and explanation of the three manners of likely fate of sediment and eroded SOC (*n*=9).

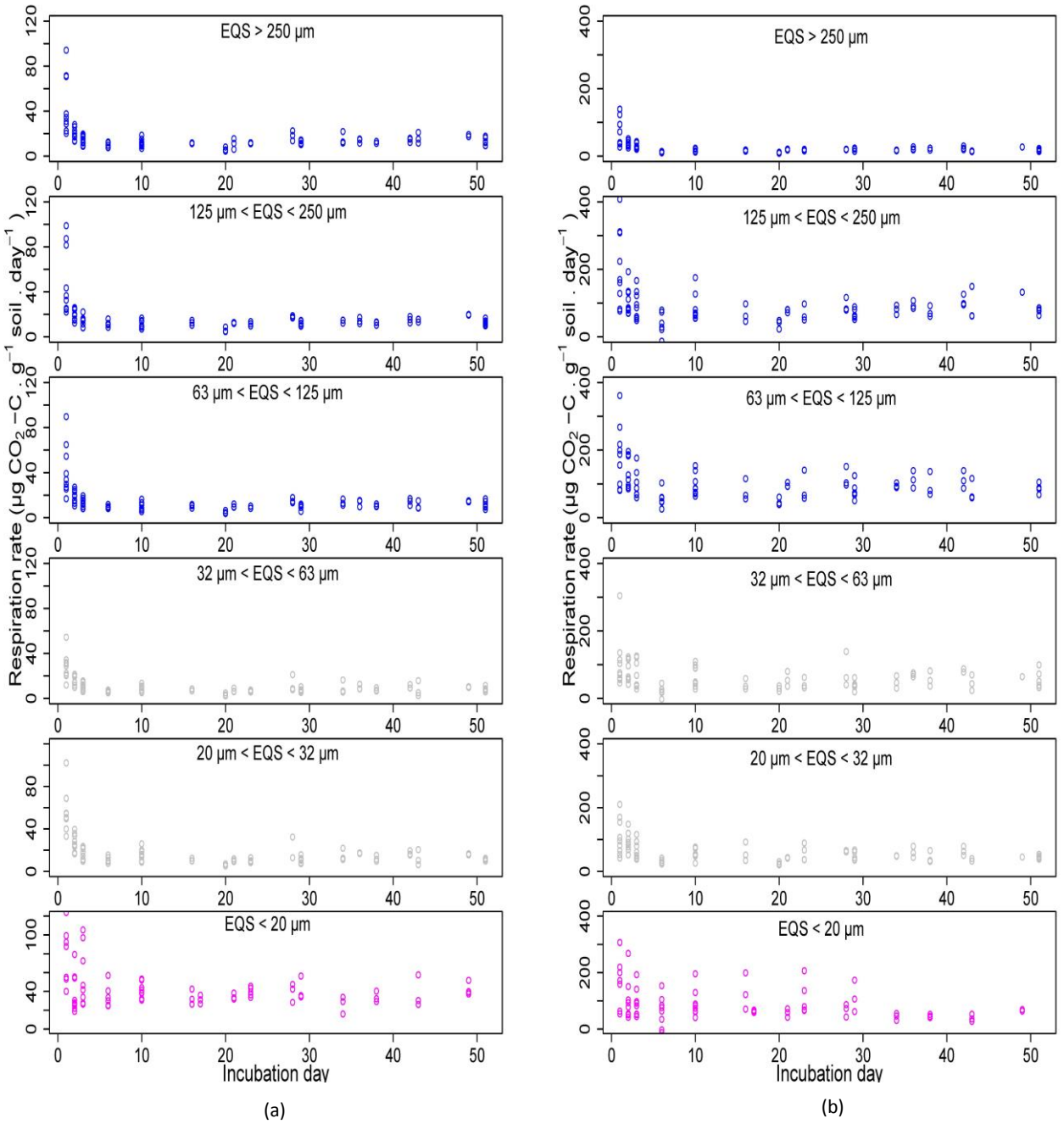

Figure 6-4. The respiration rates of eroded soil organic carbon (SOC) associated with different Equivalent Quartz Size (EQS) fractions from Möhlin (a) and Movelier (b) soil (*n*=9).

6.3.2.Long-term mineralization potential of eroded SOC fractions

The respiration rates of different SOC fractions from the two soils show similar temporal tendencies over the 50 days (Figure 6-4a, b): high rates at the beginning 10 days, followed by a rapid decline, and stayed constant during the last 30 days. The cumulative respiration rates (Figure 6-5a, b) show that most of the SOC in both the Möhlin and the Movelier sediment were more susceptible to mineralization than that in the original soils. In addition, the respiration potentials differed distinctively

across different EQS classes (Figure 6-5a, b). Among the six EQS classes, eroded SOC in the Möhlin sediment class of EQS < 20 µm was most susceptible (Figure 6-5a), while in the Movelier sediment, it was the classes of EQS from 63 to 250 µm that had the highest respiration rates (Figure 6-5b).

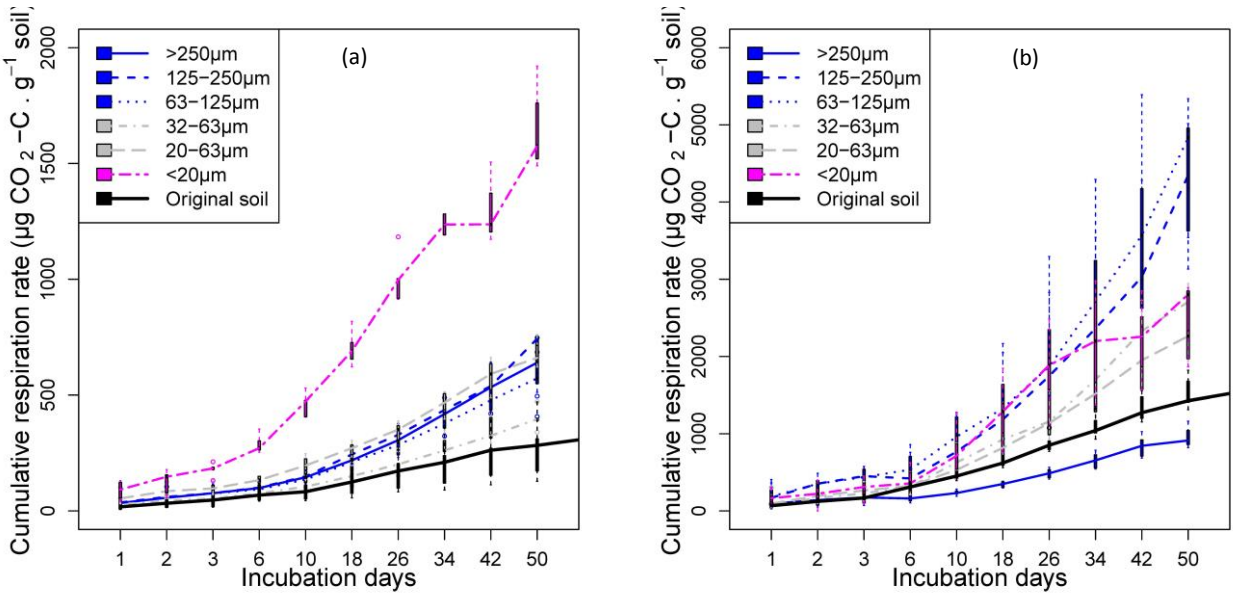

Figure 6-5. The cumulative respiration rates of eroded soil organic carbon (SOC) associated with different EQS fractions from Möhlin (a) and Movelier (b) soil over 50 days. Colors of the boxes and lines correspond to the likely fate of different eroded fractions. See section 6.2.3 for the definition and explanation of the three manners of likely fate of sediment and eroded SOC (*n*=9).

6.3.3.Erosion-induced additional SOC mineralization

The potential shares of CO_2 emission from SOC in different EQS classes are shown in Table 3. Overall, about 272 mg or 4.8% of the SOC eroded from the Möhlin soil was mineralized into CO_2 (Table 6-3). Out of that, about 63% was potentially released from the SOC that was likely to be re-deposited along hillslopes (Figure 6-6a). While the finest particles of EQS < 20 µm from the Möhlin sediment had the highest susceptibility to mineralization, they were of limited mass and hence only responsible for 12% of the entire CO_2 emission (Figure 6-6a). From the Movelier sediment, about 85 mg or 2.5% of the eroded SOC was mineralized into CO_2 (Table 6-3). Out of that, 78% was potentially released from the SOC that was likely to be re-deposited along hillslopes (Figure 6-6b). In addition, the extents of erosion-induced additional SOC mineralization differed greatly between the two soils. The CO_2 from the eroded Möhlin sediment (272 mg) was 114% more than that of the same amount of original soil (127 mg) (Table 6-3). Yet, the CO_2 released from the Movelier sediment (85 mg) was roughly equivalent (9% less) to that from the same amount of the original soil (93 mg) (Table 6-3).

Table 6-3. The summary of the amount of sediment fractions, eroded soil organic carbon (SOC), and entire CO_2 emission, and their likely spatial distribution and potential shares from fractions of three different likely fates. The additional SOC mineralization represents the additional CO_2 emissions compared to the same amount of SOC if stored in original soils.

	Möhlin			**Movelier**		
	Fractions	**SOC**	**CO_2-C**	**Fractions**	**SOC**	**CO_2-C**
Eroded sediment	430 g	5622 mg	272 mg	57 g	3463 mg	85 mg
	Likely spatial re-distribution			Likely spatial re-distribution		
Re-deposited along hillslopes	60%	63%	63%	87%	88%	78%
Possibly transferred into rivers	36%	31%	25%	9%	8%	14%
Likely transferred into rivers	4%	6%	12%	4%	4%	8%
Original soil			127 mg			93 mg
Additional CO_2 emission			+114%			-9%

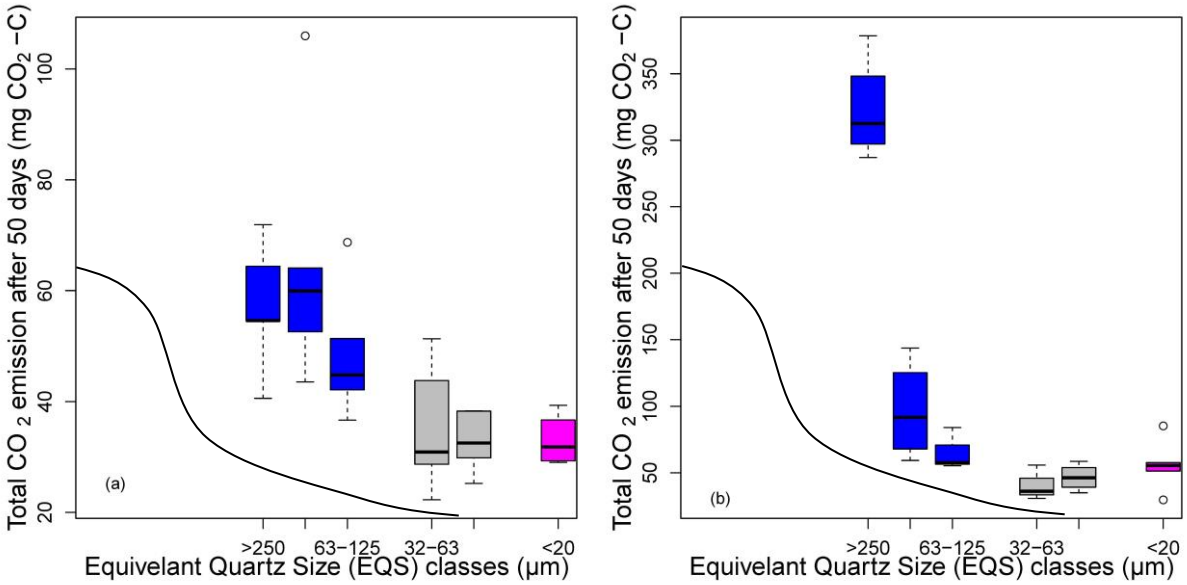

Figure 6-6. The potential shares of CO_2 emission from eroded soil organic carbon (SOC) of different likely fates after eroded from the Möhlin (a) and Movelier soil (b). The curves represent a hillslope profile, helping to visualize the likely transit of eroded sediment from the eroding site on the slope shoulder, to the colluvial depositional site on slope tail, and further to the alluvial or aquatic system. The colors of the boxes correspond to their likely fate. See section 6.2.3 for the definition and explanation of the three manners of likely fate of sediment and eroded SOC (*n*=9).

6.4. Discussion

6.4.1. Aggregation skewing the spatial re-distribution of eroded SOC

The contrasting SOC distributions between the six EQS classes and the mineral particle size classes of both the Möhlin and Movelier soil clearly demonstrate the potential effects of aggregation to the fate of eroded SOC. The results show that 63% of eroded SOC from the Möhlin sediment is likely be re-

deposited along hillslopes (Figure 6-2a). This is strongly contrasting against the mineral particle specific SOC distribution of original Möhlin soil, which suggests that 79% SOC would be likely to be transferred into rivers with mineral particles finer than 32 µm (Table 6-1). Such contradictory estimates on the spatial re-distribution of eroded SOC are mostly attributed to the effects of aggregation in facilitating the settling velocity of individual mineral particles, and thus reducing the likely transport distance of the associated SOC. These findings confirm the observations in previous reports (Hu et al., 2013b; Hu and Kuhn, 2014), where the terrestrial SOC deposition from the same Möhlin soil is 31% greater than the mineral particle specific SOC distribution would suggest. An even more pronounced skew of SOC distribution was observed in the Movelier sediment (Figure 6-2b compared with Table 6-1). Such effects of aggregation onto the transport distance of eroded SOC illustrate that current slope-scale carbon balances should ascribe more credits to the terrestrial SOC deposition, and accordingly attribute less to loss SOC to the aquatic system.

Table 6-4 Comparison between the soil organic carbon (SOC) stock of a nominal 25 cm layer of Movelier topsoil on the foot-slope of a colluvial depositional site, which is theoretically composed of only three Equivalent Quartz Size (EQS) classes, and the SOC stock of average original Movelier in the same top layer of 25 cm, as often applied in previous literature.

	EQS class (µm)	SOC concentration ($mg \cdot g^{-1}$)	Density ($g \cdot cm^{-3}$)	Depth (cm)	SOC stock ($kg \cdot m^{-2}$)	SOC stock on average ($kg \cdot m^{-2}$)	Relative differences (%)[a]	Relative difference on average (%)[a]
Re-deposited sediment fractions	> 250	38.1	1.5	25	14.3	17.5	4.9	-11.4
	125 to 250	49.6	1.8	25	22.3		-32.9	
	63 to125	49.1	1.3	25	16.0		-6.1	
Original Movelier	NA	42.8	1.4	25	15.0	15.0	NA	NA

NOTE: a) Minus (-) means underestimation compared to original Movelier soil; Plus (+) means overestimation compared to original Movelier soil.

The potential SOC stock of a nominal 25 cm layer of Movelier topsoil on the foot-slope of a colluvial depositional site, assumingly composed of aggregates EQS > 63 µm, would be 17.5 $kg \cdot m^{-2}$ on average (Table 6-4). The potential SOC stock from the same 25 cm layer of the original Movelier soil would be only 15.0 $kg \cdot m^{-2}$, or 11.4% lower than that on the foot-slope of a colluvial depositional site. This 11.4% SOC enrichment of the Movelier sediment re-deposited in the terrestrial system in general agrees with the 15.5% enrichment estimated from the Möhlin sediment in Hu and Kuhn (2014). As a second type of aggregated soil, the SOC enrichment of the Movelier sediment re-deposited in the terrestrial system confirms the skewing effects of aggregation onto SOC re-distribution. While two types of soil such as the Möhlin and Movelier cannot fully represent the global soil diversities, such 15.5% and 11.4% SOC enrichment in re-deposited sediment implies that under-estimation of terrestrial SOC deposition in current

carbon balances (e.g., Berhe et al., 2007; Dlugoß et al., 2012; van Oost et al., 2012) could be considerable. Consequently, ignoring the effects of aggregation onto re-distribution of eroded SOC would bear a considerable risk of overestimating the erosion-induced carbon sink effects. Our results reaffirm the possibility that preferential re-deposition of SOC-enriched aggregates into terrestrial systems might be roughly on the same magnitude of the currently estimated carbon sink strength van Oost et al. (2007), thereby making the erosion-induced sink effects approach zero.

6.4.2.Erosion induced additional CO_2 to the atmosphere

The erosion-induced mineralization of eroded SOC would add a further error onto the currently estimated carbon sink effects. Our data show that the mineralization of the Möhlin sediment was significantly increased by 114%, compared to the same amount of original Möhlin soil (Table 6-3). It can be attributed to the relatively poor aggregation of the Möhlin soil (Table 6-1), which was apt to break coarse aggregates into finer fractions upon raindrop impact, releasing the otherwise encapsulated SOC to the environment. Such observation agrees with the statement made by Lal and his colleagues that erosion and transport processes tend to break down aggregates, thereby exposing previously protected SOC to the environment and thus potentially contributing additional CO_2 to the atmosphere (Polyakov and Lal, 2004; Lal and Pimentel, 2008; Polyakov and Lal, 2008). Further disintegration of aggregates after repeated erosion and deposition processes are speculated to induce more additional CO_2 emissions (van Hemelryck et al., 2010; Kuhn, 2013). However, the total CO_2 emissions from the Movelier sediment were not as appreciably accelerated by erosion as those from the Möhlin sediment (Table 6-3). It can be explained by their different degrees of aggregation of the two soils (Table 6-1). Among the six EQS classes of the Movelier sediment, the eroded aggregates of EQS between 63 and 250 µm had the highest respiration rates. These aggregates, suggested by the great aggregate stability of the original Movelier soil (Table 6-1), probably barely broke down during erosion and transport. They thus were less likely to introduce extra exposure of SOC to be mineralized. Under the same simulated rainfall conditions, the distinct degrees of sensitivity to erosion-induced mineralization demonstrate the diverse effects of aggregation to the likely fate of eroded SOC. Similar discrepancies can also be captured from the two reports from Polyakov and Lal. On the silt loam used in Polyakov and Lal (2004), the mineralization rate in mid-size sediment fractions (53 to 250 µm) was 2 to 4 times greater than that from coarse and fine fractions. Nevertheless, on the clay loam investigated in Polyakov and Lal (2008), the amount of CO_2 released from coarse size sediment fractions (0.282 g $C \cdot kg^{-1}$ $soil \cdot d^{-1}$) was 9 times greater than that in fine fractions (0.032 g $C \cdot kg^{-1}$ $soil \cdot d^{-1}$). Overall, the mineralization potential of eroded SOC differed from that of SOC stored in intact soil. The significance of erosion-induced additional SOC mineralization is dependent on the degrees of aggregation and the quality of SOC in different fractions. This thus urges further investigation on the potential effects of different aggregation degrees onto the fate of eroded SOC.

6.5. Chapter conclusion

This study aimed to identify the significance of the aggregation effects onto the re-deposition of eroded SOC and its susceptibility to mineralization during transport. The results demonstrate that effects of aggregation considerably reduced the likely transport distance of eroded SOC, and hence potentially skewed its re-distribution towards the terrestrial deposition. The skewing pattern of SOC re-distribution was more pronounced in the better-aggregated silty clay from Movlier than in the silty loam from Möhlin. Such findings may profoundly alter our current understanding of erosion-induced lateral SOC transfer from eroding to depositional sites. Since soil is mostly eroded in form of aggregates, our results necessitate that current slope-scale carbon balances should incorporate the terrestrial SOC deposition. The effects of aggregation on the re-distribution and subsequent fate of eroded SOC were also exacerbated by the mineralization of eroded SOC. Over 50 days, the mineralization of the Möhlin sediment significantly increased compared to the same amount of original soil. This could add a further error onto current carbon sink effects. Yet the roughly equivalent CO_2 emissions from the Movelier sediment to the original Movelier soil indicate that more research is required to get a full understanding of the effects of different degrees of aggregation onto the fate of eroded SOC. Overall, the potential terrestrial SOC re-deposition and the increased mineralization of eroded SOC suggest that soil erosion is more likely to be a source of atmospheric CO_2. More field sampling along hillslopes on a wider range of soils under various rainfall regimes across larger erosion scales are required.

Chapter 7

Summary and Conclusions

7.1. Summary of primary results from each experiment

The aim of this study was to investigate the potential impacts of the temporal variation of SOC erosion and the spatial variation of SOC deposition on the fate of eroded SOC on hillslopes. By addressing these aims, this study is intended to improve our current understanding of the potential role of soil erosion, as a sink or source to atmospheric CO_2. Four specific knowledge gaps were thus identified: 1) crusting and erosion-induced temporal variation of SOC erosion; 2) significance of inherent inter-replicate variability under ideally controlled conditions; 3) aggregation effects on the likely transport distance of eroded SOC; 4) erosion-induced mineralization of eroded SOC during transport. A series of experiments was conducted to address these knowledge gaps (Table 1-2). Experimental designs, results, discussions and conclusions of each experiment were described in different chapters. Primary results and conclusions of all the experiments are summarized here as an overview of this study.

Chapter 2 described the temporal variation of SOC enrichment during prolonged rainfall events observed from the *SOC-Variability* experiment. Two silty loams of different tillage managements were subjected to a simulated rainfall of intensity 30 mm h^{-1} for 6 h. Runoff and sediment were sampled every 30 min, and the entire rainfall events were repeated for ten times. The SOC enrichment ratio (ER_{SOC}) of eroded sediment from both soils varied with rainfall time, increased first, peaked around achieving runoff steady-state, and declined afterwards (Figure 2-4). The variation of ER_{SOC} from the organically farmed soil always delayed and was less pronounced than that from the conventionally managed soil. The results of this *SOC-Variability* experiment illustrate that the ER_{SOC} of eroded sediment cannot be constant or always greater than unity, but varies with rainfall time due to the evolvement of crusting and erosion. This agrees with conservation of mass that the ER_{SOC} of sediment must be balanced over time by a decline of SOC in the source area material. While the prolonged rainfall (6 h) used here is very limited in its applicability under natural conditions, observations in this study caution that a "constant" ER_{SOC} of sediment is biased, leading to an overestimation of SOC erosion, unless the ER_{SOC} was determined for the entire crust formation.

Chapter 3 mainly examined the significance of two types of variability during SOC erosion events conducted in the *SOC-Variability* experiment: 1) the simulated rainfall was repeated ten times under most achievably uniform conditions, to enable statistical analysis of inter-replicate variability caused by the

non-eliminable variations of rainfall characteristics, soil properties, erosion, crusting and their interactions; and 2) a two-step erosion model was developed based on the infiltration, runoff and soil erosion data obtained from six selected sub-events to examine the systematic variability derived from crusting evolvement over rainfall time. The results show that: i) the inter-replicate variability of runoff and soil erosion rates considerably declined over rainfall time (Figure 3-6). Yet, even after maximum runoff and erosion rates were reached, the inter-replicate variability still remained between 15 and 39%, indicating the existence of significant inter-replicate variability even under ideally controlled conditions; and ii) the increasingly improved predictions with extending event durations (Figure 3-7 and 3-8) suggest that SOC erosion may inevitably bear a systematic variability, due to crusting evolvement and temporally varying SOC enrichment ratios. Thus, observations from short events cannot be directly extrapolated to predict soil and SOC loss over prolonged events and vice versa.

Chapter 4 mainly described the design and operation rationale of a settling tube apparatus in *SOC-Settling* experiment. In order to exclude the bias estimation in current soil erosion models induced by mineral particle size distribution, a settling tube apparatus was built up to fractionate soils according to the settling velocities of actual aggregate fractions. By comparing the different distributions of SOC between aggregates and dispersed mineral particles (Figure 4-6), the results show that aggregation strongly affects settling velocities as opposed to the texture of mineral grains. Soil aggregation status, therefore, should be considered in erosion models. This also illustrates that settling velocity is a suitable parameter to physically connect the re-distribution of eroded SOC to overland flow transport processes.

In Chapter 5, the settling tube apparatus was applied to fractionate eroded sediment generated from the experiment *SOC-Aggregation 1*. The results indicate that: 1) aggregation effects considerably facilitate the settling velocities of individual mineral particles, and thus reduce the likely transport distance of the associated SOC, potentially skewing the re-deposition of SOC-rich aggregates towards the terrestrial system. In current slope-scale carbon balance calculations, SOC stock at eroding sites is often presumed to equal the SOC stock observed in the topsoil of colluvial depositional sites (Table 5-4). Thus, the preferentially deposited SOC-rich aggregates in topsoil of colluvial depositional sites would lead to an overestimation of total SOC loss from eroding sites. Conversely, assuming SOC stock observed in the topsoil of colluvial depositional sites corresponds to SOC stocks observed in the topsoil at eroding sites, would neglect the potential enrichment of SOC in sediment fractions that is preferentially deposited on hill slopes. This would thus lead to an underestimation of SOC mineralization during transport. In both cases, SOC transferred to the aquatic system would be overestimated. 2) Erosion was prone to accelerate the mineralization of eroded SOC immediately after erosion, and thus might contribute additional CO_2 to the atmosphere (Figure 5-5 and 5-7). This would potentially generate a further error into the carbon source-

sink balances, particularly when repeated erosion and deposition processes along hill-slopes prompt further disintegration of large aggregates, thereby resulting in advanced SOC exposure and mineralization.

The experiment *SOC-Aggregation 2* in Chapter 6 was mainly an extension of the experiment *SOC-Aggregation 1,* to compare the results observed from a single soil to two types of soil (a silty loam and silty clay). The experiment *SOC-Aggregation 2* also monitored the long-term mineralization potential of eroded SOC fractions. The results once again demonstrate that aggregation of source soil and thus that of sediment considerably reduces the likely transport distance of eroded SOC, and hence potentially skews its re-distribution towards the terrestrial system (Figure 6-3). In addition, over 50 days, about 5% of the eroded SOC from the silty loam were mineralized into atmospheric CO_2, which was 114% more than the same amount of SOC if stored in original soil would potentially release (Figure 6-5, Table 6-3). An even more considerable skewing pattern of SOC spatial distribution was observed on the silty clay. But the eroded SOC fraction from the silty clay was not as significantly increased as that from the silty loam (Table 6-3). This is principally attributed to the greater SOC content and aggregate stability in this silty clay, better resisting aggregates breakdown and thus protecting the encapsulated SOC during erosion and transport. Compatible performance observed from the two soils suggest that erosion and transport process tend to significantly accelerate the mineralization of eroded SOC, and thus may contribute extra atmospheric CO_2 than erosion would have not occurred. However, the diverse significances of such accelerating effects observed from the two soils further highlight the need to study the potential effects of different aggregation degrees onto the fate of eroded SOC.

7.2. General conclusions

This study aimed to detect the potential impacts of temporal variation of SOC erosion and spatial variation of SOC deposition on the fate of eroded SOC on hillslopes. A series of laboratory experiments were conducted to address these aims. Results observed in this study cast a new light onto our current understanding of slope-scale carbon balances. The crusting and erosion-induced temporal variation of SOC enrichment ratios observed in this study cautions the use of constant or average SOC enrichment ratios to estimate long-term or large-scale selective carbon erosion. It also illustrates the potential risk of bias estimation induced by temporal and inter-replicate variability during linear extrapolation in erosion modeling. Hence, the evolvement of crusting formation over time must be assessed in the field to fairly reflect the possible variation of SOC erosion against time.

The spatial variation during SOC re-deposition observed in this study shows that aggregation effects reduce the likely transport distance of eroded SOC considerably, and hence potentially skew the preferential deposition of SOC-rich coarse sediment fractions toward the terrestrial system. Slope-scale

carbon balances, drawn only from the SOC stocks either on site of erosion or colluvial deposition, may not adequately distinguish the SOC likely re-deposited in terrestrial systems from the portion potentially transferred to aquatic systems. Hence, the potential effects of aggregation onto the likely transport distance of SOC must be included into erosion models (e.g., as a soil erodibility parameter). This then demands current slope-scale carbon balances to ascribe more credits to the terrestrial deposition of eroded SOC, and accordingly less share of eroded SOC transferred to the aquatic system. Such findings may profoundly alter our current understanding of erosion-induced lateral SOC transfer, further suggesting that current recognition on the deep burial of SOC at long-term depositional sites and the accordingly derived CO_2 sink strength would be over-estimated. Significantly accelerated mineralization of eroded SOC during transport adds a further error onto current carbon sink effects. Overall, results from this study suggest that soil erosion is more likely to be a source of atmospheric CO_2. More field investigations on a wider range of soils under various rainfall regimes across larger scales are required in the future to ascertain and further quantify the effects of soil erosion as a source of atmospheric CO_2.

7.3. Potential research in the future

This study was based on laboratory experiments with a limited range of soil types under certain patterns of simulated rainfalls. Erosion plots were relatively small, and transport distances were rather short. Elements in soil erosion and deposition processes, such as transport processes, vegetation coverage, and SOC uptake, were not accounted for. This limits the application of the observations in this study to other erosion scenarios. Therefore, potential research can focus on following directions in the future:

1) Field experiments and monitoring are required to determine the relevance of crusting for the ER_{SOC} under more complex natural conditions, and to examine the applicability of the temporal variation of ER_{SOC} to other erosion scenarios.

2) Soils of different texture, structure and various SOC contents should be examined systematically to investigate the potential of different degrees of aggregation onto the potential transport distance of eroded SOC.

3) Effects of varying rainfall characteristics (e.g., rainfall intensity, multiple rainfall events), a range of crust and moisture conditions of the soil surface, as well as soil management onto SOC transport should also be investigated to extend the findings observed under controlled simulated rainfall conditions to more patterns of natural transport processes.

4) Dissolved SOC transfer and its mineralization potential should also be included in future experiments to fully account for all the relevant elements of carbon fluxes, especially the potential impacts of erosion onto carbon dynamics in the atmosphere and the aquatic system.

5) After obtaining sufficient data from different soil types, rainfall patterns, and soil management, aggregation effects on the likely transport distance of eroded SOC should be included as a soil erodibility parameter to strengthen current soil erosion models.

References

Agassi, M. and Bradford, J. M.: Methodologies for interrill soil erosion studies, Soil Tillage Res., 49(4), 277–287, 1999.

Aksoy, H. and Kavvas, M. L.: A review of hillslope and watershed scale erosion and sediment transport models, Catena, 64(2-3), 247–271, doi:10.1016/j.catena.2005.08.008, 2005.

Anderson, K. and Kuhn, N. J.: Variations in soil structure and reflectance during a controlled crusting experiment, Int. J. Remote Sens., 29(12), 3457–3475, doi:10.1080/01431160701767435, 2008.

Armstrong, A., Quinton, J. N., Heng, B. C. P. and Chandler, J. H.: Variability of interrill erosion at low slopes, Earth Surf. Process. Landf., 36(1), 97–106, doi:10.1002/esp.2024, 2011.

Assouline, S. and Ben-Hur, M.: Effects of rainfall intensity and slope gradient on the dynamics of interrill erosion during soil surface sealing, Catena, 66(3), 211–220, doi:10.1016/j.catena.2006.02.005, 2006.

Barthes, B. and Roose, E.: Aggregate stability as an indicator of soil susceptibility to runoff and erosion; validation at several levels, CATENA, 47(2), 133–149, 2002.

Berhe, A. A.: Decomposition of organic substrates at eroding vs. depositional landform positions, Plant Soil, 350(1-2), 261–280, doi:10.1007/s11104-011-0902-z, 2011.

Berhe, A. A., Harte, J., Harden, J. W. and Torn, M. S.: The significance of the erosion-induced terrestrial carbon sink, BioScience, 57(4), 337–346, 2007.

Berhe, A. A., Suttle, K. B., Burton, S. D. and Banfield, J. F.: Contingency in the direction and mechanics of soil organic matter responses to increased rainfall, Plant Soil, 358(1-2), 371–383, doi:10.1007/s11104-012-1156-0, 2012.

Beuselinck, L., Govers, G., Steegen, A. and Hairsine, P. B.: Experiments on sediment deposition by overland flow, IAHS Publ., 91–96, 1998.

Beuselinck, L., Govers, G., Steegen, A., Hairsine, P. B. and Poesen, J.: Evaluation of the simple settling theory for predicting sediment deposition by overland flow, Earth Surf. Process. Landf., 24, 993–1007, 1999a.

Beuselinck, L., Govers, G., Steegen, A. and Quine, T. A.: Sediment transport by overland flow over an area of net deposition, Hydrol. Process., 13, 2769–2782, 1999b.

Beuselinck, L., Steegen, A., Govers, G., Nachtergaele, J., Takken, I. and Poesen, J.: Characteristics of sediment deposits formed by intense rainfall events in small catchments in the Belgian Loam Belt, Geomorphology, 32(1), 69–82, 2000.

Billings, S. A., Buddemeier, R. W., deB. Richter, D., Van Oost, K. and Bohling, G.: A simple method for estimating the influence of eroding soil profiles on atmospheric CO $_2$: ATMOSPHERIC C POOL AND SOIL EROSION, Glob. Biogeochem. Cycles, 24(2), n/a–n/a, doi:10.1029/2009GB003560, 2010.

Le Bissonnais, Y.: Experimental study and modelling of soil surface crusting processes, Catena, Supplement(17), 13–28, 1990.

Le Bissonnais, Y.: Aggregate stability and assessment of soil crustability and erodibility: I. Theory and methodology, Eur. J. Soil Sci., 47(4), 425–437, 1996.

Le Bissonnais, Y., Benkhadra, H., Chaplot, V., Fox, D., King, D. and Daroussin, J.: Crusting, runoff and sheet erosion on silty loamy soils at various scales and upscaling from m< sup> 2</sup> to small catchments, Soil Tillage Res., 46(1), 69–80, 1998.

Le Bissonnais, Y., Bruand, A. and Jamagne, M.: Laboratory experimental study of soil crusting: Relation between aggregate breakdown mechanisms and crust stucture, Catena, 16(4), 377–392, 1989.

Le Bissonnais, Y., Cerdan, O., Lecomte, V., Benkhadra, H., Souchère, V. and Martin, P.: Variability of soil surface characteristics influencing runoff and interrill erosion, Catena, 62(2-3), 111–124, doi:10.1016/j.catena.2005.05.001, 2005.

Le Bissonnais, Y., Renaux, B. and Delouche, H.: INTERACTIONS BETWEEN SOIL PROPERTIES AND MOISTURE-CONTENT IN CRUST FORMATION, RUNOFF AND INTERRILL EROSION FROM TILLED LOESS SOILS, CATENA, 25(1-4), 33–46, 1995.

Boix-Fayos, C., de Vente, J., Martínez-Mena, M., Barberá, G. G. and Castillo, V.: The impact of land use change and check-dams on catchment sediment yield, Hydrol. Process., 22(25), 4922–4935, doi:10.1002/hyp.7115, 2008.

Borselli, L., Torri, D., Poesen, J. and Sanchis, P.: Effects of water quality on infiltration, runoff and interrill erosion processes during simulated rainfall, EARTH Surf. Process. Landf., 26(3), 329–342, 2001.

Bradford, J. M. and Huang, C.: Interrill soil erosion as affected by tillage and residue cover, Soil Tillage Res., 31(4), 353–361, 1994.

Brady, N. C. and Weil, R. R.: The Nature and Properties of Soils, 13th ed., Pearson Education, New Jersey, US., 2002.

Bremenfeld, S., Fiener, P. and Govers, G.: Effects of interrill erosion, soil crusting and soil aggregate breakdown on in situ CO2 effluxes, Catena, 104, 14–20, doi:10.1016/j.catena.2012.12.011, 2013.

Bryan, R. B. and Luk, S. H.: Laboratory experiments on the variation of soil erosion under simulated rainfall, Geoderma, 26, 245–265, 1981.

Bryan, R. B. and de Ploey, J.: Comparability of soil erosion measurements with different laboratory rainfall simulators, Catena, (Ed: Jan de Ploey, Rainfall Simulation, Runoff and Soil Erosion, Supplement 4), 33–56, 1983.

Cambardella, C. A. and Elliott, E. T.: Carbon and nitrogen dynamics of soil organic matter fractions from cultivated grassland soils, SOIL Sci. Soc. Am. J., 58(1), 123–130, 1994.

Cerda, A. and Garcia-Fayos, P.: The influence of slope angle on sediment, water and seed losses on badland landscapes, Geomorphology, 18, 77–90, 1997.

Chen, Y., Tarchitzky, J., Brouwer, J., Morin, J. and Banin, A.: Scanning electron microscope observation on soil crusts and their formation, Soil Sci., 130, 49–55, 1980.

Christensen, B. T.: Physical fractionation of soil and structural and functional complexity in organic matter turnover, Eur. J. Soil Sci., 52(3), 345–353, 2001.

Darboux, F. and Le Bissonnais, Y.: Changes in structural stability with soil surface crusting: consequences for erodibility estimation, Eur. J. Soil Sci., 58(5), 1107–1114, doi:10.1111/j.1365-2389.2007.00906.x, 2007.

Dietrich, W. E.: Settling velocity of natural particles, Water Resour. Res., 18(6), 1615–1626, 1982.

Dietrich, W. E., Wilson, C. J., Montgomery, D. R., McKean, J. and Bauer, R.: Erosion thresholds and land surface morphology, Geology, 20(8), 675–679, 1992.

Dlugoß, V., Fiener, P., Van Oost, K. and Schneider, K.: Model based analysis of lateral and vertical soil carbon fluxes induced by soil redistribution processes in a small agricultural catchment: MODELLING SOIL

REDISTRIBUTION & SOIL CARBON DYNAMICS, Earth Surf. Process. Landf., 37(2), 193–208, doi:10.1002/esp.2246, 2012.

Doetterl, S., Six, J., Van Wesemael, B. and Van Oost, K.: Carbon cycling in eroding landscapes: geomorphic controls on soil organic C pool composition and C stabilization, Glob. Change Biol., 18(7), 2218–2232, doi:10.1111/j.1365-2486.2012.02680.x, 2012.

Droppo, I. G., Leppard, G. G., Flannigan, D. T. and Liss, S. N.: The freshwater floc: a functional relationship of water and organic and inorganic floc constituents affecting suspended sediment properties, Water. Air. Soil Pollut., 99(1-4), 43–54, 1997.

Dunkerley, D.: Rain event properties in nature and in rainfall simulation experiments: a comparative review with recommendations for increasingly systematic study and reporting, Hydrol. Process., 22(22), 4415–4435, doi:10.1002/hyp.7045, 2008.

Ferguson, R. I. and Church, M.: A Simple Universal Equation for Grain Settling Velocity, J. Sediment. Res., 74(6), 933–937, 2004.

Fiener, P., Dlugoß, V., Korres, W. and Schneider, K.: Spatial variability of soil respiration in a small agricultural watershed — Are patterns of soil redistribution important?, Catena, 94, 3–16, doi:10.1016/j.catena.2011.05.014, 2012.

Fiener, P., Govers, G. and Oost, K. V.: Evaluation of a dynamic multi-class sediment transport model in a catchment under soil-conservation agriculture, Earth Surf Process Landf., 33(11), 1639–1660, 2008a.

Fiener, P., Govers, G. and Oost, K. V.: Evaluation of a dynamic multi-class sediment transport model in a catchment under soil-conservation agriculture, Earth Surf. Process. Landf., 33(11), 1639–1660, doi:10.1002/esp.1634, 2008b.

Fitzjohn, C., Ternan, J. and Williams, A.: Soil moisture variability in a semi-arid gully catchment: implications for runoff and erosion control, CATENA, 32(1), 55–70, 1998.

Flanagan, D. C. and Nearing, M. A.: Sediment particle sorting on hillslope profiles in the WEPP model, Trans. ASAE, 43(3), 573–583, 2000.

Fox, D. M. and Bryan, R. B.: The relationship of soil loss by interrill erosion to slope gradient, Catena, 38(3), 211–222, 2000.

Fox, D. M., Bryan, R. B. and Price, A. G.: The influence of slope angle on final infiltration rate for interrill conditions, Geoderma, 80(1), 181–194, 1997.

Govers, G. and Poesen, J.: Assessment of the interrill and rill contributions to total soil loss from an upland field plot, Geomorphology, 1(4), 343–354, 1988.

Govers, G., Quine, T. A., Desmet, P. J. J. and Walling, D. E.: The relative contribution of soil tillage and overland flow erosion to soil redistribution on agricutlural land, EARTH Surf. Process. Landf., 21, 929–946, 1996.

Gregorich, E. G., Greer, K. J., Anderson, D. W. and Liang, B. C.: Carbon distribution and losses: erosion and deposition effects, Soil Tillage Res., 47(3), 291–302, 1998.

Hairsine, P. B., Sander, G. C., Rose, C. W., Parlange, J.-Y., Hogarth, W. L., Lisle, I. and Rouhipour, H.: Unsteady soil erosion due to rainfall impact: a model of sediment sorting on the hillslope, J. Hydrol., 220(3), 115–128, 1999.

Hairsine, P. and McTainsh, G.: The Griffith tube: A simple settling tube for the measurement of settling velocity of aggregates, School of Australian Environmental Studies, Griffith University. [online] Available from: http://online.sfsu.edu/jerry/geo_642/refs/GriffithTube.pdf (Accessed 17 September 2013), 1986.

Harden, J. W., Sharpe, J. M., Parton, W. J., Ojima, S., Fries, T. L., Huntington, T. G. and Dabney, S. M.: Dynamic replacement and loss of soil carbon on eroding cropland, Glob. Biogeochem. Cycles, 13(4), 885–901, doi:10.1029/1999GB900061, 1999.

Heil, J. W., Juo, A. S. R. and McInnes, K. J.: Soil Properties Influencing Surface Sealing of Some Sandy Soils in the Sahel, Soil Sci., 162(7), 459–469, 1997.

Van Hemelryck, H., Fiener, P., van Oost, K., Govers, G. and Merckx, R.: The effect of soil redistribution on soil organic carbon: an experimental study, Biogeosciences, 7(12), 3971–3986, doi:10.5194/bg-7-3971-2010, 2010.

Van Hemelryck, H., Govers, G., Van Oost, K. and Merckx, R.: Evaluating the impact of soil redistribution on the in situ mineralization of soil organic carbon, Earth Surf. Process. Landf., 36(4), 427–438, doi:10.1002/esp.2055, 2011.

Hoffmann, T., Mudd, S. M., van Oost, K., Verstraeten, G., Erkens, G., Lang, A., Middelkoop, H., Boyle, J., Kaplan, J. O., Willenbring, J. and Aalto, R.: Short Communication: Humans and the missing C-sink: erosion and burial of soil carbon through time, Earth Surf. Dyn., 1(1), 45–52, doi:10.5194/esurf-1-45-2013, 2013.

Hu, Y. and Fister, W.: Soil organic carbon erosion from two silty loam soils - a laboratory rainfall experiment, in Poster at Session GM 4.2 “Erosion and terrestrial carbon cycle”, in General Assembly of European Geoscience Union, Vienna., 2011.

Hu, Y., Fister, W. and Kuhn, N. J.: Inter-replicate variability and duration-related systematic variability in organic carbon erosion modeling,, In preparation.

Hu, Y., Fister, W. and Kuhn, N. J.: Temporal variation of SOC enrichment from interrill erosion over prolonged rainfall simulations, Agriculture, 3(4), 726–740, 2013a.

Hu, Y., Fister, W., Rüegg, H.-R., Kinnell, P. A. and Kuhn, N. J.: The Use of Equivalent Quartz Size and Settling Tube Apparatus to Fractionate Soil Aggregates by Settling Velocity, Geomorphol. Tech. Online Ed. Br. Soc. Geomorphol., Section–1, 2013c.

Hu, Y. and Kuhn, N. J.: Aggregates reduce transport distance of soil organic carbon: are our balances correct?, Biogeosciences Discuss., 11, 1–31, doi:10.5194/bgd-11-1-2014, 2014.

IPCC: Climate change 2013: the physical science basis : Working Group I contribution to the fifth assessment report of the Intergovernmental Panel on Climate Change., 2014.

Iserloh, T., Fister, W., Seeger, M., Willger, H. and Ries, J. B.: A small portable rainfall simulator for reproducible experiments on soil erosion, Soil Tillage Res., 124, 131–137, doi:10.1016/j.still.2012.05.016, 2012.

Iserloh, T., Ries, J. B., Arnáez, J., Boix-Fayos, C., Butzen, V., Cerdà, A., Echeverría, M. T., Fernández-Gálvez, J., Fister, W., Geißler, C., Gómez, J. A., Gómez-Macpherson, H., Kuhn, N. J., Lázaro, R., León, F. J., Martínez-Mena, M., Martínez-Murillo, J. F., Marzen, M., Mingorance, M. D., Ortigosa, L., Peters, P., Regüés, D., Ruiz-Sinoga, J. D., Scholten, T., Seeger, M., Solé-Benet, A., Wengel, R. and Wirtz, S.: European small portable rainfall simulators: A comparison of rainfall characteristics, Catena, 110, 100–112, doi:10.1016/j.catena.2013.05.013, 2013.

Jacinthe, P. A. and Lal, R.: A mass balance approach to assess carbon dioxide evolution during erosional events, Land Degrad. Dev., 12(4), 329–339, doi:10.1002/ldr.454, 2001.

Jacinthe, P. A., Lal, R. and Kimble, J. M.: Assessing water erosion impacts on soil carbon pools and fluxes, in Assessment Methods for Soil Carbon, pp. 427–450, CRC Press, Boca Raton. [online] Available from: http://books.google.ch/books?hl=en&lr=&id=kgiYYADtQx0C&oi=fnd&pg=PA427&dq=assessing+water+erosion+impacts+on+soil+carbon+pools+and+fluxes&ots=JF-H2Tp2Y0&sig=iFTGwmNO4PcD0k4xLpbzgjdA_80#v=onepage&q=assessing%20water%20erosion%20impacts%20on%20soil%20carbon%20pools%20and%20fluxes&f=false (Accessed 7 February 2014), 2001.

Jacinthe, P., Lal, R. and Kimble, J.: Carbon dioxide evolution in runoff from simulated rainfall on long-term no-till and plowed soils in southwestern Ohio, SOIL TILLAGE Res., 66(1), 23–33, 2002a.

Jacinthe, P.-A., Lal, R. and Kimble, J. M.: Carbon dioxide evolution in runoff from simulated rainfall on long-term no-till and plowed soils in southwestern Ohio, Soil Tillage Res., 66(1), 23–33, 2002b.

Jacinthe, P.-A., Lal, R., Owens, L. B. and Hothem, D. L.: Transport of labile carbon in runoff as affected by land use and rainfall characteristics, Soil Tillage Res., 77(2), 111–123, doi:10.1016/j.still.2003.11.004, 2004.

Jin, K., Cornelis, W. M., Gabriels, D., Baert, M., Wu, H. J., Schiettecatte, W., Cai, D. X., De Neve, S., Jin, J. Y., Hartmann, R. and Hofman, G.: Residue cover and rainfall intensity effects on runoff soil organic carbon losses, Catena, 78(1), 81–86, doi:10.1016/j.catena.2009.03.001, 2009.

Johnson, C. P., Li, X. and Logan, B. E.: Settling Velocities of Fractal Aggregates, Env. Sci Techool, 30, 1911–1918, 1996.

Kaiser, M., Berhe, A. A., Sommer, M. and Kleber, M.: Application of ultrasound to disperse soil aggregates of high mechanical stability, J. Plant Nutr. Soil Sci., 175(4), 521–526, doi:10.1002/jpln.201200077, 2012.

Kimaro, D. N., Poesen, J., Msanya, B. M. and Deckers, J. A.: Magnitude of soil erosion on the northern slope of the Uluguru Mountains, Tanzania: Interrill and rill erosion, Catena, 75(1), 38–44, doi:10.1016/j.catena.2008.04.007, 2008.

Kinnell, P.: Raindrop-impact-induced erosion processes and prediction: a review, Hydrol. Process., 19(14), 2815–2844, doi:10.1002/hyp.5788, 2005.

Kinnell, P. I. A.: Particle travel distances and bed and sediment compositions associated with rain-impacted flows, Earth Surf. Process. Landf., 26(7), 749–758, doi:10.1002/esp.221, 2001.

Kinnell, P. I. A.: Raindrop-induced saltation and the enrichment of sediment discharged from sheet and interrill erosion areas, Hydrol. Process., 26(10), 1449–1456, doi:10.1002/hyp.8270, 2012.

Kinnell, P. I. A. and McLachlan, C.: An injection barrel for the top entry sedimentation tube,, 1988.

Kuhn, N., Bryan, R. and Navar, J.: Seal formation and interrill erosion on a smectite-rich Kastanozem from NE-Mexico, CATENA, 52(2), 149–169, doi:10.1016/S0341-8162(02)00091-7, 2003.

Kuhn, N. J.: Erodibility of soil and organic matter: independence of organic matter resistance to interrill erosion, Earth Surf. Process. Landf., 32(5), 794–802, doi:10.1002/esp.1486, 2007.

Kuhn, N. J.: Erosion and climate, Nat. Geosci., 3 [online] Available from: https://physiogeo.unibas.ch/pubs/pdfs/KuhnNJ10.pdf (Accessed 19 May 2014a), 2010.

Kuhn, N. J.: Rainfall Simulation Experiments on Crusting and Interrill Sediment Organic Matter Content on a Silt Loam from Devon, ERDE, 141(4), 283–300, 2010b.

Kuhn, N. J.: Assessing lateral organic Carbon movement in small agricultural catchments, Publ. Zur Jahrestag. Schweiz. Geomorphol. Ges. Ed Graf C, 29, 151–164, 2013.

Kuhn, N. J. and Armstrong, E. K.: Erosion of organic matter from sandy soils: Solving the mass balance, Catena, 98, 87–95, doi:10.1016/j.catena.2012.05.014, 2012.

Kuhn, N. J., Armstrong, E. K., Ling, A. C., Connolly, K. L. and Heckrath, G.: Interrill erosion of carbon and phosphorus from conventionally and organically farmed Devon silt soils, CATENA, 91, 94–103, doi:10.1016/j.catena.2010.10.002, 2012.

Kuhn, N. J. and Bryan, R. B.: Drying, soil surface condition and interrill erosion on two Ontario soils, Catena, 57(2), 113–133, doi:10.1016/j.catena.2003.11.001, 2004.

Kuhn, N. J., Hoffmann, T., Schwanghart, W. and Dotterweich, M.: Agricultural soil erosion and global carbon cycle: controversy over?, Earth Surf. Process. Landf., 1033–1038, doi:10.1002/esp.1796, 2009.

Lal, R.: Soil erosion and the global carbon budget, Environ. Int., 29(4), 437–450, doi:10.1016/S0160-4120(02)00192-7, 2003.

Lal, R., Griffin, M., Apt, J., Lave, L. and Morgan, M. G.: Managing soil carbon, Science, 304(5669), 393, 2004.

Lal, R. and Pimentel, D.: Soil erosion a carbon sink or source?, Science, 319, 1040–1041, 2008.

Levy, G. J., Levin, J. and Shainberg, I.: Prewetting rate and aging effects on seal formation and interrill soil erosion 1, SOIL Sci., 162(2), 131–139, 1997.

Leys, A., Govers, G., Gillijns, K. and Poesen, J.: Conservation tillage on loamy soils: explaining the variability in interrill runoff and erosion reduction, Eur. J. Soil Sci., 58(6), 1425–1436, doi:10.1111/j.1365-2389.2007.00947.x, 2007.

Loch, R. J.: Settling velocity–a new approach to assessing soil and sediment properties, Comput. Electron. Agric., 31(3), 305–316, 2001.

Luk, S. H. and Morgan, R. P. C.: Spatial variation of rainwash and runoff within apparently homogeneous areas, Catena, 8, 383–402, 1981.

Martínez-Mena, M., López, J., Almagro, M., Albaladejo, J., Castillo, V., Ortiz, R. and Boix-Fayos, C.: Organic carbon enrichment in sediments: Effects of rainfall characteristics under different land uses in a Mediterranean area, Catena, 94, 36–42, doi:10.1016/j.catena.2011.02.005, 2012.

Massey, H. F. and Jackson, M. L.: Selective Erosion of Soil Fertility Constituents1, Soil Sci Soc Am J, 16(4), 353–356, 1952.

McCarty, G. W. and Ritchie, J. C.: Impact of soil movement on carbon sequestration in agricultural ecosystems, Environ. Pollut., 116(3), 423–430, 2002.

MeteoSwiss: Monthly total precipitation during April, May, and June at Station Arisdorf near Möhlin from 1985 to 2012,, 2013.

Meyer, L. D.: Rainfall simulators for soil erosion research, in Soil Erosion Research Methods. Ed: Lal R., St. Lucie Press., 1994.

Moore, D. C. and Singer, M. J.: Crust formation effects on soil erosion processes, Soil Sci. Soc. Am. J., 54, 1117–1123, 1990a.

Moore, D. C. and Singer, M. J.: Crust Formation Effects on Soil Erosion Processes, Soil Sci Soc Am J, 54(4), 1117–1123, 1990b.

Mora, J. L., Guerra, J. A., Armas, C. M., Rodriguez-Rodriguez, A., Arbelo, C. D. and Notario, J. S.: Mineralization rate of eroded organic C in andosols of the Canary Islands, Sci. TOTAL Environ., 378(1-2), 143–146, doi:10.1016/j.sciotenv.2007.01.040, 2007.

Morgan, R. P. C., Quinton, J. N., Smith, R. E., Govers, G., Poesen, J. W. A., Auerswald, K., Chisci, G., Torri, D. and Styczen, M. E.: The European Soil Erosion Model (EUROSEM): a dynamic approach for predicting sediment transport from fields and small catchments, Earth Surf. Process. Landf., 23(6), 527–544, 1998.

Nadeu, E., Berhe, A. A., de Vente, J. and Boix-Fayos, C.: Erosion, deposition and replacement of soil organic carbon in Mediterranean catchments: a geomorphological, isotopic and land use change approach, Biogeosciences, 9(3), 1099–1111, doi:10.5194/bg-9-1099-2012, 2012.

Nearing, M. A., Govers, G. and Norton, L. D.: Variability in soil erosion data from replicated plots, Soil Sci. Soc. Am. J., 63(6), 1829–1835, 1999.

Nimmo, J. R. and Perkins, K. S.: Aggregate stability and size distribution, in Soil Science Society of America. Ed: Dane J. H., Topp G.C., vol. Part 4-Physical methods, pp. 317–328, Madison, Wisconsin., 2002.

North, P. F.: Towards an absolute measurement of soil structural stability using ultrasound, J. Soil Sci., 27, 451–459, 1976.

Olson, K. R.: Impacts of Tillage, Slope, and Erosion on Soil Organic Carbon Retention:, Soil Sci., 175(11), 562–567, doi:10.1097/SS.0b013e3181fa2837, 2010.

Van Oost, K., Beuselinck, L., Hairsine, P. B. and Govers, G.: Spatial evaluation of a multi-class sediment transport and deposition model, Earth Surf. Process. Landf., 29(8), 1027–1044, doi:10.1002/esp.1089, 2004.

Van Oost, K., Govers, G., Quine, T. A., Heckrath, G., Olesen, J. E., De Gryze, S. and Merckx, R.: Landscape-scale modeling of carbon cycling under the impact of soil redistribution: The role of tillage erosion, Glob. Biogeochem. Cycles, 19(4), doi:10.1029/2005GB002471, 2005.

Van Oost, K., Quine, T. A., Govers, G., De Gryze, S., Six, J., Harden, J. W., Ritchie, J. C., McCarty, G. W., Heckrath, G., Kosmas, C., Giraldez, J. V., da Silva, J. R. M. and Merckx, R.: The Impact of Agricultural Soil Erosion on the Global Carbon Cycle, Science, 318(5850), 626–629, doi:10.1126/science.1145724, 2007.

Van Oost, K., Verstraeten, G., Doetterl, S., Notebaert, B., Wiaux, F., Broothaerts, N. and Six, J.: Legacy of human-induced C erosion and burial on soil-atmosphere C exchange, Proc. Natl. Acad. Sci., 109(47), 19492–19497, doi:10.1073/pnas.1211162109, 2012.

Palis, R. G., Okwach, G., Rose, C. W. and Saffigna, P. G.: Soil erosion processes and nutrient loss. 1. The interpretation of enrichment ratio and nitrogen loss in runoff sediment, Aust. J. Soil Res., 28(4), 623–639, 1990.

Parson, A. J. and Abrahams, A. D.: Field investigations of sediment removal in interrill overland flow, in Overland Flow, pp. 307–334, Routledge Taylor & Francis Group., 1992.

Pimentel, D., Harvey, C., Resosudarmo, P., Sinclair, K., Kurz, D., McNair, M., Crist, S., Shpritz, L., Fitton, L., Saffouri, R. and Blair, R.: Environmental and economic costs of soil erosion and conservation benefits, Science, 267, 1117–1123, 1995.

Polyakov, V. and Lal, R.: Modeling soil organic matter dynamics as affected by soil water erosion, Environ. Int., 30(4), 547–556, doi:10.1016/j.envint.2003.10.011, 2004a.

Polyakov, V. O. and Lal, R.: Soil erosion and carbon dynamics under simulated rainfall, Soil Sci., 169(8), 590–599, doi:10.1097/01.ss.0000138414.84427.40, 2004b.

Polyakov, V. O. and Lal, R.: Soil organic matter and CO2 emission as affected by water erosion on field runoff plots, Geoderma, 143(1-2), 216–222, doi:10.1016/j.geoderma.2007.11.005, 2008.

Puri, A. N.: A siltometer for studying size distribution of silts and sands, Punjab Irrig. Inst. Res. Publ., 2(7), 10, 1934.

Quinton, J. N., Catt, J. A. and Hess, T. M.: The selecctive removal of phosphorus from soil: is event size important?, J Env. Qual, 30(2), 538–545, 2001.

Quinton, J. N., Govers, G., Van Oost, K. and Bardgett, R. D.: The impact of agricultural soil erosion on biogeochemical cycling, Nat. Geosci., 3(5), 311–314, doi:10.1038/ngeo838, 2010.

Ramos, M. C., Nacci, S. and Pla, I.: Soil Sealing and Its Influence on Erosion Rates for Some Soils in the Mediterranean Area, Soil Sci., 165(5), 398–403, 2000.

Rex, J. F. and Petticrew, E. L.: Pacific salmon and sediment flocculation: nutrient cycling and intergravel habitat quality, IAHS Publ., 306, 442, 2006.

Robertson, G. P., Wedin, D., Groffmann, P. M., Blair, J. M., Holland, E. A., Nadelhoffer, K. J. and Harris, D.: Soil carbon and nitrogen availability - Nitrogen mineralization, nitrification, and soil respiration potentials, in Standard Soil Method for Long-term Ecological Research. Ed: G.Philip Robertson, David C. Coleman, Caroline S. Bledsoe, Phillip Sollins, Oxford University Press, Oxford., 1999.

Rodríguez Rodríguez, A., Guerra, A., Arbelo, C., Mora, J. L., Gorrín, S. P. and Armas, C.: Forms of eroded soil organic carbon in andosols of the Canary Islands (Spain), Geoderma, 121(3-4), 205–219, doi:10.1016/j.geoderma.2003.11.009, 2004.

Römkens, M. J. M., Helming, K. and Prasad, S. N.: Soil erosion under different rainfall intensities, surface roughness, and soil water regimes, Catena, 46(2), 103–123, 2002.

Rubey, W. W.: Settling velocities of gravel, sand, and silt particles, Am. J. Sci., 225, 325–338, 1933.

Rüttimann, M., Schaub, D., Prasuhn, V. and Rüegg, W.: Measurement of runoff and soil erosion on regularly cultivated fields in Switzerland—some critical considerations, Catena, 25(1), 127–139, 1995.

Sartori, M.: The quaternary climate in loess sediments, Diss. Naturwissenschaften ETH Zürich, Nr. 13570, 2000. [online] Available from: http://e-collection.library.ethz.ch/view/eth:23643 (Accessed 23 January 2014), 2000.

Schiettecatte, W., Gabriels, D., Cornelis, W. M. and Hofman, G.: Enrichment of organic carbon in sediment transport by interrill and rill erosion processes, Soil Sci Soc Am J, 72(1), 50–55, 2008.

Sharpley, A. N.: The Selection Erosion of Plant Nutrients in Runoff, Soil Sci Soc Am J, 49(6), 1527–1534, 1985.

Singer, M. J. and Le Bissonnais, Y.: Importance of surface sealing in the erosion of some soils from a mediterranen climate, Geomorphology, 24, 79–85, 1998.

Singer, M. and Shainberg, I.: Mineral soil surface crusts and wind and water erosion, EARTH Surf. Process. Landf., 29(9), 1065–1075, 2004.

Six, J., Conant, R. T., Paul, E. A. and Paustian, K.: Stabilization mechanisms of soil organic matter: Implications for C-saturation of soils, Plant Soil, 241, 155–176, 2002.

Slattery, M. C. and Bryan, R. B.: Laboratory experiments on surface seal development and its effect on interrill erosion processes., J. Soil Sci., 43, 517–529, 1992.

Slattery, M. C. and Burt, T. P.: Particle size characteristics of suspended sediment in hillslope runoff and stream flow, Earth Surf. Process. Landf., 22(8), 705–719, 1997.

Smith, S. V., Renwick, W. H., Buddemeier, R. W. and Crossland, C. J.: Budgets of soil erosion and deposition for sediments and sedimentary organic carbon across the conterminous United States, Glob. Biogeochem. CYCLES, 15(3), 697–707, 2001.

Stallard, R. F.: Terrestrial sedimentation and the carbon cycle: Coupling weathering and erosion to carbon burial, Glob. Biogeochem. Cycles, 12(2), 231–257, 1998.

Starr, G. C., Lal, R., Malone, R., Hothem, D., Owens, L. and Kimble, J.: Modeling soil carbon transported by water erosion processes, Land Degrad. Dev., 11(1), 83–91, 2000.

Teixeira, P. C. and Misra, R. K.: Measurement and prediction of nitrogen loss by simulated erosion events on cultivated forest soils of contrasting structure, Soil Tillage Res., 83(2), 204–217, doi:10.1016/j.still.2004.07.014, 2005.

Tisdall, J. M. and Oades, J. M.: Organic matter and water-stable aggregates in soils, J. Soil Sci., 33(2), 141–163, 1982.

Tromp-van Meerveld, H. J., Parlange, J.-Y., Barry, D. A., Tromp, M. F., Sander, G. C., Walter, M. T. and Parlange, M. B.: Influence of sediment settling velocity on mechanistic soil erosion modeling: INFLUENCE OF SEDIMENT SETTLING VELOCITY, Water Resour. Res., 44(6), n/a–n/a, doi:10.1029/2007WR006361, 2008.

Vanmaercke, M., Poesen, J., Radoane, M., Govers, G., Ocakoglu, F. and Arabkhedri, M.: How long should we measure? An exploration of factors controlling the inter-annual variation of catchment sediment yield, J. Soils Sediments, 12(4), 603–619, doi:10.1007/s11368-012-0475-3, 2012.

Walker, P. H., Kinnell, P. I. A. and Patricia, G.: Transport of a non-cohesive sand mixture in rainfall and runoff experiments, Soil Sci. Soc. Am. J., 42, 793–801, 1978.

Walling, D. E.: The sediment delivery problem, J. Hydrol., 65(1), 209–237, 1983.

Walling, D. E.: Erosion and sediment yield research—some recent perspectives, J. Hydrol., 100(1), 113–141, 1988.

Wan, L., Zhang, X. P., Ma, Q., Zhang, J. J., Ma, T. Y. and Sun, Y. P.: Spatiotemporal characteristics of precipitation and extreme events on the Loess Plateau of China between 1957 and 2009: CHANGES OF PRECIPITATION AND EXTREME EVENTS ON CHINA LOESS PLATEAU, Hydrol. Process., n/a–n/a, doi:10.1002/hyp.9951, 2013.

Wang, Q., Fan, X., Qin, Z. and Wang, M.: Change trends of temperature and precipitation in the Loess Plateau Region of China, 1961–2010, Glob. Planet. Change, 92-93, 138–147, doi:10.1016/j.gloplacha.2012.05.010, 2012.

Wang, X., Cammeraat, E. L. H., Romeijn, P. and Kalbitz, K.: Soil Organic Carbon Redistribution by Water Erosion – The Role of CO2 Emissions for the Carbon Budget, edited by B. Bond-Lamberty, PLoS ONE, 9(5), e96299, doi:10.1371/journal.pone.0096299, 2014.

Wang, X., Gao, H., Tullberg, J. N., Li, H., Kuhn, N. J., Mchugh, A. and Li, Y.: Traffic and tillage effects on runoff and soil loss on the Loess Plateau of northern China, Soil Res., 46(8), 667–675, 2008.

Wang, Z., Govers, G., Steegen, A., Clymans, W., Van den Putte, A., Langhans, C., Merckx, R. and Van Oost, K.: Catchment-scale carbon redistribution and delivery by water erosion in an intensively cultivated area, Geomorphology, 124(1-2), 65–74, doi:10.1016/j.geomorph.2010.08.010, 2010.

Warrington, D. N., Mamedov, A. I., Bhardwaj, A. K. and Levy, G. J.: Primary particle size distribution of eroded material affected by degree of aggregate slaking and seal development, Eur. J. Soil Sci., 60(1), 84–93, doi:10.1111/j.1365-2389.2008.01090.x, 2009.

Wendt, R. C., Alberts, E. E. and Hjelmfelt, A. T.: Variability of Runoff and Soil Loss from Fallow Experimental Plots, Soil Sci Soc Am J, 50(3), 730–736, 1986.

Wong, K. B. and Piedrahita, R. H.: Settling velocity characterization of aquacultural solids, Aquac. Eng., 21(4), 233–246, 2000.

Wu, W. and Wang, S. S.: Formulas for sediment porosity and settling velocity, J. Hydraul. Eng., 132(8), 858–862, 2006.

Xu, L., Baldocchi, D. D. and Tang, J.: How soil moisture, rain pulses, and growth alter the response of ecosystem respiration to temperature, Glob. Biogeochem Cycles, 18(GB4002), doi:10.1029/2004GB002281, 2004.

Zehe, E., Graeff, T., Morgner, M., Bauer, A. and Bronstert, A.: Plot and field scale soil moisture dynamics and subsurface wetness control on runoff generation in a headwater in the Ore Mountains, Hydrol. EARTH Syst. Sci., 14(6), 873–889, doi:10.5194/hess-14-873-2010, 2010.

Zibilske, L. M.: Carbon mineralization., in Soil Science Society of America, vol. Methods of Soil Analysis, Madison, Wisconsin, USA., 1994.